Postprint version of paper published in Mathematical Biosciences 2017, vol. 288, p. 21-34.
The content is identical to the published paper, but without the final typesetting by the publisher.

Identifiability of large-scale non-linear dynamic network models applied to the ADM1-case study

Philippe Nimmegeers[a], Joost Lauwers[a], Dries Telen[a], Filip Logist[a], Jan Van Impe[a,b]

[a] *KU Leuven, Department of Chemical Engineering, BioTeC+ & OPTEC, Gebroeders De Smetstraat 1, 9000 Ghent, Belgium*
[b] *Corresponding author. jan.vanimpe@kuleuven.be*
Tel: +32.16.32.14.66

Abstract

In this work, both the structural and practical identifiability of the Anaerobic Digestion Model no. 1 (ADM1) is investigated, which serves as a relevant case study of large non-linear dynamic network models. The structural identifiability is investigated using the *probabilistic* algorithm, adapted to deal with the specifics of the case study (i.e., a large-scale non-linear dynamic system of differential and algebraic equations). The practical identifiability is analyzed using a Monte Carlo parameter estimation procedure for a 'non-informative' and 'informative' experiment, which are heuristically designed.
The model structure of ADM1 has been modified by replacing parameters by parameter combinations, to provide a generally locally structurally identifiable version of ADM1. This means that in an idealized theoretical situation, the parameters can be estimated accurately. Furthermore, the generally positive structural identifiability results can be explained from the large number of interconnections between the states in the network structure. This interconnectivity, however, is also observed in the parameter estimates, making uncorrelated parameter estimations in practice difficult.

Keywords: Structural identifiability, Practical identfiability, Anaerobic Digestion Model No.1, Non-linear biological models

1. Introduction

Dynamic models are essential tools for the study of large-scale bioprocesses. Due to the complexity of the processes, however, these models generally contain large numbers of (i) non-linear ordinary differential or differential alge-

braic equations (ODEs or DAEs) and (*ii*) parameters which have to be estimated. The latter issue raises questions whether the parameters can be estimated univocally (i.e., unique parameter estimates) and with sufficient accuracy and precision (which is reflected in the width of the confidence intervals on the parameter estimates). Furthermore the parameter estimates should be consistent with respect to parameter values that are reported in literature.

The problem of non-uniqueness of parameter estimates is a question of *identifiability*. This concept acts on two levels: the *structural identifiability* and the *practical identifiability*. The former refers to the structure of the model which does or does not allow the unique characterization of the parameters, even under perfect 'identification conditions'. A lack of structural identifiability could be attributed to a poor choice of model structure such as overparameterization or the inclusion of phenomena that can never be experimentally verified or refuted. The practical identifiability refers to finding accurate and precise parameter estimates considering the influence of issues such as the choice and limitation of the applied input and the measuring conditions. Since the conditions for structural identifiability are stricter than for practical identifiability, structural identifiability is in fact a *necessary condition* for practical identifiability. For a model that is not structurally identifiable, it is impossible to find reliable parameter estimates.

In this work the Anaerobic Digestion Model No. 1 (ADM1) [1] is considered as a case study of a large-scale non-linear biological network model. For the structural identifiability analysis: different measurement and input scenarios are evaluated. For the practical identifiability, the single situation in which all states are measured and all possible inputs are available, i.e., the situation that yields the best estimates, is investigated.

The contributions of this article are three-fold. Firstly, to show how an analysis of the structural and practical identifiability of a large-scale model consisting of DAEs and non-rational expressions can be performed. Secondly, to yield structural and practical identifiability results for ADM1, which are to our knowledge not available. Finally, to generalize the results of the ADM1 case study to dynamic network models: to investigate the structural aspects of the model causing the (non-)identifiability.

The outline of the work is as follows: first the ADM1 case study is presented. This also includes a statement of the identifiability problem and an overview of the analyzed cases concerning the applied inputs and measured outputs. In the next sections definitions concerning structural identifiability are stated, together with a description of the method to study it. This is followed by a description of the followed methodology for analyzing the practical identifiability. The results section starts with an overview of the structural identifiability results for the ADM1 case study. The structural aspects of the case study causing the (non-)identifiability are highlighted. Next, the results concerning the practical identifiability are presented, with a highlight on the structural aspects of the model causing the (non-)identifiability. The conclusions are presented in the last section.

2. Case study

Anaerobic Digestion Model No. 1 (ADM1) is a generic model developed by the International Water Association's Anaerobic Digestion Modelling Task Group [2, 1]. The ADM1 model knows numerous simulation applications in literature varying from anaerobic digestion of organic wastes to waste wa-

Postprint version of paper published in Mathematical Biosciences 2017, vol. 288, p. 21-34.
The content is identical to the published paper, but without the final typesetting by the publisher.

ter treatment (e.g., [3, 4, 5, 6]). Therefore it can be seen as the state-of-the-art model in anaerobic digestion. The ADM1 model network structure is depicted in Figure **??**, based on the implementation of the equations presented in Appendix A [7]. The model comprises 39 states: 24 soluble components (S_i, with $i \in \{\text{su}, \text{aa}, \text{fa}, \text{va}, \text{bu}, \text{pro}, \text{ac}, \text{h2}, \text{ch4}, \text{IC}, \text{IN}, \text{I}\}$), 3 gaseous components ($S_{\text{gas},i}$, with $i \in \{\text{h2}, \text{ch4}, \text{co2}\}$), 5 particulate composites (X_i, with $i \in \{\text{xc}, \text{ch}, \text{pr}, \text{li}, \text{I}\}$) with i being a component and 7 microbial groups (X_j, with $j \in \{\text{su}, \text{aa}, \text{fa}, \text{c4}, \text{pro}, \text{ac}, \text{h2}\}$), degrading component j. Since the reactions related to the acid-base equilibrium can be considered instantaneous, they are expressed in algebraic expressions (AEs) of index 1, following [1]. Most of the states are expressed either in terms of Chemical Oxygen Demand (COD) or kmol C or N per m^3. See Table 1 of Appendix A for an overview of all states.

ADM1 includes 22 stoichiometric, 19 composition and 37 kinetic parameters. The stoichiometric parameters express the ratios in which COD is converted from one state into another: (i) 7 biomass on component yield coefficients ($Y_i \in [0, 1]$, with i being the component consumed by the microbial group) and (ii) 15 component on component yield coefficients, ($f_{i,j} \in [0, 1]$ with i being the component produced from component j). The composition parameters N_i and C_i express the nitrogen and carbon content of a component i. They act as conversion factors between COD-based states and the inorganic nitrogen and carbon. Of the 19 composition parameters, 5 are considered to be known, i.e., the carbon content of CH_4, valeric acid, butyric acid, propionic acid and acetic acid. The kinetic parameters appear in the reaction rates of the model. They include 11 first-order constants, 7 Monod maximum growth rate and 7 saturation constants, 5 parameters concerning secondary substrate uptake or inhibition , 3 pairs of upper and lower pH-boundaries which appear

Journal homepage: http://www.sciencedirect.com/science/journal/00255564
Original file available at: http://www.sciencedirect.com/science/article/pii/S0025556417300780

in the pH-inhibition expressions and 1 liquid-gas mass transfer parameter. See Table 3 to 7 of Additional file 1 for an overview of all parameters.

In addition, there are several physico-chemical constants such as the acid-base dissociation constants and operational parameters, i.e., the liquid volume and the temperature. It is assumed that they are known and they have the default value listed in Table 7 and 8 in Appendix B [7].

Note, that in this work, more parameters are considered 'unknown' than typically the case in anaerobic digestion applications [8, 9]. The structural identifiability in these applications, however, can be deduced from the investigated more general situation. If a parameter is identifiable in the latter situation, it will also be identifiable when part of the set of parameters are assigned a numerical value.

Concerning the inputs, there are two types: the liquid inflow q_{liq} and the concentrations of the components in the inflow. Both the liquid inflow as the concentrations of the inflow are controlled. The numerical values used for the inputs are listed in Table 3 of Additional File 2 [7], except for $X_{\text{su,in}}$ which is changed from 0.0 to 0.1.

Concerning the output, it is for now assumed that all states in ADM1, both differential and algebraic, can be measured. This is in accordance with the underlying philosophy of this manuscript in finding an *upper limit* on the number of parameters that can be estimated and the corresponding quality of the estimates. For the practical identifiability analysis, the situation yielding the most informative option is chosen: both the dilution rate and the liquid flow rate are controlled and all states are measured.

Postprint version of paper published in Mathematical Biosciences 2017, vol. 288, p. 21-34.
The content is identical to the published paper, but without the final typesetting by the publisher.

Remark: In practice, liquid inflow, gaseous outflow and the dilution rate can be measured. Typically, liquid samples are taken daily, e.g. [10],[11], and some state values have to be deduced from measurements such as total COD and alkalinity. An interesting direction of research from a practitioner's point of view, could be to relax these assumptions and analyze the identifiability when only typical measurements of a digester are performed: biogas production and composition, pH, total and soluble chemical oxygen demand (COD), volatile fatty acids (VFA), total organic carbon, total inorganic carbon, Kjeldahl-Nitrogen, total inorganic nitrogen, total phosphorous, orthophosphate, total alkalinity, total solids, total volatile solids. Using the measurement-to-state mapping of Kleerebezem and Van Loosdrecht (2006) [12] or Zaher et al. (2009) [13] these measurements can be converted into the ADM1 states. A difficulty here is that direct measurement of the distinct microbial groups is not possible and including it requires estimation of the initial conditions of the different microbial groups. However, major developments in absolute quantification using quantitative polymerase chain reaction (qPCR) technique and fluorescence in situ hybridization (FISH) could create opportunities for measurement of these groups. See for instance Junicke et al. (2014) [14].

3. Mathematical methods

In the following section the concepts of structural and practical identifiability are introduced. In addition, several different methods to investigate these concepts are presented.

Journal homepage: http://www.sciencedirect.com/science/journal/00255564
Original file available at: http://www.sciencedirect.com/science/article/pii/S0025556417300780

Postprint version of paper published in Mathematical Biosciences 2017, vol. 288, p. 21-34.
The content is identical to the published paper, but without the final typesetting by the publisher.

3.1. Structural identifiability

Structural identifiability is defined following the definitions of [15]. Consider the dynamic model Σ of the form:

$$\Sigma = \begin{cases} \dfrac{\mathrm{d}\mathbf{x}}{\mathrm{d}t} = \mathbf{f}(\mathbf{x}, \mathbf{z}, \boldsymbol{\theta}, \mathbf{u}, t) & (1) \\ \mathbf{0} = \mathbf{g}(\mathbf{x}, \mathbf{z}, \boldsymbol{\theta}, \mathbf{u}, t) & (2) \\ \mathbf{y} = \mathbf{h}(\mathbf{x}, \mathbf{z}, \boldsymbol{\theta}, \mathbf{u}, t) & (3) \\ \mathbf{x}(0) = \mathbf{x}_0 & (4) \end{cases}$$

where $\mathbf{x} = [x_1, \ldots, x_{n_x}]^\intercal \in \mathbb{R}^{n_x}$ the differential state vector, $\mathbf{z} = [z_1, \ldots, z_{n_z}]^\intercal \in \mathbb{R}^{n_z}$ the algebraic state vector $\boldsymbol{\theta} = [\theta_1, \ldots, \theta_{n_\theta}]^\intercal \in \mathbb{R}^{n_\theta}$ the parameter vector, $\mathbf{u} = [u_1, \ldots, u_{n_u}]^\intercal \in \mathbb{R}^{n_u}$ the input vector, $\mathbf{y} = \left[y_1, \ldots, y_{n_y}\right]^\intercal \in \mathbb{R}^{n_y}$ the output vector, $t \in \mathbb{R}$ the time, $\mathbf{f}$ a $\mathbb{R}^{n_x}$ vector function, $\mathbf{g}$ a $\mathbb{R}^{n_z}$ vector function, $\mathbf{h}$ a $\mathbb{R}^{n_y}$ vector function expressing the output and $\mathbf{x_0} \in \mathbb{R}^{n_x}$ the initial state vector. It is assumed that for each system described by (1)-(4) there exists a set of true parameter values $\boldsymbol{\theta}^*$, which are considered to be unknown. Parameter estimation is then equivalent to finding parameter estimates $\hat{\boldsymbol{\theta}}$, that are as close as possible to the true parameter values $\boldsymbol{\theta}^*$.

Structural identifiability then relates to the question whether the true parameter values can be found from the input-output behavior, denoted with $M(\boldsymbol{\theta})$. In studying this relationship, the following idealized conditions are assumed: (i) the model is a perfect representation of the process, (ii) all data is noise-free and (iii) the input $\mathbf{u}$ can be chosen at will and (iv) the sampling is continuous. Formally, a parameter θ_{i_θ}, $i_\theta = \{1, \ldots, n_\theta\}$ is *structurally globally identifiable* if under these ideal conditions and for almost any true parameter value $\boldsymbol{\theta}^*$, the true parameter values can be uniquely estimated from input-

Journal homepage: http://www.sciencedirect.com/science/journal/00255564
Original file available at: http://www.sciencedirect.com/science/article/pii/S0025556417300780

Postprint version of paper published in Mathematical Biosciences 2017, vol. 288, p. 21-34.
The content is identical to the published paper, but without the final typesetting by the publisher.

output behavior M, i.e.,

$$M(\hat{\boldsymbol{\theta}}) = M(\boldsymbol{\theta}^*) \tag{5}$$

has the unique solution:

$$\hat{\theta}_{i_\theta} = \theta^*_{i_\theta}. \tag{6}$$

If all parameters of a model Σ are structurally globally identifiable, the model Σ is structurally globally identifiable. With 'for almost any $\boldsymbol{\theta}^*$' it is meant that structural identifiability may vary depending on the true parameter values. Often, this will only occur in singular points of the feasible parameter space. A parameter θ_{i_θ} is said to be *structurally locally identifiable* if (5) has a countable number of solutions (larger than 1) [16]. A model Σ is structurally locally identifiable if all its parameters are structurally locally identifiable. A parameter θ_{i_θ}, $i_\theta = \{1, \ldots, n_\theta\}$ is *structurally unidentifiable* or *non-identifiable* if under the previously presented idealized conditions and for almost any true parameter value $\boldsymbol{\theta}^*$, (5) has an infinite number of solutions. A model Σ is structurally unidentifiable if one of its parameters is structurally unidentifiable. If a model is unidentifiable, it is often possible to find structurally identifiable parameter combinations.

Different techniques exist to determine the structural identifiability of dynamic models, e.g., investigating the coefficients of the Taylor expansion [17] or investigating generators of the differential ideal described by the model equations [18]. In general, these techniques work well for small-scale systems, yielding a general result for the structural identifiability. However, due to the extensive symbolic calculations involved, they do not deal well with large systems, mainly due to memory considerations [19]. Therefore, the procedure followed in this work is based on the *probabilistic* algorithm of Sedoglavic [20], since it has been proven to be applicable for several large-scale models [21].

Journal homepage: http://www.sciencedirect.com/science/journal/00255564
Original file available at: http://www.sciencedirect.com/science/article/pii/S0025556417300780

The method elaborates on reformulating the identifiability problem as a problem of observability by considering the parameters as non-varying states and checking whether the initial conditions $[\mathbf{x}_0^\intercal, \boldsymbol{\theta}^\intercal]^\intercal$ are *locally algebraically observable*. Without going into the details, it can be shown [22, 23, 24] that local algebraic observability is a sufficient condition for structural local identifiability. Other names used in literature for local algebraic observability are *local distinguishability* [22], Hermann-Krener observability or *HK-observability* [25], *local generic observability* [23] and the Exact Arithmetic Rank (EAR) condition [26]. For brevity, this condition will be referred to as *observability* for the remainder of the text.

In what follows the method used to investigate the observability of $[\mathbf{x}_0^\intercal, \boldsymbol{\theta}^\intercal]^\intercal$ is briefly presented. This is followed by several modifications of the model and method needed in order to analyze the structural identifiability of ADM1. Finally, the procedure for identifying parameter combinations is explained.

3.1.1. Methodology

The probabilistic method applies to ODE systems, i.e., $n_z = 0$ for which $\mathbf{h}$ and $\mathbf{f}$ are rational functions in the parameters, states and inputs. It is assumed that the initial conditions $\mathbf{x}_0$ do not depend on the parameters. The initial conditions $\mathbf{x}_0$ and parameters $\boldsymbol{\theta}$ of the system Σ are observable if the rank of the following Jacobian evaluated for $[{\mathbf{x}_0}^{*\intercal}, \boldsymbol{\theta}^{*\intercal}]$ equals the total num-

ber of parameters and states, i.e., $n_x + n_\theta$:

$$\begin{bmatrix}
\frac{\partial h_1}{\partial x_1} & \dots & \frac{\partial h_1}{\partial x_{n_x}} & \frac{\partial h_1}{\partial \theta_1} & \dots & \frac{\partial h_1}{\partial \theta_{n_\theta}} \\
\vdots & \vdots & \vdots & \vdots & \vdots & \vdots \\
\frac{\partial h_{n_y}}{\partial x_1} & \dots & \frac{\partial h_{n_y}}{\partial x_{n_x}} & \frac{\partial h_{n_y}}{\partial \theta_1} & \dots & \frac{\partial h_{n_y}}{\partial \theta_{n_\theta}} \\
\frac{\partial \mathcal{L}_\mathbf{f} h_1}{\partial x_1} & \dots & \frac{\partial \mathcal{L}_\mathbf{f} h_1}{\partial x_{n_x}} & \frac{\partial \mathcal{L}_\mathbf{f} h_1}{\partial \theta_1} & \dots & \frac{\partial \mathcal{L}_\mathbf{f} h_1}{\partial \theta_{n_\theta}} \\
\vdots & \vdots & \vdots & \vdots & \vdots & \vdots \\
\frac{\partial \mathcal{L}_\mathbf{f} h_{n_y}}{\partial x_1} & \dots & \frac{\partial \mathcal{L}_\mathbf{f} h_{n_y}}{\partial x_{n_x}} & \frac{\partial \mathcal{L}_\mathbf{f} h_{n_y}}{\partial \theta_1} & \dots & \frac{\partial \mathcal{L}_\mathbf{f} h_{n_y}}{\partial \theta_{n_\theta}} \\
\vdots & \vdots & \vdots & \vdots & \vdots & \vdots \\
\frac{\partial \mathcal{L}_\mathbf{f}^{(n_x+n_\theta-1)} h_1}{\partial x_1} & \dots & \frac{\partial \mathcal{L}_\mathbf{f}^{(n_x+n_\theta-1)} h_1}{\partial x_{n_x}} & \frac{\partial \mathcal{L}_\mathbf{f}^{(n_x+n_\theta-1)} h_1}{\partial \theta_1} & \dots & \frac{\partial \mathcal{L}_\mathbf{f}^{(n_x++n_\theta-1)} h_1}{\partial \theta_{n_\theta}} \\
\vdots & \vdots & \vdots & \vdots & \vdots & \vdots \\
\frac{\partial \mathcal{L}_\mathbf{f}^{(n_x+n_\theta-1)} h_{n_y}}{\partial x_1} & \dots & \frac{\partial \mathcal{L}_\mathbf{f}^{(n_x+n_\theta-1)} h_{n_y}}{\partial x_{n_x}} & \frac{\partial \mathcal{L}_\mathbf{f}^{(n_x+n_\theta-1)} h_{n_y}}{\partial \theta_1} & \dots & \frac{\partial \mathcal{L}_\mathbf{f}^{(n_x+n_\theta-1)} h_{n_y}}{\partial \theta_{n_\theta}}
\end{bmatrix} \tag{7}$$

in which the Lie-derivative on the vector field $\mathbf{f}$ is introduced:

$$\mathcal{L}_\mathbf{f} := \frac{\partial}{\partial t} + \sum_{i=1}^{n_x} f_i \frac{\partial}{\partial x_i} + \sum_{j \in \mathbb{N}} \sum_{i=1}^{n_u} u_i^{(j+1)} \frac{\partial}{\partial u_i^{(j)}} \tag{8}$$

with:

$$\mathcal{L}_\mathbf{f}^{(j)} = \underbrace{\mathcal{L}_\mathbf{f} \mathcal{L}_\mathbf{f} \cdots \mathcal{L}_\mathbf{f}}_{j \text{ times}} \tag{9}$$

and $u_i^{(j)}$ the j-th derivative of u_i. To determine if a specific state/parameter is observable, it suffices to eliminate the corresponding column in (7) and see whether the rank of (7) changes.

A fully symbolic calculation of the Jacobian matrix is theoretically possible, but the equations quickly become huge. The algorithm of [20] calculates the elements of the matrix in a numerical way using rationals.

First, integers are assigned to the parameters and initial conditions. Next, the input is specified to a random integer coefficient power series. Using this input, the specified initial conditions and parameter values, a truncated power

Journal homepage: http://www.sciencedirect.com/science/journal/00255564
Original file available at: http://www.sciencedirect.com/science/article/pii/S0025556417300780

Postprint version of paper published in Mathematical Biosciences 2017, vol. 288, p. 21-34.
The content is identical to the published paper, but without the final typesetting by the publisher.

series of the states, as well as their sensitivity to the initial conditions and parameters, are calculated. Using these power series sensitivities, values for the Lie-derivatives are calculated [20]. To prevent calculations with large integer numbers, all calculations are done modulo a large prime number.

It should be remarked that the result is a *sufficient* condition for structural local identifiability. The method does not guarantee that a parameter is structurally globally identifiable. These caveats make that the method gives less general results than for instance other structural identifiability techniques, e.g. differential algebra [27].

3.1.2. Implementation aspects

Concerning the implementation of the method for the case of ADM1, three aspects are addressed:

1. The relations between the stoichiometric parameters to ascertain a correct COD balance in the system, have to be taken into account (Equations (10) to (12)). Therefore $f_{\mathrm{pr,xc}}$, $f_{\mathrm{h2,aa}}$ and $f_{\mathrm{h2,su}}$ by the expressions in terms of the other stoichiometric parameters.

$$1 = f_{\mathrm{xI,xc}} + f_{\mathrm{sI,xc}} + f_{\mathrm{ch,xc}} + f_{\mathrm{pr,xc}} + f_{\mathrm{li,xc}} \tag{10}$$

$$1 = f_{\mathrm{pro,su}} + f_{\mathrm{ac,su}} + f_{\mathrm{h2,su}} + f_{\mathrm{bu,su}} \tag{11}$$

$$1 = f_{\mathrm{va,aa}} + f_{\mathrm{bu,aa}} + f_{\mathrm{pro,aa}} + f_{\mathrm{ac,aa}} + f_{\mathrm{h2,aa}} \tag{12}$$

2. ADM1 consists of AEs which in principle cannot be analyzed with the adopted method. Therefore, instead of the 10 index-1 algebraic equa-

Journal homepage: http://www.sciencedirect.com/science/journal/00255564
Original file available at: http://www.sciencedirect.com/science/article/pii/S0025556417300780

Postprint version of paper published in Mathematical Biosciences 2017, vol. 288, p. 21-34.
The content is identical to the published paper, but without the final typesetting by the publisher.

tions, their underlying ODEs are used, i.e.,

$$\mathbf{0} = \mathbf{g}(\mathbf{x}, \boldsymbol{\theta}, \mathbf{z}, \mathbf{u}, t) \tag{13}$$

is converted into

$$\frac{\mathrm{d}\mathbf{z}}{\mathrm{d}t} = -\left(\frac{\partial \mathbf{g}}{\partial \mathbf{z}}\right)^{-1}\left(\frac{\partial \mathbf{g}}{\partial \mathbf{x}}\right)\left(\frac{\partial \mathbf{x}}{\partial t}\right) = -\left(\frac{\partial \mathbf{g}}{\partial \mathbf{z}}\right)^{-1}\left(\frac{\partial \mathbf{g}}{\partial \mathbf{x}}\right)\mathbf{f} = \mathbf{f}^{\dagger}(\mathbf{x}, \boldsymbol{\theta}, \mathbf{z}, \mathbf{u}, t). \tag{14}$$

The initial conditions of these differentiated algebraic states are determined by solving the algebraic equations, evaluated with the initial conditions of the differential states in Appendix B [7]. All values are converted to an exact rational representation.

3. The method is not able to deal with non-rational expressions although these appear in ADM1. Therefore the non-rational expressions for the pH-inhibition factors $I_{\mathrm{pH},i}$ are reformulated by introducing the parameters $k_{\mathrm{pH},i}$ and the auxiliary state ω_i, $i = \{1, \ldots, 3\}$:

$$I_{\mathrm{pH},i} = \frac{K_{\mathrm{pH},i}^{n_{\mathrm{pH},i}}}{{S_{\mathrm{h}^+}}^{n_{\mathrm{pH},i}} + K_{\mathrm{pH},i}^{n_{\mathrm{pH},i}}} \rightarrow I_{\mathrm{pH},i} = \frac{k_{\mathrm{pH},i}}{\omega_i + k_{\mathrm{pH},i}}, \quad k_{\mathrm{pH},i} = K_{\mathrm{pH},i}^{n_{\mathrm{pH},i}}, \quad \omega_i = S_{h^+}^{n_{\mathrm{pH},i}}. \tag{15}$$

The auxiliary state ω_i is added to the equations of the system:

$$\frac{\mathrm{d}\omega_i}{\mathrm{d}t} = n_{\mathrm{pH},i}\frac{\omega_i}{S_{h^+}} \cdot \frac{\mathrm{d}S_{h^+}}{\mathrm{d}t}. \tag{16}$$

Concerning the identifiability analysis, instead of the 3 pairs of upper and lower limits, the 3 pairs of parameters $n_{\mathrm{pH},i}$ and $k_{\mathrm{pH},i}$ are now investigated. However, it has to be stressed that in none of the scenarios, the 3 states ω_i are measured. Analogously as for the differentiated algebraic states, the initial conditions of the ω_i and the parameter values are

Journal homepage: http://www.sciencedirect.com/science/journal/00255564
Original file available at: http://www.sciencedirect.com/science/article/pii/S0025556417300780

Postprint version of paper published in Mathematical Biosciences 2017, vol. 288, p. 21-34.
The content is identical to the published paper, but without the final typesetting by the publisher.

numerically assigned to comply with (15).

Remark: The aforementioned adaptations impose implicit relations between the initial conditions and parameter values. which may lead to conflicting results. For instance, the method may assign ω_i and $k_{\mathrm{pH},i}$ to be non-observable while S_{h^+} and $n_{\mathrm{pH},i}$ are found to be observable. Clearly, from the observability of S_{h^+} and $n_{\mathrm{pH},i}$ and (15) ω_i is also observable. Using $k_{\mathrm{pH},i} = K_{\mathrm{pH},i}^{n_{\mathrm{pH},i}}$ and $\omega_i = S_{h^+}^{n_{\mathrm{pH},i}}$, it can then be deduced that $\mathrm{pH}_{\mathrm{UL},i} - \mathrm{pH}_{\mathrm{LL},i}$ is observable. The observability analysis is then repeated, with the observable parameters assigned a numerical value, in order to detect other observable parameters. The results presented are those after solving such *conflicting* results.

If the system is found to non-observable, one could try to find observable parameter combinations. Non-observability occurs when points on a direction in the parametric space render the input-output invariant, i.e., a so-called *symmetry*. It can be shown (see [22, 20]) that these symmetries can be calculated by calculating the kernel of the Jacobian matrix of which the columns associated with observable states/parameters are omitted.

In case the number of non-observable parameters/states is low, it is often much easier just to check whether the proposed parameter/state combinations involving non-observable parameters/states are observable, by considering their combination as a single parameter. These parameter combinations can often be discovered after close examination of the model equations. This approach is followed in this work.

Journal homepage: http://www.sciencedirect.com/science/journal/00255564
Original file available at: http://www.sciencedirect.com/science/article/pii/S0025556417300780

Postprint version of paper published in Mathematical Biosciences 2017, vol. 288, p. 21-34.
The content is identical to the published paper, but without the final typesetting by the publisher.

3.2. Practical identifiability

Structural identifiability is a necessary but not sufficient condition for finding univocal, accurate and precise parameter estimates. Experimental artefacts such as the nature and magnitude of the noise, the choice of applied inputs and measurements, the sampling rate and the form of the input may confound the solution, i.e., increase the uncertainty of the estimate. In this work, the practical identifiability analysis assesses the effect of the type of applied input and the magnitude of the noise levels.

The practical identifiability is assessed by performing parameter estimations on *in silico* data, i.e., data generated by simulations of the model.

In what follows a short description of parameter estimations and the procedure on how the quality of the estimates is assessed, are presented. This is followed by a description on how the experiments are designed.

3.2.1. Parameter estimation and quantification of uncertainty

The parameter estimations are based on the maximum likelihood criterion which searches the value of the parameter vector $\boldsymbol{\theta}$ that gives the highest likelihood to the observed data, considering the error distribution on the measurements. Under the assumptions of (*i*) no characterization error, (*ii*) independently normally distributed measurements noise and (*iii*) known and univariate variance, it can be proven that under these assumptions the maximization of the log-likelihood function (the logarithm of the likelihood function) corresponds to the minimization given in Equation (17) [15]. Note that for other distributions different maximum likelihood estimators would be ob-

Journal homepage: http://www.sciencedirect.com/science/journal/00255564
Original file available at: http://www.sciencedirect.com/science/article/pii/S0025556417300780

tained.

$$\min_{\boldsymbol{\theta}} \frac{1}{2} \sum_{i_y=1}^{n_y} \sum_{i=1}^{n_t} \frac{1}{\sigma_{i,i_y}^2} \left(y_{i_y}^{\mathrm{s}}(t_i) - y_{i_y}(t_i, \boldsymbol{\theta}) \right)^2 \tag{17}$$

with n_t the number of time points t_i, σ_{i,i_y}^2 the measurement variance on the measured values $y_{i_y}^{\mathrm{s}}(t_i)$ and $y_{i_y}(t_i, \boldsymbol{\theta})$ the predicted values.

In order to quantify the quality of the estimates, Monte Carlo resampling analyses are performed. The rationale is that a set of measurements $\mathbf{y}^{\mathrm{s}}$ is a particular realization of a *true* profile on which random noise is superimposed. The practical identifiability is then based on the estimates of the finite number of realizations of $\mathbf{y}^{\mathrm{s}}$. Practically, an *in silico* reference profile is generated using the true parameter value $\boldsymbol{\theta}^*$.

Note that the inverse of the Fisher Information Matrix (FIM) defined by the model and the experimental design could also be used as a measure for the quality of the estimates. However, the Fisher information matrix only provides a linear approximation, while Monte Carlo simulations provide a real measure of the actual distribution of the parameter estimates in a setting with measurement noise. Furthermore, the authors opted for Monte Carlo simulations over the Fisher information matrix computation as it involves only the repetitions of multiple parameter estimations while for the FIM also the sensitivities with respect to the parameters are required. For the first experiment, the FIM approach would result in 2900 (i.e. number of estimated parameters (71 parameters+29 initial conditions)×29 dynamic states) in addition to the original states.

The following statistics are used: the mean $\bar{\boldsymbol{\theta}}_{\mathrm{MC}}$, the standard deviation $\boldsymbol{\sigma}_{\mathrm{MC}}$

and the covariance matrix $\mathbf{P}_{\mathrm{MC}}$ of the n_{it} realizations:

$$\bar{\boldsymbol{\theta}}_{\mathrm{MC}} = \sum_{i=1}^{n_{\mathrm{it}}} \frac{1}{n_{\mathrm{it}}} \hat{\boldsymbol{\theta}}_i \tag{18}$$

$$\boldsymbol{\sigma}_{\mathrm{MC}} = \sqrt{\sum_{i=1}^{n_{\mathrm{it}}} \frac{1}{n_{\mathrm{it}}} \left(\hat{\boldsymbol{\theta}}_i - \bar{\boldsymbol{\theta}}_{\mathrm{MC}}\right)^2} \tag{19}$$

$$\mathbf{P}_{\mathrm{MC}} = \sum_{i=1}^{n_{\mathrm{it}}} (\hat{\boldsymbol{\theta}}_i - \bar{\boldsymbol{\theta}}_{\mathrm{MC}})(\hat{\boldsymbol{\theta}}_i - \bar{\boldsymbol{\theta}}_{\mathrm{MC}}). \tag{20}$$

These are then used to calculate the relative bias $\mathrm{Bias}_{\mathrm{rel},i_\theta}$ and the relative standard deviation $\sigma_{\mathrm{rel},i_\theta}$ for each parameter or initial condition i_θ:

$$\mathrm{Bias}_{\mathrm{rel},i_\theta} = \frac{\theta^*_{i_\theta} - \bar{\theta}_{\mathrm{MC},i_\theta}}{\theta^*_{i_\theta}} \tag{21}$$

$$\sigma_{\mathrm{rel},i_\theta} = \frac{\sigma_{\mathrm{MC},i_\theta}}{\theta^*_{i_\theta}}. \tag{22}$$

For large-scale models with many parameters, inspection of the different elements of the covariance matrix can be difficult to interpret. Alternatively, the matrix $\mathbf{P}'_{\mathrm{MC}}$ with elements $P'_{\mathrm{MC},i_\theta,j_\theta}$, $i_\theta = 1,\ldots,n_\theta + n_x$, $j_\theta = 1,\ldots,n_\theta + n_x$ which consists of roots of the absolute value of the normalized covariances, is calculated:

$$P'_{\mathrm{MC},i_\theta,j_\theta} = \sqrt{\left|\frac{P_{\mathrm{MC},i_\theta,j_\theta}}{\theta^*_{i_\theta}\theta^*_{j_\theta}}\right|}. \tag{23}$$

In this way, the diagonal elements of $\mathbf{P}'_{\mathrm{MC}}$ correspond with the absolute value of the relative standard deviations. Note that this measure looks very similar to the Pearson correlation coefficient ($R_{\mathrm{Pearson}} = \frac{P_{\mathrm{MC},i_\theta,j_\theta}}{\sigma_{i_\theta}\sigma_{j_\theta}}$, with σ_{i_θ} and σ_{j_θ} the standard deviations of the i_θ-th and j_θ-th parameter), a measure for the linear dependence between different variables. Since ADM1 is a highly

Journal homepage: http://www.sciencedirect.com/science/journal/00255564
Original file available at: http://www.sciencedirect.com/science/article/pii/S0025556417300780

nonlinear model and a nonlinear dependence between the parameters has to be covered, the authors considered normalized covariances to investigate the (nonlinear) dependence between different variables.

The number of realizations was chosen such that the addition of an extra realization changes the Monte Carlo estimates $\bar{\boldsymbol{\theta}}_{\mathrm{MC},i_\theta}$ and $\boldsymbol{\sigma}_{\mathrm{MC},i_\theta}$ less than 2%. This is mostly reached at around 100 iterations.

The overall quality of the Monte Carlo analysis is based on the average normalized root mean squared errors, R_1, the normalized average error between the predictions and the measurements and R_2, the normalized average error between the predictions and the true values. To assess the simulated measurements, the average normalized mean squared error between the measured and the true values R_3 is calculated:

$$R_1 = \sqrt{\frac{1}{n_{\mathrm{it}}}\frac{1}{n_t}\frac{1}{n_y}\sum_{i=1}^{n_{\mathrm{it}}}\sum_{i_t=1}^{n_t}\sum_{i_y=1}^{n_y}\frac{(y_{i_y,i_t}-y^{\mathrm{s}}_{i_y,i_t})^2}{\sigma^2_{i_y}}} \tag{24}$$

$$R_2 = \sqrt{\frac{1}{n_{\mathrm{it}}}\frac{1}{n_t}\frac{1}{n_y}\sum_{i=1}^{n_{\mathrm{it}}}\sum_{i_t=1}^{n_t}\sum_{i_y=1}^{n_y}\frac{(y_{i_y,i_t}-y^{*}_{i_y,i_t})^2}{\sigma^2_{i_y}}} \tag{25}$$

$$R_3 = \sqrt{\frac{1}{n_{\mathrm{it}}}\frac{1}{n_t}\frac{1}{n_y}\sum_{i=1}^{n_{\mathrm{it}}}\sum_{i_t=1}^{n_t}\sum_{i_y=1}^{n_y}\frac{(y^{\mathrm{s}}_{i_y,i_t}-y^{*}_{i_y,i_t})^2}{\sigma^2_{i_y}}} \tag{26}$$

3.2.2. Design of experiments

The experiment is designed in order to find the 'best' profile to estimate the parameters, concerning the choice of outputs, inputs and the applied input profile within the experimental boundaries, e.g., maximum concentrations,

duration of experiment. In that way, an upper limit concerning the practical identifiability is sought, i.e., to show that the parameter *can* be uniquely identified on experimental data. The design is made on heuristic rules and guidelines.

The heuristic rules focus on obtaining accurate estimates for the kinetic parameters. Primarily because these parameters appear in a non-linear way in the equations, and are thus, are the most challenging in the estimation.

The general guideline followed is that the concentrations of the states involved in the reaction kinetics, including inhibitory functions, are such that the complete range of different kinetic values are active.

More specifically, for Monod-type kinetics, shown in Equation (27), the adoption of this general guideline is logical.

$$\mu(S) = \frac{\mu_{max} S}{K_S + S} \tag{27}$$

For very small concentrations of substrate S, $\rho \approx \mu_{max}/K_S$. For high concentrations $\rho \approx \mu_{max}$. Thus, in order to estimate both parameters well, both extremes have to be reached approximately. Several sources [28, 29, 30] recommend $S < 0.1K_S$ and $S > K_S$ or $S > 2K_S$.

For the secondary substrate uptake and inhibition functions, the value of the associated uptake or inhibition constant will only have an effect if the secondary substrate concentrations are low and high respectively. For the practical identifiability of these functions, the requirement is that the secondary

substrate has low concentrations for the secondary substrate uptake functions or high concentrations for the secondary substrate inhibition functions.

Practically, the evaluation of an experiment concerning the practical identifiability of the kinetic parameters will be determined by plotting the range of concentrations of the states on the kinetic expressions.

3.3. Software

The structural identifiability tests are performed using the Maple `observabilityTest` tool of [20], with the aforementioned adjustments to take into account the implementation of AEs and non-rational expressions.

The parameter estimation problem is a dynamic optimization problem, which is solved in an in-house developed software called `Pomodoro` [31], [32]. This software can be downloaded from `http://cit.kuleuven.be/biotec/software/pomodoro` or `https://perswww.kuleuven.be/~u0093798/software.php` and the cited work [31], can be found on `http://www.student.kuleuven.be/~s0212066/pomodoro/`.

States and controls are discretized following an orthogonal collocation framework. In this approach, the value of the states are, like the parameters and the initial conditions, considered to be optimization variables [33]. The control variables are discretized as== piecewise constant. This usually results in a very large but structured non-linear programming (NLP) problem. The maximum number of allowed iterations was 2000 and the relative convergence tolerance was 1E−7.

To increase calculation speed and stability, all states and parameters in the

Postprint version of paper published in Mathematical Biosciences 2017, vol. 288, p. 21-34.
The content is identical to the published paper, but without the final typesetting by the publisher.

parameter estimation loop have been normalized. Additionally, a small value of 1E−10 is added to the denominator ($S_{\text{bu}} + S_{\text{va}}$) in Equation (8) and (9) of Appendix A to avoid division by zero due to numerical errors. To prevent too sudden changes of input, changes in input variables are 'spread' in a ramp over the course of 1 day (i.e., the derivative of the input with respect to time is constrained).

The assigned lower and upper bounds for the optimization variables are the following:

- parameters: $\boldsymbol{\theta}^*/4$ and $4 \times \boldsymbol{\theta}^*$, with an upper limit of 0.999 for the stoichiometric parameters
- states: $0.2 \times \min \mathbf{x}^*(t)$ and $1.8 \times \max \mathbf{x}^*(t), \quad t = 0, \ldots, n_t$
- initial conditions: $\mathbf{x}(0)^*/2$ and $\mathbf{x}(0)^* \times 2$

with $\boldsymbol{\theta}^*$ the true parameter value and $\mathbf{x}(t)^*$ the true profile, i.e., without noise. As initial guess, $\mathbf{x}(t)^*$ was given for the states and initial conditions and $\boldsymbol{\theta}^*$ for the parameters. Additionally, the relationships between the stoichiometric parameters of Equations (10) to (12) are given as extra constraints on the parameters. Finally, the differences between the lower and upper pH-inhibition levels, i.e., $\text{pH}_{\text{UL,aa}} - \text{pH}_{\text{LL,aa}}$, $\text{pH}_{\text{UL,h2}} - \text{pH}_{\text{LL,h2}}$ and $\text{pH}_{\text{UL,ac}} - \text{pH}_{\text{LL,ac}}$, are constrained to be less than 2.5.

All computations are done on a Intel® Core™ $i7 - 3770$, with 8 CPUs at 3.40 GHz each and 16 Gb of RAM.

Journal homepage: http://www.sciencedirect.com/science/journal/00255564
Original file available at: http://www.sciencedirect.com/science/article/pii/S0025556417300780

Postprint version of paper published in Mathematical Biosciences 2017, vol. 288, p. 21-34.
The content is identical to the published paper, but without the final typesetting by the publisher.

4. Results and discussion

4.1. Structural identifiability

The results of the observability analyses of the different scenarios are summarized in Table 1 and discussed next. Each observability analysis of ADM1 took between 35-45 minutes to calculate.

Table 1: The results of the parameters of ADM1 for the scenarios with inputs q_{liq} and/or $S_{x,in}$. Observability is equivalent to structurally locally identifiable.

Measurement	**Result**
All states	All parameters observable excl. C_{sI}, C_{xI}
Any state excl. S_{I}, X_{I}, $S_{\mathrm{cat^+}}$, $S_{\mathrm{an^-}}$	All parameters observable excl. $f_{\mathrm{sI,xc}}$, $f_{\mathrm{xI,xc}}$, C_{sI}, C_{xI}, $S_{\mathrm{I}}(0)$, $X_{\mathrm{I}}(0)$, $S_{\mathrm{cat^+}}(0)$, $S_{\mathrm{an^-}}(0)$
S_{I}	All parameters observable excl. C_{sI}, C_{xI}, $X_{\mathrm{I}}(0)$, $S_{\mathrm{cat^+}}(0)$, $S_{\mathrm{an^-}}(0)$
X_{I}	All parameters observable excl. C_{sI}, C_{xI}, $S_{\mathrm{I}}(0)$, $S_{\mathrm{cat^+}}(0)$, $S_{\mathrm{an^-}}(0)$
$S_{\mathrm{cat^+}}$	None observable excl. $S_{\mathrm{cat^+}}(0)$
$S_{\mathrm{an^-}}$	None observable excl. $S_{\mathrm{an^-}}(0)$

Concerning the observability results, it is found that in all six measurement cases in Table 1 , the non-observable parameters are related to the soluble and particulate inerts (i.e., the carbon compositions C_{sI} and C_{xI} and the stoichiometric yield of COD from particulate components to soluble $f_{\mathrm{sI,xc}}$ and particulate inerts $f_{\mathrm{xI,xc}}$). Since only the total free inorganic carbon is measured in the system, it is impossible to determine how much carbon is fixed in either the particulate or soluble inerts. Thus, the non-observability of the two parameters results from the structure of the model. In addition, if particulate or soluble inerts are not measured, it cannot be determined how much COD is fixed in each of the states, since they are both dead ends in the degradation pathway (**??**). This explains the non-observability of $f_{\mathrm{xI,xc}}$ and $f_{\mathrm{sI,xc}}$.

Journal homepage: http://www.sciencedirect.com/science/journal/00255564
Original file available at: http://www.sciencedirect.com/science/article/pii/S0025556417300780

Postprint version of paper published in Mathematical Biosciences 2017, vol. 288, p. 21-34.
The content is identical to the published paper, but without the final typesetting by the publisher.

In the cases in which the corresponding states are not measured, the initial concentrations of soluble inerts (S_{I}), particulate inerts (X_{I}), cations (S_{cat^+}) and anions (S_{an^-}) are not observable. Furthermore, if only cation or anion concentrations are measured, no parameters are observable due to the fact that these states *only* 'interact' with the other states in the ion-balance of Equation (87) of Appendix A. In this equation, only their difference $S_{\mathrm{cat}^+} - S_{\mathrm{an}^-}$ appears. Hence, without measuring the anions or cations separately, these states cannot be estimated separately.

4.1.1. Parameter combinations

Because the results in Table 1 show several non-observable parameters/states, it is of interest to look for observable parameter combinations that involve the non-observable parameters/states. Although mathematical techniques exist to identify these parameter combinations automatically, i.e., the calculation of Lie point symmetries (see [20]), the limited number of non-observable parameters/states enables to manually check parameter/state combinations such that there is no need to apply them in the case of ADM1. The proposed parameter combinations are listed in Table 2 and their observability is verified by substituting the mentioned non-observable parameters by the accompanying parameter combination and recalculating the observability of the system. The original model structure and the structure with the two first proposed parameter combinations are shown in Figure 2. Note that no combination of states exists to estimate $S_{\mathrm{I}}(0)$ or $X_{\mathrm{I}}(0)$ when these states are not measured.

Journal homepage: http://www.sciencedirect.com/science/journal/00255564
Original file available at: http://www.sciencedirect.com/science/article/pii/S0025556417300780

Postprint version of paper published in Mathematical Biosciences 2017, vol. 288, p. 21-34.
The content is identical to the published paper, but without the final typesetting by the publisher.

Table 2: Observable parameter combinations, based on the results of Table 1. Note that observability is equivalent to structurally locally identifiable.

Non-observable parameters/states	Observable parameter/state combination
C_{sI}, C_{xI}	$(f_{\mathrm{sI,xc}}C_{\mathrm{sI}} + f_{\mathrm{xI,xc}}C_{\mathrm{xI}})$
$f_{\mathrm{sI,xc}}$, $f_{\mathrm{xI,xc}}$	$(f_{\mathrm{sI,xc}} + f_{\mathrm{xI,xc}})$
S_{cat^+}, S_{an^-}	$(S_{\mathrm{an}^-} - S_{\mathrm{cat}^+})$

4.1.2. Structural aspects

The found results can be explained from the model structure.

Firstly, as already mentioned, the properties of the states that are dead ends in the model structure are not observable, unless they are measured directly. Secondly, the good structural identifiability properties can be attributed to the large number of interactions between the different states: forward *and* backward (i.e., for reversible reaction fluxes). These interactions are discussed in depth in Appendix C.

4.2. Practical identifiability

As discussed in the Methods section, the influence of the choice of the applied input and the magnitude of noise are investigated. The first aspect will be handled by investigation of a 'non-informative' and an 'informative' experiment. For each of the two experiments different noise levels are analyzed. Since it was found that the parameters C_{I} and C_{xI} are not structurally identifiable, the structurally identifiable parameter combination $C_{\mathrm{I}} = f_{sI,xc}C_{sI} + f_{xI,xc}C_{xI}$ is estimated instead. In addition, the role of the N-limiting parameter $K_{\mathrm{IN,lim}}$ is solely numerical and it will not be included in the parameter estimation procedure. Hence, 71 parameters and 29 initial conditions (i.e., corresponding to the 29 original dynamic states) that need to be estimated.

Journal homepage: http://www.sciencedirect.com/science/journal/00255564
Original file available at: http://www.sciencedirect.com/science/article/pii/S0025556417300780

Postprint version of paper published in Mathematical Biosciences 2017, vol. 288, p. 21-34.
The content is identical to the published paper, but without the final typesetting by the publisher.

The outline of these sections is as follows: First, the general experimental and process conditions are stated. This is followed by an overview of the designed experiments. Next, the results are presented and discussed. Finally, the results for ADM1 are generalized.

4.2.1. Experimental and process conditions

In order to work with a structurally (locally) identifiable model, the parameter C_I as defined in Table 2 is used instead of the composition parameters C_{sI} and C_{xI}.

The initial conditions are the obtained steady-states when the liquid inflow as described in Appendix B is applied with a volumetric flow rate $q_{\mathrm{liq}} = 85$ $\mathrm{m^3 d^{-1}}$. This relatively low rate induces lower biomass concentrations such that the system is easier to 'excite', i.e., induce a change in concentrations. This steady-state is calculated by simulation over a period of 1000 days.

The noise is normally distributed $\mathcal{N}(0, \sigma^2_{i_y})$ with a constant variance for each output y_{i_y}. The variance of the distribution equals the square of a set percentage of the initial conditions. Different percentage levels will be investigated.

Samples are taken 4 times per day, which is a high number for an anaerobic digestion system. Higher values are not considered due to the additional computational burden.

The parameter $K_{\mathrm{IN,lim}}$ associated with N as a limiting substrate is assigned its true parameter value of 1E−4, since this parameter is more of a numerical

nature than of a physical one [7].

For this experiment design, all state variables are considered to be measured. Admittedly, this is unrealistic but helps establishing an upper limit on what can be estimated for ADM1.

Concerning the applied input of the system, several boundaries are set. The applied controls are the liquid inflow q_{liq}, the input concentrations of cations $S_{\text{cat}^+,\text{in}}$ and $S_{\text{an}^-,\text{in}}$ representing added bases and acids, monosaccharides $S_{\text{su,in}}$ and amino acids $S_{\text{aa,in}}$. It will be seen that the control of just these variables, leads to satisfactory results concerning the specified design specifications. Based on the solubility of monosaccharides and amino acids, a maximum concentration for $S_{\text{su,in}}$ and $S_{\text{aa,in}}$ is determined. In that respect, the monosaccharides are assumed to be D-glucose with a maximum solubility at 35°C of 612 gCOD L^{-1} [34] and the amino acids are assumed to be a mixture of amino acids originating from the decomposition of casein with a maximum solubility of about 20 gCOD L^{-1}. Cations and anions are added in the form concentrated strong bases and acids, e.g., NaOH and HCl such as reported by [35]. There are no specific limitations on the total amount of added substrate.

4.2.2. Overview of performed experiments

Based on the discussed conditions and limitations, two experiments are designed. The first acts as a non-informative experiment, in which only the dilution rate (or hydraulic retention time) is changed.

Experiment 1.

The motivation for this first experiment is to get an idea on what is achiev-

able when performing only a simple control action. At the beginning of this experiment, the liquid inflow q_{liq} is doubled from 85 m^3d^{-1} to 170 m^3d^{-1} so that the dilution rate d increases from 0.025 d^{-1} to 0.05 d^{-1}. This dilution rate is maintained for 50 days so that the system evolves from the steady-state SS_1 to steady-state SS_2. This is depicted in Figure 3. Note that for this experiment 100 parameters are estimated (i.e., 71 parameters and 29 initial conditions).

Experiment 2.

In the second experiment, the heuristic guidelines discussed in Section 3.2.2 are applied. In order to activate the full spectrum of the kinetic expressions, a second experiment is proposed in which a change in liquid inflow is combined with the addition of extra intermediate components in the liquid feed while taking into account the previously considered experimental limitations. To prevent the extra inflow of intermediate components to be directly consumed by the available biomass and leading to accompanying biomass growth, the reaction rates are kept low by reducing the pH to 4 by adding acid in the form of anions (S_{an^-}). At this pH, the substrate uptake rates are practically zero. The concentration of monosaccharides and amino acids are then raised, taking into consideration the limits as determined in Section 4.2.1. This is maintained for 10 days. Afterwards, the pH is then gradually raised to the starting point by adding bases in the form of cations (S_{cat^+}), as well as the liquid inflow q_{liq} which is changed from 85 m^3d^{-1} to 170 m^3d^{-1} after 25 days. The applied input profiles for $S_{\text{su,in}}$, $S_{\text{aa,in}}$, q_{liq} and the desired pH profile are shown in Figure 4. Note that for this experiment 98 parameters are estimated (i.e., 71 parameters and 27 initial conditions).

For both experiments, four different noise levels are imposed. The standard

deviations of the Gaussian noise are 5%, 10%, 15% and 25% of the initial values listed in Table 2 of Appendix B.

A successful parameter estimation took between 5 and 20 minutes.

Several numerical issues did arise during the implementation of this specific experiment. This concerns the tracking of the desired pH-profile and the concentrations of inorganic carbon and hydrogen. Following modifications have been applied to the model to address these issues:

1. To enable the desired pH-profile, the concentration profiles of $S_{\mathrm{an}^-,\mathrm{in}}$ - $S_{\mathrm{cat}^+,\mathrm{in}}$ depicted in Figure 5 has to be applied. Since the required changes in this profile are too sudden to apply the desired pH-profile in a piecewise fashion with time step of 0.25 d, the pH-profile $\mathrm{pH}(t)$ itself is enforced in the model. Furthermore, the algebraic equation concerning the ion balance in Equation (87) of Appendix A has been changed to:

$$0 = 100 \cdot [S_{\mathrm{h}^+}(t) - 10^{-\mathrm{pH}(t)}]. \tag{28}$$

   The factor 100 is inserted for a better tracking. Conceptually, this kind of alterations can be thought of as the introduction of a *perfect* controller, which instantaneously feeds the acids and bases to the system, according to Figure 5. Note that due to this tracking, the states S_{an^-} and S_{cat^+} become irrelevant and are removed from the equations.

2. A limiting substrate inhibition for H_2 (S_{h2}) and inorganic carbon (S_{IC}) are included to prevent negative concentrations for S_{h2} and S_{IC}. Note that such functions were already included for inorganic nitrogen S_{IN} in

the form of $K_{\mathrm{IN,lim}}$. The used inhibition functions are the following:

$$I_{\mathrm{IC,lim}} = \frac{S_{\mathrm{IC}}}{S_{\mathrm{IC}} + K_{\mathrm{IC,lim}}} \tag{29}$$

$$I_{\mathrm{h2,lim}} = \frac{S_{\mathrm{h2}}}{S_{\mathrm{h2}} + K_{\mathrm{h2,lim}}} \tag{30}$$

with $K_{\mathrm{h2,lim}} = 10^{-5}$ and $K_{\mathrm{h2,lim}} = 10^{-8}$. These factors are added to the S_{h2} and S_{IC} consuming reactions. These are the uptake of lipids S_{li} in ρ_4, the uptake of valeric acid Sv_{va} in ρ_8, the uptake of butyric acid S_{bu} in ρ_9 and the uptake of hydrogen S_{h2} for S_{IC}. This is also the single S_{h2} consuming reaction. The inclusion of these inhibition factors has no effect on the state profiles for experiment 1.

The majority of the resulting state profiles are depicted, together with a more in-depth discussion in Appendix D. The resulting state profiles are plotted on the kinetic expressions in Figure 6. It is clear that for all kinetic expressions, the values of the states are spread out over the entire spectrum. Importantly, for the Monod type kinetics, the concentrations lie both above and below the reference concentration of the saturation constant, which corresponds with a rate of $\mu_{\mathrm{max}}/2$.

Parameter estimation results

In this section the parameter estimation results for the two experiments at the 4 noise levels are presented and discussed. A Monte Carlo parameter estimate will be labeled 'good', 'mediocre' or 'bad' when its relative bias or standard deviation, as defined in Equation (21) and (22) is below 5%, between 5% and

572 25% and above 25%, respectively.

573 *Experiment 1.*

574 The performance of the Monte Carlo analysis for the 4 different noise levels,
575 i.e., 5%, 10%, 15% and 25% is presented in Table 3 with the statistics defined
576 in Equations (24) to (25). Since $R_1 \approx 1$, the error between the measurement
577 and the predictions is almost equivalent to measurement error. The error be-
578 tween the true and predicted values are about 10 %, which is acceptable to
579 good.

Table 3: Performance of the Monte Carlo analysis for experiment 1.

Noise	R_1	R_2	R_3
5%	0.9945	0.1002	0.9996
10%	0.9878	0.0848	0.9926
15%	0.9895	0.0841	0.9937
25%	0.9901	0.0902	0.9929

580 The parameter estimation results are listed in Table 1 and 2 of Appendix E in
581 which the bias and the observed standard deviation are reported. Generally
582 speaking, the results are rather poor, and as expected, the parameter esti-
583 mates become worse with increasing measurement noise.

584 In order to asses the independence of the parameter estimates, the 'relative
585 covariance' $\mathbf{P}'_{\mathrm{MC}}$ as defined Equation (23) is constructed. For brevity, only the
586 5% noise level case is calculated, depicted in Figure 7. There are 2720 pairs
587 with no or weak interdependence (less than 5 %), 1746 pairs with moderate
588 interdependence (between 5 and 25%)and 484 pairs of strongly related (more
589 than 25%) parameter estimates in the upper triangle of the matrix. This does
590 not include the diagonal elements of the matrix which represent absolute val-
591 ues of the single parameter relative standard deviations. The lower triangle is
592 the mirror image of the upper triangle.

Postprint version of paper published in Mathematical Biosciences 2017, vol. 288, p. 21-34.
The content is identical to the published paper, but without the final typesetting by the publisher.

There are several trends that can be observed. First, there is generally a considerable interdependence between the parameters. Also, the parameters that were found to have large relative standard deviations, are also the ones that have strong relations with others. In Figure 7 it can be seen that if a row or column has dark marker on the diagonal, it is very likely to have another dark or gray marker on its row or column.

There are two blocks of parameters with little interdependence to other parameters. This can be seen on the figure as columns or rows with only a rather limited amount of gray markers. These are the first order kinetic parameters (36.-40.) and the initial conditions (72.-100.). Additionally, there are several blocks of parameters that generally have intermediate interdependence with other parameters. These are the pH-inhibition levels (66.-71.), the LCFA from lipids yield $f_{\mathrm{fa,li}}$ (1.) and the biomass yield coefficients (2.-8.).

The rest of the parameter estimates generally show substantial interdependence, although several big blocks of particularly strong interdependence can be observed. These consist of the relations between the kinetic parameters concerning S_{su}, S_{aa}, S_{pro} S_{fa}, S_{bu}, S_{va} S_{h2}, S_{ac} (41.-58.) , the associated stoichiometric parameters (14.-22.) and all composition parameters. Exceptions are the saturation constant for the acetic acid degradation $K_{\mathrm{S,ac}}$ (55.) and the carbon content of the inerts C_I (28.). In Appendix E, these results are explained from the structure and the equations.

In conclusion, this simple experiment showed several problems concerning the practical identifiability of the parameters of ADM1. Because of the rather limited spread of the states on the kinetic expressions, most kinetic parameters could not be estimated properly. Moreover, many of the parameter estimates

Journal homepage: http://www.sciencedirect.com/science/journal/00255564
Original file available at: http://www.sciencedirect.com/science/article/pii/S0025556417300780

show significant interdependence between each other. Nevertheless, for this simple experiment, adequate results were obtained for the disintegration kinetics, the hydrolysis kinetics, the liquid-gas mass transfer constant and the initial conditions of the states. Also, the saturation constant for acetate uptake is reasonably well estimated. It is safe to say that, if these parameters can be estimated in such a non-exciting experiment as Experiment 1, they can be considered practically identifiable.

Experiment 2.

The performance of the Monte Carlo analysis for the 4 different noise levels, i.e., 5%, 10%, 15% and 25% is reported in Table 4. The successful parameter estimations took about 25-45 minutes to solve. The time needed in unsuccessful parameter estimation varied between about 5-45 minutes.

Table 4: Performance of the Monte Carlo analysis for experiment 2.

Noise	R_1	R_2	R_3
5%	4.2813	4.2507	0.9939
10%	6.3492	6.1943	0.9920
15%	5.1050	4.8934	0.9932
25%	4.8305	5.0734	0.9923

Because $R_3 \approx 1$, the data on which the Monte Carlo analysis was performed, is assumed to be compliant with the assumptions concerning random sampling. Generally speaking the number of failed parameter estimations is higher for Experiment 2 than for Experiment 1. Comparing R_1 and R_2 in Table 4 with R_1 and R_2 in Table 3 clearly shows that the quality of the estimates is much lower than for Experiment 1. The error is several factors larger than the measurement errors. A possible explanation for this error is a bias in the parameter estimations. To check if there is a bias in the parameter estimations, the average normalized mean error between the predictions and the samples

Postprint version of paper published in Mathematical Biosciences 2017, vol. 288, p. 21-34.
The content is identical to the published paper, but without the final typesetting by the publisher.

Noise level	S_1	S_2
5%	0.6028	0.6033
10%	0.5542	0.5542
15%	0.6002	0.5990
25%	0.4384	0.4374

Table 5: S_1 and S_2 of the Monte Carlo analysis for experiment 2.

(S_1) and the true values (S_2), introduced in Equation (31) and (32), were calculated. For an accurate parameter estimation, both S_1 and S_2 should be around zero. The results for the different noise levels are listed in Table 5

$$S_1 = \frac{1}{n_{\text{it}}}\frac{1}{n_t}\frac{1}{n_y}\sum_{i=1}^{n_{\text{it}}}\sum_{i_t=1}^{n_t}\sum_{i_y=1}^{n_y}\frac{(y_{i_y,i_t} - y^{\text{s}}_{i_y,i_t})}{\sigma_{i_y}} \tag{31}$$

$$S_2 = \frac{1}{n_{\text{it}}}\frac{1}{n_t}\frac{1}{n_y}\sum_{i=1}^{n_{\text{it}}}\sum_{i_t=1}^{n_t}\sum_{i_y=1}^{n_y}\frac{(y_{i_y,i_t} - y^{*}_{i_y,i_t})}{\sigma_{i_y}} \tag{32}$$

It is clear that there is a positive bias in the results: the prediction values are generally higher than the true values or measurements. This is due to the fact that the values of some states almost become zero. See for instance the profile of S_{nh3} in Figure 8. During the acidification of the system, the value drops from $4.5 \cdot 10^{-3}$ to about 10^{-6}. Since the noise is normally distributed with a standard deviation equal to about 5%-25% of $4.5 \cdot 10^{-3}$, negative measurement values are 'observed'. Hence, there could be Monte Carlo realizations with measurements such that the solution that maximizes the likelihood as defined in Equation (17), goes below zero. These solutions, however, are forbidden due to the imposed lower bounds. Therefore solutions will be selected that have only positive states and are, hence, positively biased in comparison to the measurements and the true values. It is believed that this parameter estimation behavior is also responsible for the large number of failed parameter estimates.

Journal homepage: http://www.sciencedirect.com/science/journal/00255564
Original file available at: http://www.sciencedirect.com/science/article/pii/S0025556417300780

Postprint version of paper published in Mathematical Biosciences 2017, vol. 288, p. 21-34.
The content is identical to the published paper, but without the final typesetting by the publisher.

This problem cannot be solved in straightforward way. Either the assumptions on the noise are changed by making them for instance proportional to the value of the state, or the biased estimates are used. The latter option is chosen since the former implies a change of the practical experimental conditions.

The parameter estimates results for the successful experiments are listed in Table 3 and 4 of Appendix E in which the bias and the observed standard deviation are reported. Note that because of the pH-control with cations $S_{\mathrm{cat}^+,\mathrm{in}}$ and anions $S_{\mathrm{an}^-,\mathrm{in}}$, the states S_{cat^+} and S_{an^-} are no longer included in the model. Thus, the initial conditions $S_{\mathrm{cat}^+}(0)$ and $S_{\mathrm{an}^-}(0)$ are no longer estimated. The total number of parameters and unknowns for this Experiment is thus 98. The results of Table 3 and 4 are discussed in detail in Appendix E.

In terms of relative parameter bias (cfr. Equation (21)) and parameter standard deviation (cfr. Equation (22)), (and considering the successful experiments) the results are generally better than for Experiment 1. For instance, for the case of 5% noise, there are 92 'good' entries, 69 'moderate' entries and 39 'bad' entries, i.e., the relative bias or standard deviation is lower than 5%, between 5% and 25% and higher than 25%, respectively. This is better than the 86 'good' entries, 42 'moderate' and 72 'bad' entries for Experiment 1.

It is apparent that the parameters associated with the states, i.e., the stoichiometric, composition, kinetic, and decay parameters, that were directly excited, i.e., S_{su} and S_{aa} are estimated well. This is in addition to the parameters that were already found to be practically identifiable in Experiment 1. The other parameters associated with the other states are also better estimated, with the exception for the parameters associated with the degradation of S_{fa} and

Journal homepage: http://www.sciencedirect.com/science/journal/00255564
Original file available at: http://www.sciencedirect.com/science/article/pii/S0025556417300780

S_{ac}. Especially for the latter, the estimates are very poor. Thus, the idea behind the heuristic design, i.e., a sufficiently large domain of state values, is not sufficient to guarantee practical identifiability for the all non-linear expressions. A clue to a better experiment design is the observation that the direct excitation of the states through the change of input, resulted in 'sharper' peaks in the concentration profile of S_{su} and S_{aa} than for the other states (see Figure 8).

To investigate the interdependence between the estimates, the normalized covariance matrix as defined in Equation (23) is calculated and depicted in Figure 9. Only the result for the 5% noise level is analyzed. Again, values below 5 % are considered to correspond with weak or no relation between the parameter, values between 5% and 25% correspond to a moderate relation and values higher than 25% indicate a strong relation between the parameters.

There are 2720 pairs with no or weak interdependence, 1901 pairs with moderate interdependence and 294 pairs of strongly related parameter estimates in the upper triangle of the matrix. This does not include the diagonal elements of the matrix which represent absolute values of the single parameter relative standard deviations. In comparison with the first experiment, there are less strong interdependencies. However, there a bit more moderate interdependencies.

Generally, the results of the covariance matrix correspond with what was concluded on the results of Tables 3 and 4 of Appendix E. In this experiment, in addition to the parameters that were already found to be practically identifiable in the first experiment, the parameters concerning the S_{aa} and S_{su} show little interdependency with other parameters.

In conclusion, this informative experiment showed that through the direct excitation of the mono-saccharides and amino acids, the associated degradation kinetic, stoichiometric and composition parameters are practically identifiable in the stated experimental conditions.

If the results of the two experiments are combined, it shows that at least the first-order kinetic parameters (36.-40.), the stoichiometric parameters associated with the degradation of lipids (1.), monosaccharides (14.-17.) and amino acids (18.-22.), the composition of amino acids and monosaccharides (29., 31., 33), two of the 3 pH-inhibition level pairs (66.-67., 70.-71.) and the saturation constant for acetic acid degradation (55.) are practically identifiable. This does not mean that the other parameters are *not* practically identifiable, just that they were not practically identifiable in the designed experiment. Based on the results described in this manuscript, there is still room for improvement in the design of the experiment. For instance, all states can directly be excited, rather than exciting a selected few and relying on the interconnectivity of the model to excite the other states indirectly.

Also, the results are specific for the considered set of true parameter values, the nature of the noise, the choice of available inputs and outputs and under the assumption that the anaerobic digestion system is in reality described by the ADM1. Nevertheless, they are indicative on what can be expected from a parameter estimation procedure on real data.

Postprint version of paper published in Mathematical Biosciences 2017, vol. 288, p. 21-34.
The content is identical to the published paper, but without the final typesetting by the publisher.

5. Conclusions

In this work, the structural and practical identifiability of the Anaerobic Digestion Model No. 1 is analyzed as an example of a large-scale non-linear biological network model, consisting of algebraic equations and non-rational expressions.

The authors have presented modifications to the model, in terms of parameter combinations of structurally nonidentifiable parameters to yield an as good as fully locally structurally identifiable model structure. The *probabilistic* algorithm of [20] has been applied to investigate the structural identifiability for different input and output scenarios.

Furthermore, the generally positive structural identifiability results can be explained from the large number of interconnections between the states in the network structure. This interconnectivity, however, is also observed in the parameter estimates, making uncorrelated parameter estimations in practice difficult. Structural non-identifiability occurs at structural dead-ends in the ADM1 network as the inerts and for the anions/cations which are only appearing in pairs in the equations.

The practical identifiability of the model is analyzed by solving repeatedly large-scale parameter estimation problems. Based on a non-informative and an informative experiment the practical identifiability of the ADM1 case study was analyzed. At least the following parameters were found to be practically identifiable: (*i*) the first-order kinetic parameters except the biomass decay constants, (*ii*) the stoichiometric parameters associated with the degradation of lipids, monosaccharides, and amino acids, (*iii*) the composition of amino

Journal homepage: http://www.sciencedirect.com/science/journal/00255564
Original file available at: http://www.sciencedirect.com/science/article/pii/S0025556417300780

acids and monosaccharides, (iv) two of the 3 pH-inhibition levels and (v) the saturation constant for acetic acid degradation.

Generally speaking it is found that it is better to directly excite the states by means of the input, than relying on the interactions of the biological network to indirectly excite the states of interest. Additionally, the case study shows a strong interconnectivity between the states. This interconnectivity is also observed in the covariances of the parameter estimates. Therefore, it is not recommended to estimate parameters as if the reactions are completely separated.

Acknowledgements

This work was supported by KU Leuven [PFV/10/002 Center-of-Excellence Optimization in Engineering (OPTEC), DT is supported by PDM grant 2015/134], Fonds Wetenschappelijk Onderzoek Vlaanderen [G.0930.13 and KAN2013 1.5.189.13] and the Belgian Science Policy Office (DYSCO) [IAP VII/19]. Our gratitude goes to Prof. A. Sedoglavic for the free use of the `observabilityTest` Maple tool.

References

[1] D. Batstone, J. Keller, I. Angelidaki, S. Kalyuzhnyi, S. Pavlostathis, A. Rozzi, W. Sanders, H. Siegrist, V. Vavilin, The IWA anaerobic digestion model No 1 (ADM1), Water Science and Technology 45 (10) (2002) 65–73.

[2] D. J. Batstone, J. Keller, I. Angelidaki, Anaerobic Digestion Model No. 1, IWA Publishing, 2002.

[3] F. Blumensaat, J. Keller, Modelling of two-stage anaerobic digestion using the IWA anaerobic digestion model no. 1 (ADM1), Water Research 39 (1) (2005) 171–183.

[4] S. Weinrich, M. Nelles, Critical comparison of different model structures for the applied simulation of the anaerobic digestion of agricultural energy crops, Bioresource Technology 178 (2015) 306 – 312.

[5] N. Kythreotou, G. Florides, S. A. Tassou, A review of simple to scientific models for anaerobic digestion, Renewable Energy 71 (2014) 701 – 714.

[6] C. Mendes, K. Esquerre, L. M. Queiroz, Application of anaerobic digestion model no. 1 for simulating anaerobic mesophilic sludge digestion, Waste Management 35 (2015) 89 – 95.

[7] C. Rosen, U. Jeppsson, Aspects on ADM1 implementation within the BSM2 framework, [Online]. Available: http://ftp.iea.lth.se/publications/Reports/LTH-IEA-7224.pdf (2006).

[8] K. Koch, M. Lübken, T. Gehring, M. Wichern, H. Horn, Biogas from grass silage–measurements and modeling with ADM1, Bioresource Technology 101 (21) (2010) 8158–8165.

[9] F. Mairet, O. Bernard, M. Ras, L. Lardon, J.-P. Steyer, Modeling anaerobic digestion of microalgae using ADM1, Bioresource Technology 102 (13) (2011) 6823–6829.

[10] I. Ntaikou, H. N. Gavala, G. Lyberatos, Application of a modified anaerobic digestion model 1 version for fermentative hydrogen production from

sweet sorghum extract by ruminococcus albus, International Journal of Hydrogen Energy 35 (8) (2010) 3423 – 3432.

[11] V. Razaviarani, I. D. Buchanan, Calibration of the anaerobic digestion model no. 1 (adm1) for steady-state anaerobic co-digestion of municipal wastewater sludge with restaurant grease trap waste, Chemical Engineering Journal 266 (2015) 91 – 99.

[12] R. Kleerebezem, M. Van Loosdrecht, Waste characterization for implementation in ADM1, Biotechnology and Bioengineering 54 (4) (2006) 167–174.

[13] U. Zaher, P. Buffiere, J.-P. Steyer, S. Chen, A procedure to estimate proximate analysis of mixed organic wastes, Water Environment Research 81 (2009) 407–415.

[14] H. Junicke, B. Abbas, J. Oentoro, M. van Loosdrecht, M. Kleerebezem, Absolute quantification of individual biomass concentrations in a methanogenic cocultre, AMB express 35 (4) (2014) 1–8.

[15] E. Walter, L. Pronzato, Identification of Parametric Models from Experimental Data, Springer Verlag, Heidelberg, 1997.

[16] K. Godfrey, J. DiStefano, Identifiability of model parameters, in: E. Walter (Ed.), Identifiability of Parametric Models, Pergamon Press, Oxford, 1987, pp. 1–20.

[17] H. Pohjanpalo, System identifiability based on the power series expansion of the output, Mathematical Biosciences 41 (1) (1978) 21–33.

[18] M. Saccomani, S. Audoly, L. D'Angio, Parameter identiability of nonlinear systems: the role of initial conditions, Automatica 39 (4) (2003) 619–632.

[19] O. Chiş, J. R. Banga, E. Balsa-Canto, GenSSI: a software toolbox for structural identifiability analysis of biological models, Bioinformatics 27 (18) (2011) 2610–2611.

[20] A. Sedoglavic, A probalistic algorithm to test local algebraic observability in polynomial time, Journal of Symbolic Computation 33 (2002) 735–755.

[21] J. Karlsson, M. Anguelova, M. Jirstrand, An efficient method for structural identifiability analysis of large dynamic systems, in: Procs of the 16th IFAC Symposium on System Identification, Brussels (Belgium), 2012, pp. 941–946.

[22] M. Anguelova, Observability and identifiabiltiy of nonlinear systems with applications in biology, Ph.D. thesis, Dept. Mathematical Science, Chalmers University of Technology and Göteborg University, Göteborg (2007).

[23] S. Diop, Y. Wang, Equivalence between algebraic observability and local generic observability, in: Proceedings of the 32nd Conference on Decision and Control, Vol. 3, San Antonio, TX (USA), 1993, pp. 2864 – 2865.

[24] R. Hermann, A. J. Krener, Nonlinear controllability and observability, IEEE Transactions on Automatic Control 22 (5) (1977) 728–740.

[25] E. Sontag, A concept of local observability, Systems and Control Letters 5 (1) (1984) 41–47.

[26] A. Raue, J. Karlsson, M. Saccomani, M. Jirstrand, T. J., Comparison of approaches for parameter identifiability analysis of biological systems, Bioinformatics 30 (10) (2014) 1140–1148.

[27] G. Bellu, M. P. Saccomani, S. Audoly, L. D'Angiò, DAISY: a new software tool to test global identifiability of biological and physiological sys-

tems, Computer methods and programs in biomedicine 88 (1) (2007) 52–61.

[28] C. D. Knightes, C. A. Peters, Statistical analysis of nonlinear parameter estimation for monod biodegradation kinetics using bivariate data, Biotechnology and bioengineering 69 (2) (2000) 160–170.

[29] T. G. Ellis, D. S. Barbeau, B. F. Smets, C. L. Grady Jr, Respirometric technique for determination of extant kinetic parameters describing biodegradation, Water Environment Research 68 (5) (1996) 917–926.

[30] A. Holmberg, On the practical identifiability of microbial growth models incorporating michaelis-menten type nonlinearities, Mathematical Biosciences 62 (1) (1982) 23–43.

[31] S. S. Bhonsale, D. Telen, D. Vercammen, M. Vallerio, J. Hufkens, P. Nimmegeers, F. Logist, J. Van Impe, Pomodoro - an open source toolkit for multiobject optimal control, and model based control and estimation, Preprint submitted to Expert Systems with Applications.

[32] S. Bhonsale, M. Vallerio, D. Telen, D. Vercammen, F. Logist, J. Van Impe, SolACE: An open source package for nolinear model predictive control and state estimation for (bio)chemical processes, in: Proceedings of the 26th European Symposium on Computer Aided Process Engineering. Portoroz, Slovenia., June 12th - 15th, 2016.

[33] L. T. Biegler, Nonlinear Programming: Concepts, Algorithms, and Applications to Chemical Processes, Society for Industrial and Applied Mathematics (Philadelphia, USA), 2010, Chapter 10: Simultaneous Methods for Dynamic Optimization.

[34] L. A. Alves, J. B. Almeida e Silva, M. Giulietti, Solubility of d-glucose in

water and ethanol/water mixtures, Journal of Chemical & Engineering Data 52 (6) (2007) 2166–2170.

[35] D. Strik, A. Domnanovich, P. Holubar, A pH-based control of ammonia in biogas during anaerobic digestion of artificial pig manure and maize silage, Process Biochemistry 41 (6) (2006) 1235–1238.

Postprint version of paper published in Mathematical Biosciences 2017, vol. 288, p. 21-34.
The content is identical to the published paper, but without the final typesetting by the publisher.

876 ## Figures

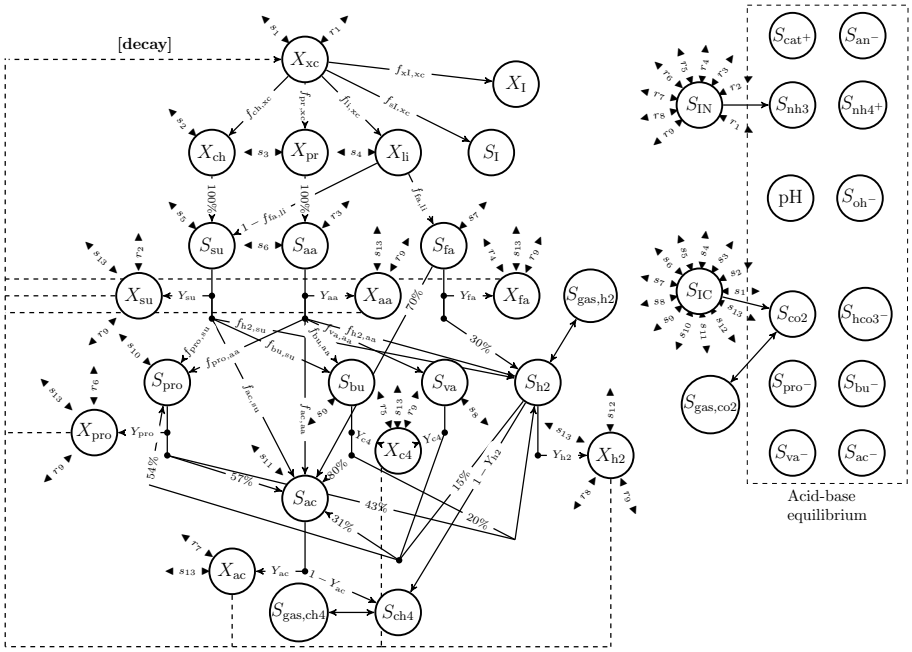

Figure 1: **Reaction network of ADM1.** The structure of ADM1 [1], on which the stoichiometric parameters $f_{i,j}$ and Y_i are indicated. Inorganic nitrogen S_{IC} and carbon S_{IN} are source/sink components that collect or make up excess or deficiencies of carbon and nitrogen, due to different N- or C-compositions of the different components in the system, indicated with r_i and s_i respectively. A separate system defines the acid-base equilibrium. The microbial metabolism on the substrates is inhibited by the pH-level, limiting inorganic nitrogen, ammonia and hydrogen.

Journal homepage: http://www.sciencedirect.com/science/journal/00255564
Original file available at: http://www.sciencedirect.com/science/article/pii/S0025556417300780

Postprint version of paper published in Mathematical Biosciences 2017, vol. 288, p. 21-34.
The content is identical to the published paper, but without the final typesetting by the publisher.

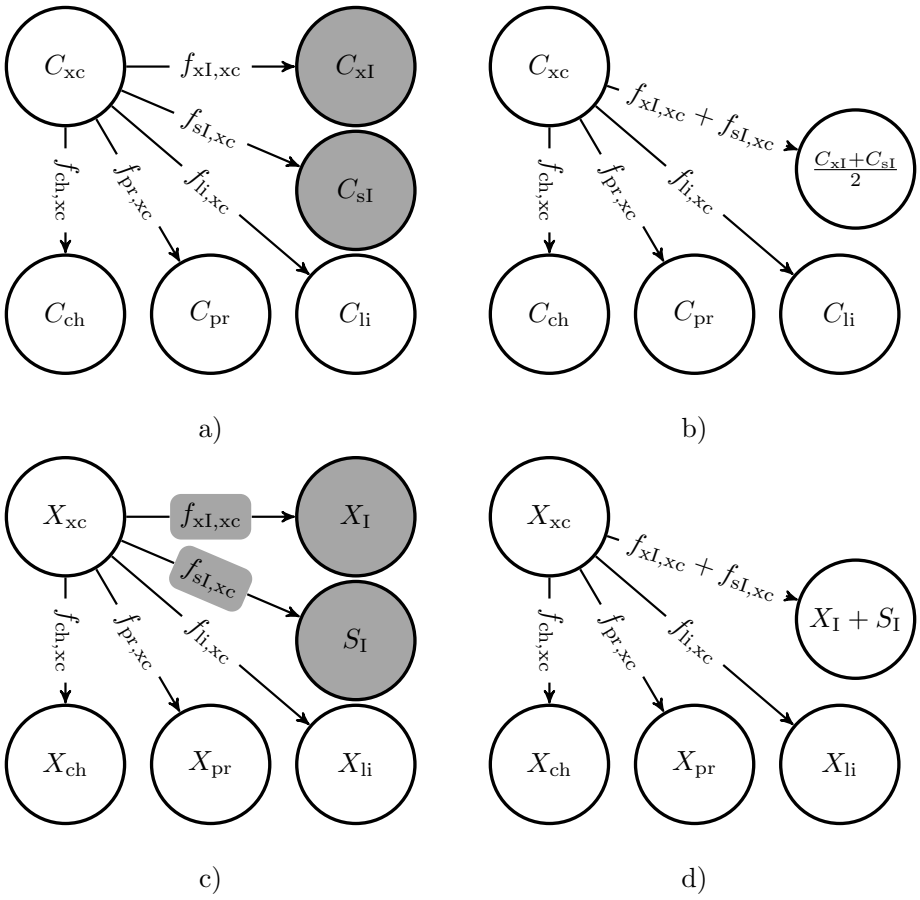

Figure 2: **Proposed parameter combinations for ADM1.** The distribution of carbon from the degradation of X_{xc} as described in *a*) the original equations of ADM1 and *b*) with the proposed parameter combination. The distribution of COD when none of the inerts are measured as described in as described in *c*) the original equations of ADM1 and *d*) with the proposed parameter combination. Dark gray indicates unidentifiability.

Journal homepage: http://www.sciencedirect.com/science/journal/00255564
Original file available at: http://www.sciencedirect.com/science/article/pii/S0025556417300780

Postprint version of paper published in Mathematical Biosciences 2017, vol. 288, p. 21-34.
The content is identical to the published paper, but without the final typesetting by the publisher.

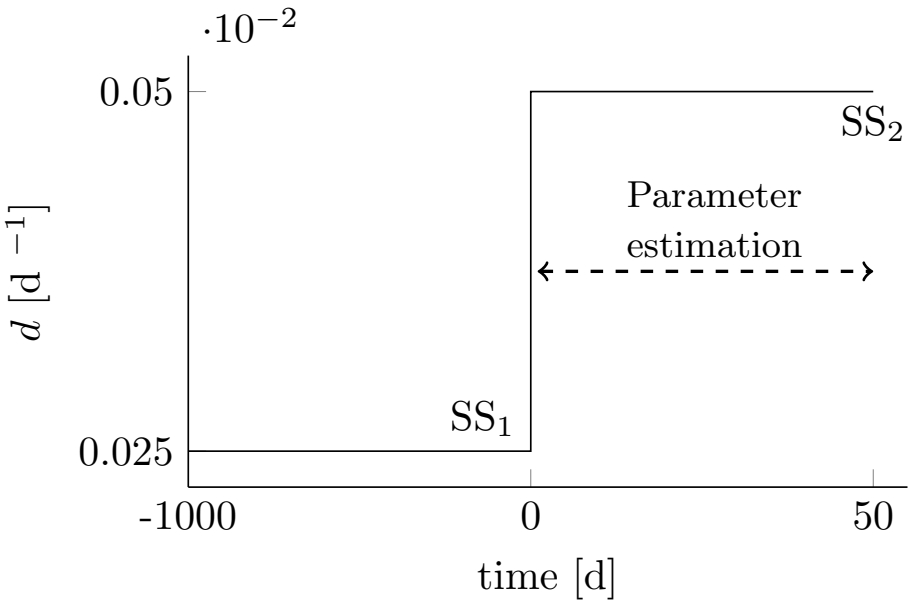

Figure 3: **Dilution rate d as a function of time for Experiment 1**. The profile starts from a steady-state (SS$_1$) obtained by applying a dilution rate of 0.025 days^{-1} for 1000 days. The dilution rate is then increased to 0.05 days^{-1} for 50 days. Eventually the system will reach a new steady-state SS$_2$. The profile considered for the parameter estimation is indicated by the double arrow.

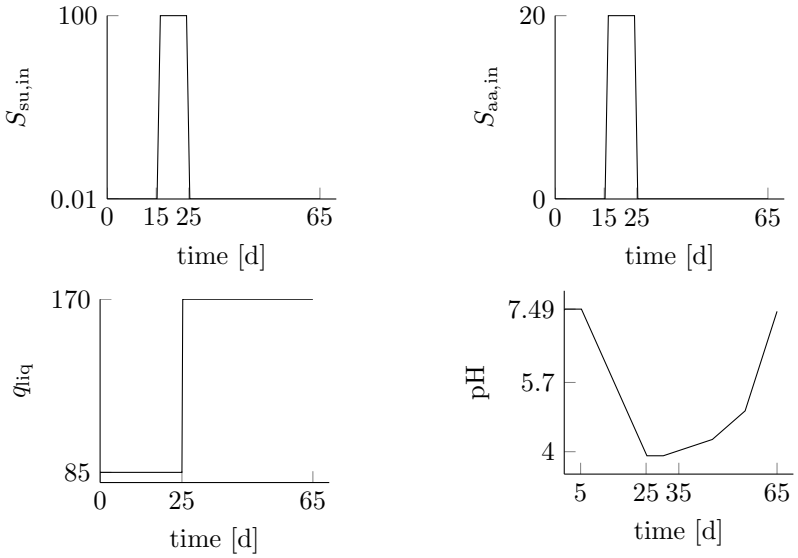

Figure 4: **Applied input for Experiment 2.** Input concentrations of $S_{\text{su,in}}$, $S_{\text{an,in}}$, q_{liq} and the desired pH profile of experiment 2.

Postprint version of paper published in Mathematical Biosciences 2017, vol. 288, p. 21-34.
The content is identical to the published paper, but without the final typesetting by the publisher.

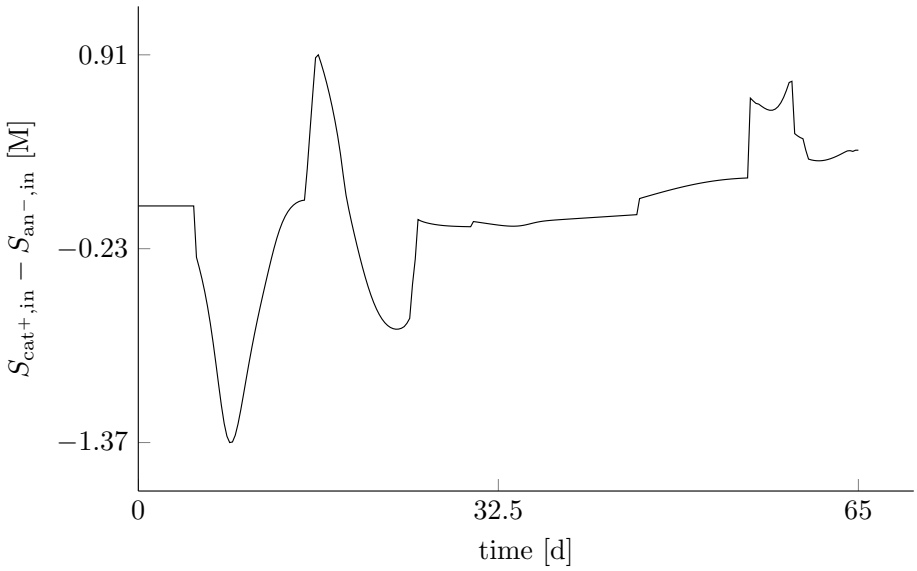

Figure 5: **The applied $S_{\mathrm{cat}^+,\mathrm{in}} - S_{\mathrm{an}^-,\mathrm{in}}$.** $S_{\mathrm{cat}^+,\mathrm{in}} - S_{\mathrm{an}^-,\mathrm{in}}$ profile needed to obtain the pH-profile of Figure 4.

Journal homepage: http://www.sciencedirect.com/science/journal/00255564
Original file available at: http://www.sciencedirect.com/science/article/pii/S0025556417300780

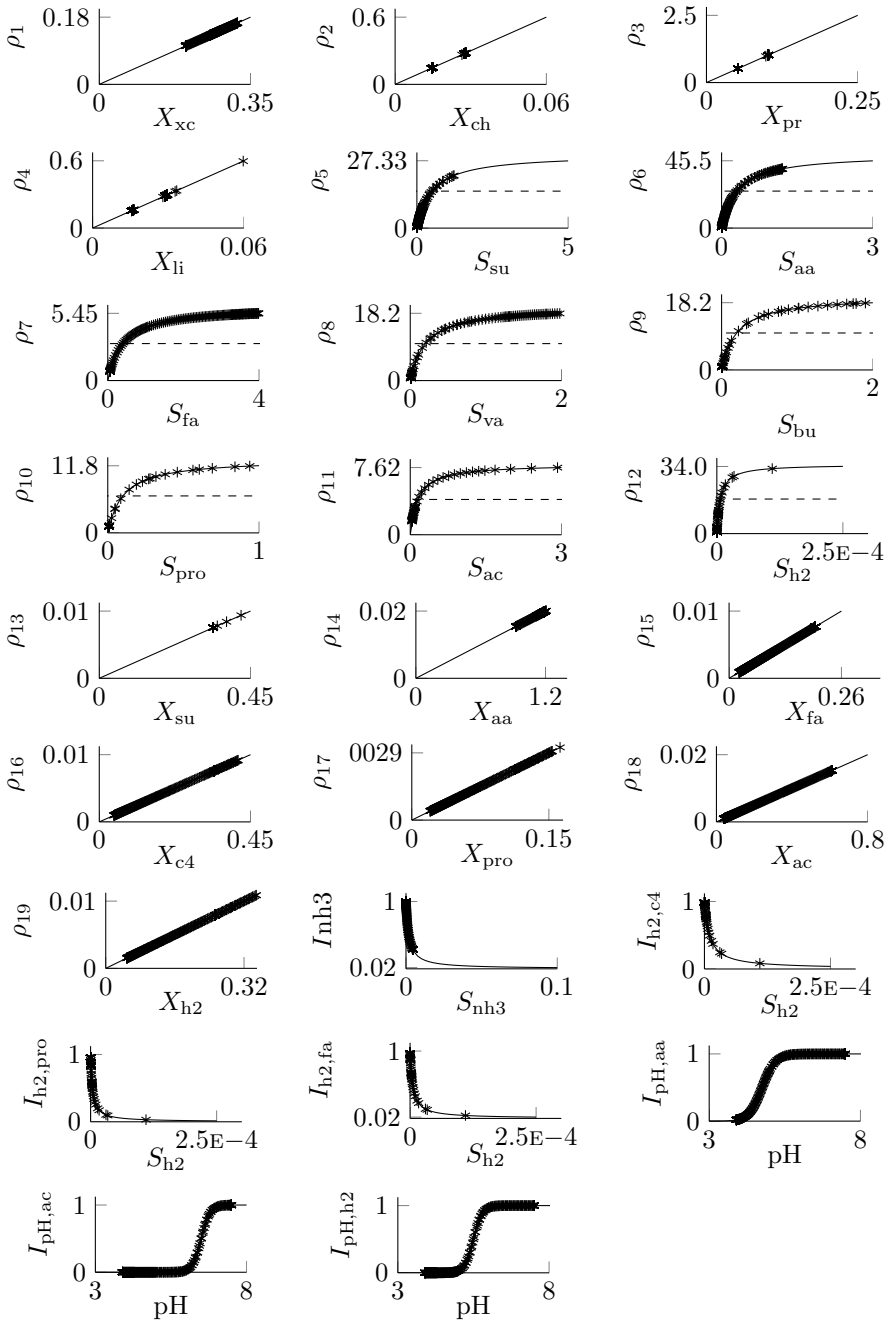

Figure 6: **Plot of the simulation results of Experiment 2 on the reaction rates of ADM1.** The value $\mu_{max}/2$ is indicated with a dashed line (- -).

Postprint version of paper published in Mathematical Biosciences 2017, vol. 288, p. 21-34.
The content is identical to the published paper, but without the final typesetting by the publisher.

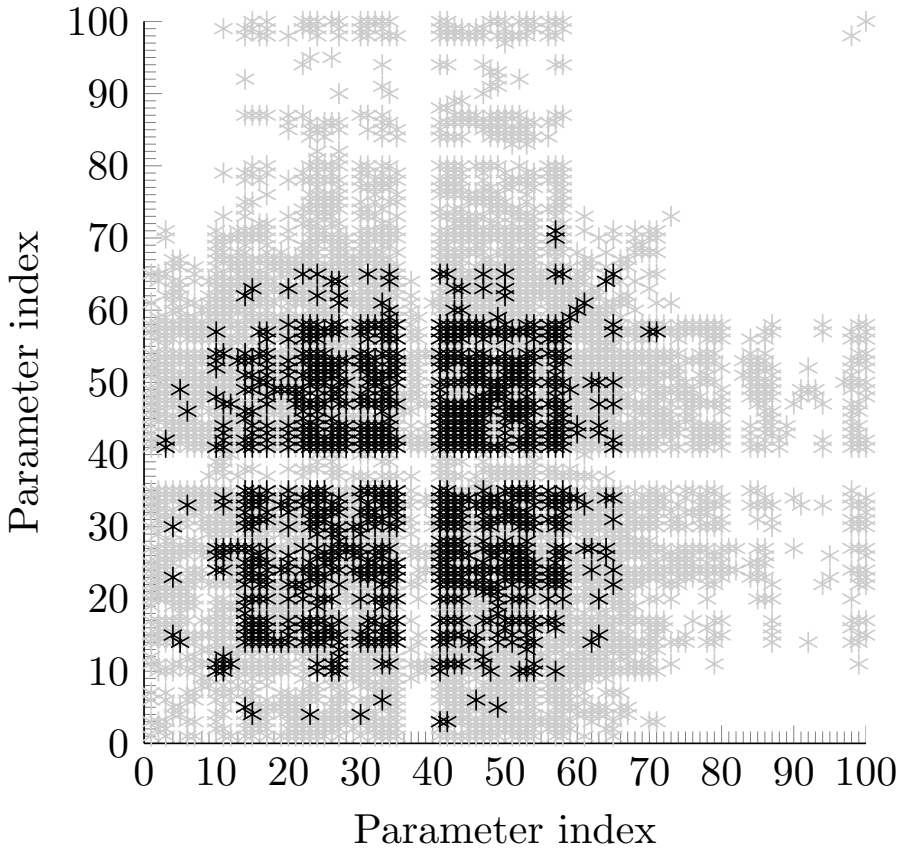

Figure 7: **Square root of the absolute relative covariances for the parameters estimates at a 5% noise level for Experiment 1.** The parameter numbering of Appendix E is used. A root of an absolute covariance higher than 25% is indicated in black. A root of an absolute covariance in between 5% and 25% is indicated in grey. Roots of absolute covariances lower than 5 % are not indicated.

Postprint version of paper published in Mathematical Biosciences 2017, vol. 288, p. 21-34.
The content is identical to the published paper, but without the final typesetting by the publisher.

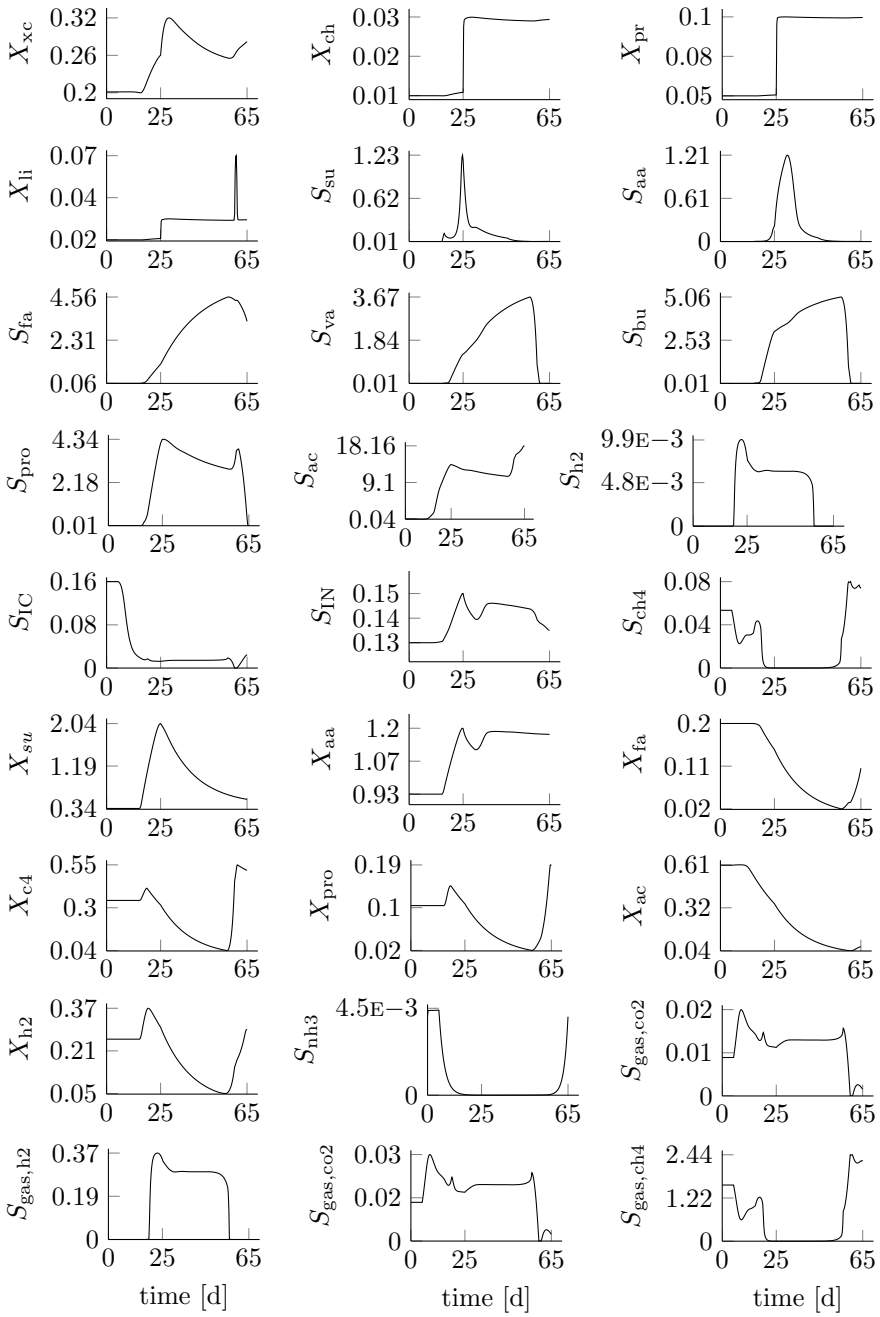

Figure 8: **Concentration profiles of most states in Experiment 2.**

Journal homepage: http://www.sciencedirect.com/science/journal/00255564
Original file available at: http://www.sciencedirect.com/science/article/pii/S0025556417300780

Postprint version of paper published in Mathematical Biosciences 2017, vol. 288, p. 21-34.
The content is identical to the published paper, but without the final typesetting by the publisher.

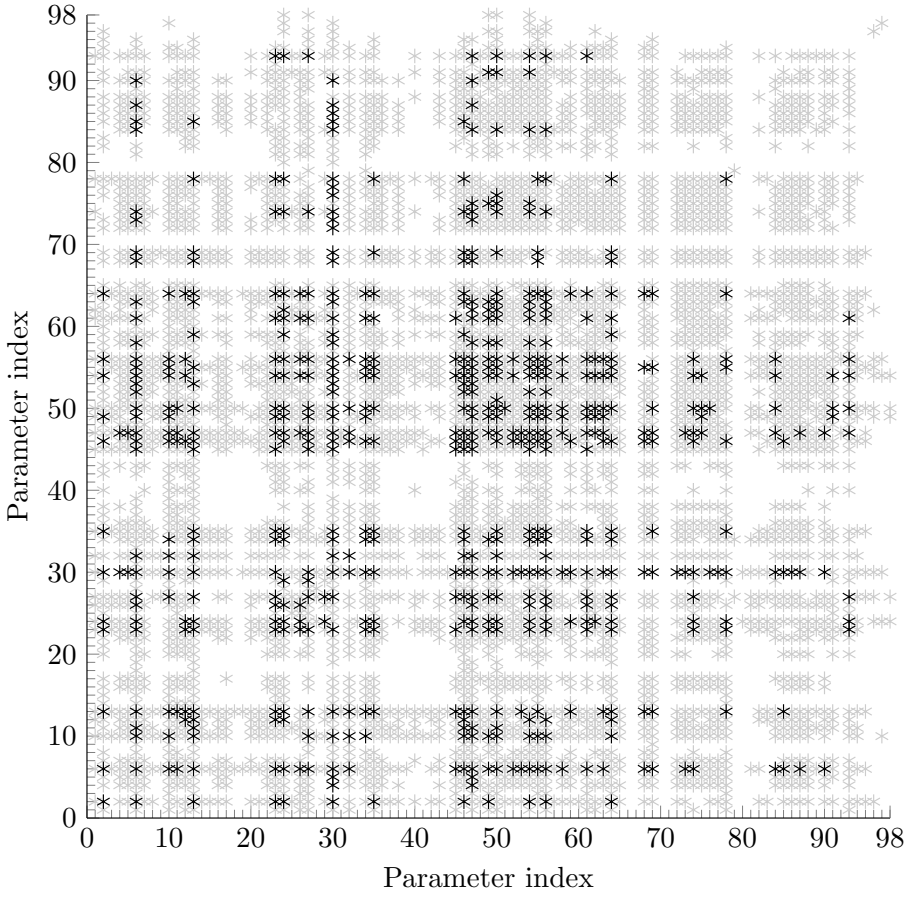

Figure 9: **Square root of the absolute relative covariances for the parameters estimates at a 5% noise level for Experiment 2.** The parameter numbering of Appendix E is used. A root of an absolute covariance higher than 25% is indicated in black. A root of an absolute covariance in between 5% and 25% is indicated in gray. Roots of absolute covariances lower than 5 % are not indicated.

Journal homepage: http://www.sciencedirect.com/science/journal/00255564
Original file available at: http://www.sciencedirect.com/science/article/pii/S0025556417300780

Postprint version of paper published in Mathematical Biosciences 2017, vol. 288, p. 21-34.
The content is identical to the published paper, but without the final typesetting by the publisher.

Appendix A. Description of ADM1

Appendix B. Numerical values of states and parameters values

Appendix C. Relations between ADM1 model structure and structural identifiability results

Appendix D. In-depth discussion of the state profiles in Experiment 2

Appendix E. Parameter estimation results

Journal homepage: http://www.sciencedirect.com/science/journal/00255564
Original file available at: http://www.sciencedirect.com/science/article/pii/S0025556417300780

Postprint version of paper published in Mathematical Biosciences 2017, vol. 288, p. 21-34.
The content is identical to the published paper, but without the final typesetting by the publisher.

Appendix A. Description of ADM1

In this appendix, the states, parameters, reactions and equations of ADM1 that are used in this article are listed. The state vector and parameter vector given by $\mathbf{x}$ and $\boldsymbol{\theta}$.

$$\mathbf{x} = \begin{Bmatrix} S_{\mathrm{su}} \\ S_{\mathrm{aa}} \\ S_{\mathrm{fa}} \\ S_{\mathrm{va}} \\ S_{\mathrm{bu}} \\ S_{\mathrm{pro}} \\ S_{\mathrm{ac}} \\ S_{\mathrm{h2}} \\ S_{\mathrm{ch4}} \\ S_{\mathrm{IC}} \\ S_{\mathrm{IN}} \\ S_{\mathrm{I}} \\ X_{\mathrm{xc}} \\ X_{\mathrm{ch}} \\ X_{\mathrm{pr}} \\ X_{\mathrm{li}} \\ X_{\mathrm{I}} \\ X_{\mathrm{su}} \\ X_{\mathrm{aa}} \\ X_{\mathrm{fa}} \\ X_{\mathrm{c4}} \\ X_{\mathrm{pro}} \\ X_{\mathrm{ac}} \\ X_{\mathrm{h2}} \\ S_{\mathrm{gas,h2}} \\ S_{\mathrm{gas,ch4}} \\ S_{\mathrm{gas,co2}} \\ S_{\mathrm{cat}^+} \\ S_{\mathrm{an}^-} \\ S_{\mathrm{va}^-} \\ S_{\mathrm{bu}^-} \\ S_{\mathrm{pro}^-} \\ S_{\mathrm{ac}^-} \\ S_{\mathrm{oh}^-} \\ S_{\mathrm{h}^+} \\ S_{\mathrm{hco3}^-} \\ S_{\mathrm{co2}} \\ S_{\mathrm{nh4}^+} \\ S_{\mathrm{nh3}} \end{Bmatrix} \tag{1}$$

Journal homepage: http://www.sciencedirect.com/science/journal/00255564
Original file available at: http://www.sciencedirect.com/science/article/pii/S0025556417300780

Postprint version of paper published in Mathematical Biosciences 2017, vol. 288, p. 21-34.
The content is identical to the published paper, but without the final typesetting by the publisher.

States

Table 1: Overview of the states.

State	Description	Unit
S_{su}	Soluble monosaccharides	kg COD m^{-3}
S_{aa}	Soluble amino acids	kg COD m^{-3}
S_{fa}	Soluble long chain fatty acids	kg COD m^{-3}
S_{va}	Soluble valeric acid	kg COD m^{-3}
S_{bu}	Soluble butyric acid	kg COD m^{-3}
S_{pro}	Soluble propionic acid	kg COD m^{-3}
S_{ac}	Soluble acetic acid	kg COD m^{-3}
S_{h2}	Soluble hydrogen	kg COD m^{-3}
S_{ch4}	Soluble methane	kg COD m^{-3}
S_{IC}	Soluble inorganic carbon	kmol C m^{-3}
S_{IN}	Soluble inorganic nitrogen	kmol N m^{-3}
S_{I}	Soluble inerts	kg COD m^{-3}
X_{xc}	Particulate composites	kg COD m^{-3}
X_{ch}	Particulate carbohydrates	kg COD m^{-3}
X_{pr}	Particulate proteins	kg COD m^{-3}
X_{li}	Particulate lipids	kg COD m^{-3}
X_{I}	Particulate inerts	kg COD m^{-3}
X_{su}	Monosaccharide degraders (biomass)	kg COD m^{-3}
X_{aa}	Amino acid degraders (biomass)	kg COD m^{-3}
X_{fa}	Fatty acid degraders (biomass)	kg COD m^{-3}
X_{c4}	Valeric and butyric acid degraders (biomass)	kg COD m^{-3}
X_{pro}	Propionic acid degraders (biomass)	kg COD m^{-3}
X_{ac}	Acetic acid degraders (biomass)	kg COD m^{-3}
X_{h2}	Hydrogen degraders (biomass)	kg COD m^{-3}
$S_{gas,h2}$	Gaseous hydrogen	kg COD m^{-3}
$S_{gas,ch4}$	Gaseous methane	kg COD m^{-3}
$S_{gas,co2}$	Gaseous carbon dioxide	kg COD m^{-3}
S_{cat^+}	Cations	kmol m^{-3}
S_{an^-}	Anions	kmol m^{-3}
S_{va^-}	Valerate	kg COD m^{-3}
S_{bu^-}	Butyrate	kg COD m^{-3}
S_{pro^-}	Propionate	kg COD m^{-3}
S_{ac^-}	Acetate	kg COD m^{-3}
S_{oh^-}	Hydroxide	kmol H^+ m^{-3}
S_{h^+}	Proton	kg COD m^{-3}
S_{hco3^-}	Bicarbonate	kmol C m^{-3}
S_{co2}	Soluble carbon dioxide	kmol C m^{-3}
S_{nh4^+}	Ammonium	kmol N m^{-3}
S_{nh3}	Ammonia	kmol N m^{-3}

Journal homepage: http://www.sciencedirect.com/science/journal/00255564
Original file available at: http://www.sciencedirect.com/science/article/pii/S0025556417300780

Postprint version of paper published in Mathematical Biosciences 2017, vol. 288, p. 21-34.
The content is identical to the published paper, but without the final typesetting by the publisher.

Reactions

Table 2: Reaction rates.

Symbol	Description	Symbol	Description
ρ_1	Disintegration of X_{xc}	ρ_{12}	Methanogenesis of S_{h2}
ρ_2	Hydrolysis of X_{ch}	ρ_{13}	Decay of X_{su}
ρ_3	Hydrolysis of X_{pr}	ρ_{14}	Decay of X_{aa}
ρ_4	Hydrolysis of X_{li}	ρ_{15}	Decay of X_{fa}
ρ_5	Acidogenesis of S_{su}	ρ_{16}	Decay of X_{c4}
ρ_6	Acidogenesis of S_{aa}	ρ_{17}	Decay of X_{pro}
ρ_7	Acidogenesis of S_{fa}	ρ_{18}	Decay of X_{ac}
ρ_8	Acetogenesis of S_{va}	ρ_{19}	Decay of X_{h2}
ρ_9	Acetogenesis of S_{bu}	$\rho_{T,8}$	liquid-gas transfer S_{h2}
ρ_{10}	Acetogenesis of S_{pro}	$\rho_{T,9}$	liquid-gas transfer S_{ch4}
ρ_{11}	Methanogenesis S_{ac}	$\rho_{T,10}$	liquid-gas transfer S_{co2}

Parameters

Table 3: Stoichiometric parameters.

Symbol	Description	Symbol	Description
$f_{\mathrm{sI,xc}}$	Yield of S_{I} on X_{xc}	$f_{\mathrm{pro,aa}}$	Yield of S_{pro} on S_{aa}
$f_{\mathrm{ch,xc}}$	Yield of X_{ch} on X_{xc}	$f_{\mathrm{va,aa}}$	Yield of S_{va} on S_{aa}
$f_{\mathrm{pr,xc}}$	Yield of X_{pr} on X_{xc}	$f_{\mathrm{ac,su}}$	Yield of S_{ac} on S_{su}
$f_{\mathrm{xI,xc}}$	Yield of X_{I} on X_{xc}	$f_{\mathrm{pro,su}}$	Yield of S_{pro} on S_{su}
$f_{\mathrm{li,xc}}$	Yield of X_{li} on X_{xc}	$f_{\mathrm{h2,su}}$	Yield of S_{h2} on S_{su}
$f_{\mathrm{ac,aa}}$	Yield of S_{ac} on S_{aa}	$f_{\mathrm{bu,su}}$	Yield of S_{bu} on S_{su}
$f_{\mathrm{bu,aa}}$	Yield of S_{bu} on S_{aa}	$f_{\mathrm{fa,li}}$	Yield of S_{fa} on X_{li}
$f_{\mathrm{h2,aa}}$	Yield of S_{h2} on S_{aa}		
Y_{su}	Yield of X_{su}	Y_{pro}	Yield of X_{pro}
Y_{aa}	Yield of X_{aa}	Y_{c4}	Yield of X_{c4}
Y_{fa}	Yield of X_{fa}	Y_{h2}	Yield of X_{h2}
Y_{ac}	Yield of X_{ac}		

Table 4: Composition parameters.

Symbol	Description	Symbol	Description
C_{aa}	C content S_{aa}	C_{pr}	C content X_{pr}
C_{ac}	C content S_{ac}	C_{pro}	C content S_{pro}
C_{bac}	C content X_{su}	C_{sI}	C content S_{I}
C_{bu}	C content S_{bu}	C_{su}	C content X_{ch}
C_{ch}	C content X_{ch}	C_{va}	C content S_{va}

Journal homepage: http://www.sciencedirect.com/science/journal/00255564
Original file available at: http://www.sciencedirect.com/science/article/pii/S0025556417300780

Postprint version of paper published in Mathematical Biosciences 2017, vol. 288, p. 21-34.
The content is identical to the published paper, but without the final typesetting by the publisher.

C_{ch4}	C content S_{ch4}	C_{xc}	C content X_{xc}
C_{fa}	C content S_{fa}	C_{xI}	C content X_I
C_{li}	C content X_{li}		
N_{aa}	N content S_{aa} and X_{pr}	N_I	N content S_I and X_I
N_{bac}	N content X_{su}, X_{aa}, X_{fa}, X_{ac}, X_{pro}, X_{c4} and X_{h2}	N_{xc}	N content X_{xc}

Table 5: Kinetic parameters.

Symbol	Description	Symbol	Description
k_{dis}	First-order ρ_1	$k_{dec,Xaa}$	First-order ρ_{14}
$k_{hyd,ch}$	First-order ρ_2	$k_{dec,Xfa}$	First-order ρ_{15}
$k_{hyd,pr}$	First-order ρ_3	$k_{dec,Xc4}$	First-order ρ_{16}
$k_{hyd,li}$	First-order ρ_4	$k_{dec,Xpro}$	First-order ρ_{17}
$k_{m,su}$	Maximum rate ρ_5	$k_{dec,Xac}$	First-order ρ_{18}
$K_{S,su}$	Saturation ρ_5	$k_{dec,Xh2}$	first-order ρ_{19}
$k_{m,aa}$	Maximum rate ρ_6	$K_{IN,lim}$	Limiting-N inhib. $\rho_5 - \rho_{12}$
$K_{S,aa}$	Saturation ρ_6	$K_{I,h2,fa}$	H_2-inhibition ρ_7
$k_{m,fa}$	Maximum rate ρ_8	$K_{I,h2,c4}$	H_2-inhibition ρ_8 and ρ_9
$K_{S,fa}$	Saturation ρ_8	$K_{I,h2,pro}$	H_2-inhibition ρ_{10}
$k_{m,c4}$	Maximum rate ρ_9 and ρ_{10}	$K_{I,nh3}$	NH_3-inhibition ρ_{11}
$K_{S,c4}$	Saturation ρ_9 and ρ_{10}	$pH_{LL,aa}$	Lower limit pH-inhib. $\rho_5 - \rho_{10}$
$k_{m,pro}$	Maximum rate ρ_{10}	$pH_{UL,aa}$	Upper limit pH-inhib. $\rho_5 - \rho_{10}$
$K_{S,pro}$	Saturation ρ_{10}	$pH_{LL,h2}$	Lower limit pH-inhib. ρ_{11}
$k_{m,ac}$	Maximum rate ρ_{11}	$pH_{UL,h2}$	Upper limit pH-inhib. ρ_{11}
$K_{S,ac}$	Saturation ρ_{11}	$pH_{LL,ac}$	Lower limit pH-inhib. ρ_{12}
$k_{m,h2}$	Maximum rate ρ_{12}	$pH_{UL,ac}$	Upper limit pH-inhib. ρ_{12}
$K_{S,h2}$	Saturation ρ_{12}	k_La	Liquid-gas mass-transfer
$k_{dec,Xsu}$	First-order ρ_{13}		

Table 6: Physico-chemical constants.

Symbol	Description	Symbol	Description
K_w	Dissociation constant water	$K_{H,co2}$	Henry constant S_{co2}
$K_{a,va}$	Dissociation constant S_{va}	$K_{H,h2}$	Henry constant S_{h2}
$K_{a,bu}$	Dissociation constant S_{bu}	$K_{H,ch4}$	Henry constant S_{ch4}
$K_{a,pro}$	Dissociation constant S_{pro}	R	Universal gas constant
$K_{a,ac}$	Dissociation constant S_{ac}	p_{h2o}	Vapor pressure water
$K_{a,co2}$	Dissociation constant S_{co2}	p_{atm}	Atmospheric pressure
$K_{a,IN}$	Dissociation constant S_{nh4+}		

Journal homepage: http://www.sciencedirect.com/science/journal/00255564
Original file available at: http://www.sciencedirect.com/science/article/pii/S0025556417300780

Postprint version of paper published in Mathematical Biosciences 2017, vol. 288, p. 21-34.
The content is identical to the published paper, but without the final typesetting by the publisher.

Table 7: Operating parameters.

Symbol	Description	Symbol	Description
T	Temperature	q_{in}	Liquid flow rate in digester
V_{liq}	Liquid volume	V_{gas}	Gaseous volume
S_{in}, X_{in}	Inflow of component S or X	k_p	Gas outflow resistance

Equations

From Equations (2) to (23), the reaction rates are given. The inhibition terms are given in Equations (24) to (31). The ODEs are given in Equations (35) to (78). The AEs are given in Equations (88) to (97).

The reaction rates ρ_i are the following:

$$\rho_1 = k_{\text{dis}} X_{\text{c}} \tag{2}$$
$$\rho_2 = k_{\text{hyd,ch}} X_{\text{ch}} \tag{3}$$
$$\rho_3 = k_{\text{hyd,pr}} X_{\text{pr}} \tag{4}$$
$$\rho_4 = k_{\text{hyd,li}} X_{\text{li}} \tag{5}$$
$$\rho_5 = k_{\text{m,su}} \frac{S_{\text{su}}}{K_{\text{S,su}} + S_{\text{su}}} X_{\text{su}} I_{\text{IN,lim}} I_{\text{pH,aa}} \tag{6}$$
$$\rho_6 = k_{\text{m,aa}} \frac{S_{\text{aa}}}{K_{\text{S,aa}} + S_{\text{aa}}} X_{\text{aa}} I_{\text{IN,lim}} I_{\text{pH,aa}} \tag{7}$$
$$\rho_7 = k_{\text{m,fa}} \frac{S_{\text{fa}}}{K_{\text{S,fa}} + S_{\text{fa}}} X_{\text{fa}} I_{\text{IN,lim}} I_{\text{pH,aa}} I_{\text{h2,fa}} \tag{8}$$
$$\rho_8 = k_{\text{m,c4}} \frac{S_{\text{va}}}{K_{\text{S,c4}} + S_{\text{va}}} X_{\text{c4}} \frac{S_{\text{va}}}{S_{\text{bu}} + S_{\text{va}}} I_{\text{IN,lim}} I_{\text{pH,aa}} I_{\text{h2,c4}} \tag{9}$$
$$\rho_9 = k_{\text{m,c4}} \frac{S_{\text{bu}}}{K_{\text{S,c4}} + S_{\text{bu}}} X_{\text{c4}} \frac{S_{\text{bu}}}{S_{\text{bu}} + S_{\text{va}}} I_{\text{pH,aa}} I_{\text{h2,c4}} \tag{10}$$
$$\rho_{10} = k_{\text{m,pro}} \frac{S_{\text{pro}}}{K_{\text{S,pro}} + S_{\text{pro}}} X_{\text{pro}} I_{\text{IN,lim}} I_{\text{pH,aa}} I_{\text{h2,pro}} \tag{11}$$
$$\rho_{11} = k_{\text{m,ac}} \frac{S_{\text{ac}}}{K_{\text{S,ac}} + S_{\text{ac}}} X_{\text{ac}} I_{\text{IN,lim}} I_{\text{pH,ac}} I_{\text{nh3}} \tag{12}$$
$$\rho_{12} = k_{\text{m,h2}} \frac{S_{\text{h2}}}{K_{\text{S,h2}} + S_{\text{h2}}} X_{\text{h2}} I_{\text{IN,lim}} I_{\text{pH,h2}} \tag{13}$$
$$\rho_{13} = k_{\text{dec,Xsu}} X_{\text{su}} \tag{14}$$
$$\rho_{14} = k_{\text{dec,Xaa}} X_{\text{aa}} \tag{15}$$
$$\rho_{15} = k_{\text{dec,Xfa}} X_{\text{fa}} \tag{16}$$
$$\rho_{16} = k_{\text{dec,Xc4}} X_{\text{c4}} \tag{17}$$
$$\rho_{17} = k_{\text{dec,Xpro}} X_{\text{pro}} \tag{18}$$
$$\rho_{18} = k_{\text{dec,Xac}} X_{\text{ac}} \tag{19}$$

Journal homepage: http://www.sciencedirect.com/science/journal/00255564
Original file available at: http://www.sciencedirect.com/science/article/pii/S0025556417300780

$$\rho_{19} = k_{\mathrm{dec,Xh2}} X_{\mathrm{h2}} \tag{20}$$
$$\rho_{\mathrm{T},8} = k_{\mathrm{L}} a(S_{\mathrm{h2}} - K_{\mathrm{H,h2}} RT S_{\mathrm{gas,h2}}) \tag{21}$$
$$\rho_{\mathrm{T},9} = k_{\mathrm{L}} a(S_{\mathrm{ch4}} - K_{\mathrm{H,ch4}} RT S_{\mathrm{gas,ch4}}) \tag{22}$$
$$\rho_{\mathrm{T},10} = k_{\mathrm{L}} a(S_{\mathrm{co2}} - K_{\mathrm{H,co2}} RT S_{\mathrm{Xgas,co2}}) \tag{23}$$

The inhibition terms are the following:

$$I_{\mathrm{h2,fa}} = \frac{K_{\mathrm{I,h2,fa}}}{K_{\mathrm{I,h2,fa}} + S_{\mathrm{h2}}} \tag{24}$$
$$I_{\mathrm{h2,c4}} = \frac{K_{\mathrm{I,h2,c4}}}{K_{\mathrm{I,h2,c4}} + S_{\mathrm{h2}}} \tag{25}$$
$$I_{\mathrm{h2,pro}} = \frac{K_{\mathrm{I,h2,pro}}}{K_{\mathrm{I,h2,pro}} + S_{\mathrm{h2}}} \tag{26}$$
$$I_{\mathrm{nh3}} = \frac{K_{\mathrm{I,nh3}}}{K_{\mathrm{I,nh3}} + S_{\mathrm{nh3}}} \tag{27}$$
$$I_{\mathrm{IN,lim}} = \frac{S_{\mathrm{IN}}}{S_{\mathrm{IN}} + K_{\mathrm{S,IN}}} \tag{28}$$
$$I_{\mathrm{pH,aa}} = \frac{K_{\mathrm{pH}}^{n_{\mathrm{aa}}}}{S_{\mathrm{h^+}}^{n_{\mathrm{aa}}} + K_{\mathrm{pH},aa}^{n_{\mathrm{aa}}}} \tag{29}$$
$$I_{\mathrm{pH,ac}} = \frac{K_{\mathrm{pH}}^{n_{\mathrm{ac}}}}{S_{\mathrm{h^+}}^{n_{\mathrm{ac}}} + K_{\mathrm{pH,aa}}^{n_{\mathrm{ac}}}} \tag{30}$$
$$I_{\mathrm{pH},h2} = \frac{K_{\mathrm{pH}}^{n_{\mathrm{h2}}}}{S_{\mathrm{h^+}}^{n_{\mathrm{h2}}} + K_{\mathrm{pH},h2}^{n_{\mathrm{h2}}}} \tag{31}$$

with:

$$K_{\mathrm{pH,aa}} = 10^{\frac{\mathrm{pH_{aa,LL}} + \mathrm{pH_{aa,UL}}}{2}}, \quad n_{\mathrm{pH,aa}} = \frac{3}{\mathrm{pH_{aa,UL}} - \mathrm{pH_{aa,LL}}} \tag{32}$$
$$K_{\mathrm{pH,ac}} = 10^{\frac{\mathrm{pH_{ac,LL}} + \mathrm{pH_{aa,UL}}}{2}}, \quad n_{\mathrm{pH,ac}} = \frac{3}{\mathrm{pH_{ac,UL}} - \mathrm{pH_{ac,LL}}} \tag{33}$$
$$K_{\mathrm{pH,h2}} = 10^{\frac{\mathrm{pH_{h2,LL}} + \mathrm{pH_{h2,UL}}}{2}}, \quad n_{\mathrm{pH,h2}} = \frac{3}{\mathrm{pH_{aa,UL}} - \mathrm{pH_{h2,LL}}} \tag{34}$$

The following differential and algebraic equations make up the model:

$$\frac{\mathrm{d}S_{\mathrm{su}}}{\mathrm{d}t} = \frac{q_{\mathrm{in}}}{V_{\mathrm{liq}}}(S_{\mathrm{su,in}} - S_{\mathrm{su}}) + \rho_2 + (1 - f_{\mathrm{fa,li}})\rho_4 - \rho_5 \tag{35}$$
$$\frac{\mathrm{d}S_{\mathrm{aa}}}{\mathrm{d}t} = \frac{q_{\mathrm{in}}}{V_{\mathrm{liq}}}(S_{\mathrm{aa},in} - S_{\mathrm{aa}}) + \rho_3 - \rho_6 \tag{36}$$
$$\frac{\mathrm{d}S_{\mathrm{fa}}}{\mathrm{d}t} = \frac{q_{\mathrm{in}}}{V_{\mathrm{liq}}}(S_{\mathrm{fa,in}} - S_{\mathrm{fa}}) + f_{\mathrm{fa,li}}\rho_4 - \rho_7 \tag{37}$$
$$\frac{\mathrm{d}S_{\mathrm{va}}}{\mathrm{d}t} = \frac{q_{\mathrm{in}}}{V_{\mathrm{liq}}}(S_{\mathrm{va,in}} - S_{\mathrm{va}}) + (1 - Y_{\mathrm{aa}})f_{\mathrm{va,aa}}\rho_6 - \rho_8 \tag{38}$$

Journal homepage: http://www.sciencedirect.com/science/journal/00255564
Original file available at: http://www.sciencedirect.com/science/article/pii/S0025556417300780

$$\frac{\mathrm{d}S_{\mathrm{bu}}}{\mathrm{d}t} = \frac{q_{\mathrm{in}}}{V_{\mathrm{liq}}}(S_{\mathrm{bu,in}} - S_{\mathrm{bu}}) + (1 - Y_{\mathrm{su}})f_{\mathrm{bu,su}}\rho_5 \tag{39}$$

$$+ (1 - Y_{\mathrm{aa}})f_{\mathrm{bu,aa}}\rho_6 - \rho_9 \tag{40}$$

$$\frac{\mathrm{d}S_{\mathrm{pro}}}{\mathrm{d}t} = \frac{q_{\mathrm{in}}}{V_{\mathrm{liq}}}(S_{\mathrm{pro,in}} - S_{\mathrm{pro}}) + (1 - Y_{\mathrm{su}})f_{\mathrm{pro,su}}\rho_5$$
$$+ (1 - Y_{\mathrm{aa}})f_{\mathrm{pro,aa}}\rho_6 + (1 - Y_{\mathrm{c4}})0.54\rho_8 - \rho_{10} \tag{41}$$

$$\frac{\mathrm{d}S_{\mathrm{ac}}}{\mathrm{d}t} = \frac{q_{\mathrm{in}}}{V_{\mathrm{liq}}}(S_{\mathrm{ac,in}} - S_{\mathrm{ac}}) + (1 - Y_{\mathrm{su}})f_{\mathrm{ac,su}}\rho_5$$
$$+ (1 - Y_{\mathrm{aa}})f_{\mathrm{ac,aa}}\rho_6 + (1 - Y_{\mathrm{fa}})0.7\rho_7$$
$$+ (1 - Y_{\mathrm{c4}})0.31\rho_8 + (1 - Y_{\mathrm{c4}})0.8\rho_9$$
$$+ (1 - Y_{\mathrm{pro}})0.57\rho_{10} - \rho_{11} \tag{42}$$

$$\frac{\mathrm{d}S_{\mathrm{h2}}}{\mathrm{d}t} = \frac{q_{\mathrm{in}}}{V_{\mathrm{liq}}}(S_{\mathrm{h2,in}} - S_{\mathrm{h2}}) + (1 - Y_{\mathrm{su}})f_{\mathrm{h2,su}}\rho_5$$
$$+ (1 - Y_{\mathrm{aa}})f_{\mathrm{h2,aa}}\rho_6 + (1 - Y_{\mathrm{fa}})0.3\rho_7$$
$$+ (1 - Y_{\mathrm{c4}})0.15\rho_8 + (1 - Y_{\mathrm{c4}})0.2\rho_9$$
$$+ (1 - Y_{\mathrm{pro}})0.43\rho_{10} - \rho_{12} - \rho_{\mathrm{T},8} \tag{43}$$

$$\frac{\mathrm{d}S_{\mathrm{ch4}}}{\mathrm{d}t} = \frac{q_{\mathrm{in}}}{V_{\mathrm{liq}}}(S_{\mathrm{ch4,in}} - S_{\mathrm{ch4}}) + (1 - Y_{\mathrm{ac}})\rho_{11} + (1 - Y_{\mathrm{h2}})\rho_{12}$$
$$- \rho_{\mathrm{T},9} \tag{44}$$

$$\frac{\mathrm{d}S_{\mathrm{IC}}}{\mathrm{d}t} = \frac{q_{\mathrm{in}}}{V_{\mathrm{liq}}}(S_{\mathrm{IC,in}} - S_{\mathrm{IC}}) - \sum_{j=1}^{19}\left(\sum_{i=1-9,11-24} C_i v_{i,j}\rho_j\right)$$
$$- \rho_{\mathrm{T},10} \tag{45}$$

$$\frac{\mathrm{d}S_{IN}}{\mathrm{d}t} = \frac{q_{\mathrm{in}}}{V_{\mathrm{liq}}}(S_{IN,in} - S_{IN}) - Y_{\mathrm{su}}N_{\mathrm{bac}}\rho_5$$
$$+ (N_{\mathrm{aa}} - Y_{\mathrm{aa}}N_{\mathrm{bac}})\rho_6 - Y_{\mathrm{fa}}N_{\mathrm{bac}}\rho_7$$
$$- Y_{\mathrm{c4}}N_{\mathrm{bac}}\rho_8 - Y_{\mathrm{c4}}N_{\mathrm{bac}}\rho_9 - Y_{\mathrm{pro}}N_{\mathrm{bac}}\rho_{10}$$
$$- Y_{\mathrm{ac}}N_{\mathrm{bac}}\rho_{11} - Y_{\mathrm{h2}}N_{\mathrm{bac}}\rho_{12} \tag{46}$$
$$+ (N_{\mathrm{bac}} - N_{\mathrm{xc}})\sum_{i=13}^{19}\rho_i$$
$$+ (N_{\mathrm{xc}} - f_{\mathrm{xI,xc}}N_{\mathrm{I}} - f_{\mathrm{sI,xc}}N_{\mathrm{I}} - f_{\mathrm{pr,xc}}N_{\mathrm{aa}})\rho_1$$

$$\frac{\mathrm{d}S_{\mathrm{I}}}{\mathrm{d}t} = \frac{q_{\mathrm{in}}}{V_{\mathrm{liq}}}(S_{\mathrm{I,in}} - S_{\mathrm{I}}) + f_{\mathrm{sI,xc}}\rho_1 \tag{47}$$

$$\frac{\mathrm{d}X_{\mathrm{c}}}{\mathrm{d}t} = \frac{q_{\mathrm{in}}}{V_{\mathrm{liq}}}(X_{\mathrm{c,in}} - X_{\mathrm{c}}) - \rho_1 + \sum_{i=13}^{19}\rho_i \tag{48}$$

$$\frac{\mathrm{d}X_{\mathrm{ch}}}{\mathrm{d}t} = \frac{q_{\mathrm{in}}}{V_{\mathrm{liq}}}(X_{\mathrm{ch,in}} - X_{\mathrm{ch}}) + f_{\mathrm{ch,xc}}\rho_1 - \rho_2 \tag{49}$$

Journal homepage: http://www.sciencedirect.com/science/journal/00255564
Original file available at: http://www.sciencedirect.com/science/article/pii/S0025556417300780

$$\frac{\mathrm{d}X_{\mathrm{pr}}}{\mathrm{d}t} = \frac{q_{\mathrm{in}}}{V_{\mathrm{liq}}}(X_{\mathrm{pr,in}} - X_{\mathrm{pr}}) + f_{\mathrm{pr,xc}}\rho_1 - \rho_3 \tag{50}$$

$$\frac{\mathrm{d}X_{\mathrm{li}}}{\mathrm{d}t} = \frac{q_{\mathrm{in}}}{V_{\mathrm{liq}}}(X_{\mathrm{li,in}} - X_{\mathrm{li}}) + f_{\mathrm{li,xc}}\rho_1 - \rho_4 \tag{51}$$

$$\frac{\mathrm{d}X_{\mathrm{su}}}{\mathrm{d}t} = \frac{q_{\mathrm{in}}}{V_{\mathrm{liq}}}(X_{\mathrm{su,in}} - X_{su}) + Y_{\mathrm{su}}\rho_5 - \rho_{13} \tag{52}$$

$$\frac{\mathrm{d}X_{\mathrm{aa}}}{\mathrm{d}t} = \frac{q_{\mathrm{in}}}{V_{\mathrm{liq}}}(X_{\mathrm{aa,in}} - X_{\mathrm{aa}}) + Y_{\mathrm{aa}}\rho_6 - \rho_{14} \tag{53}$$

$$\frac{\mathrm{d}X_{\mathrm{fa}}}{\mathrm{d}t} = \frac{q_{\mathrm{in}}}{V_{\mathrm{liq}}}(X_{\mathrm{fa,in}} - X_{\mathrm{fa}}) + Y_{\mathrm{fa}}\rho_7 - \rho_{15} \tag{54}$$

$$\frac{\mathrm{d}X_{\mathrm{c4}}}{\mathrm{d}t} = \frac{q_{\mathrm{in}}}{V_{\mathrm{liq}}}(X_{\mathrm{c4,in}} - X_{\mathrm{c4}}) + Y_{\mathrm{c4}}\rho_8 + Y_{\mathrm{c4}}\rho_9 - \rho_{16} \tag{55}$$

$$\frac{\mathrm{d}X_{\mathrm{pro}}}{\mathrm{d}t} = \frac{q_{\mathrm{in}}}{V_{\mathrm{liq}}}(X_{\mathrm{pro,in}} - X_{\mathrm{pro}}) + Y_{\mathrm{pro}}\rho_{10} - \rho_{17} \tag{56}$$

$$\frac{\mathrm{d}X_{\mathrm{ac}}}{\mathrm{d}t} = \frac{q_{\mathrm{in}}}{V_{\mathrm{liq}}}(X_{\mathrm{ac,in}} - X_{\mathrm{ac}}) + Y_{\mathrm{ac}}\rho_{11} - \rho_{18} \tag{57}$$

$$\frac{\mathrm{d}X_{\mathrm{h2}}}{\mathrm{d}t} = \frac{q_{\mathrm{in}}}{V_{\mathrm{liq}}}(X_{\mathrm{h2,in}} - X_{\mathrm{h2}}) + Y_{h2}\rho_{12} - \rho_{19} \tag{58}$$

$$\frac{\mathrm{d}X_{\mathrm{I}}}{\mathrm{d}t} = \frac{q_{\mathrm{in}}}{V_{\mathrm{liq}}}(X_{\mathrm{I,in}} - X_{\mathrm{I}}) + f_{\mathrm{xI,xc}}\rho_1 \tag{59}$$

$$\frac{\mathrm{d}S_{\mathrm{cat^+}}}{\mathrm{d}t} = \frac{q_{\mathrm{in}}}{V_{\mathrm{liq}}}(S_{\mathrm{cat^+,in}} - S_{\mathrm{cat^+}}) \tag{60}$$

$$\frac{\mathrm{d}S_{\mathrm{an^-}}}{\mathrm{d}t} = \frac{q_{\mathrm{in}}}{V_{\mathrm{liq}}}(S_{\mathrm{an^-,in}} - S_{\mathrm{an^-}}) \tag{61}$$

$$\frac{\mathrm{d}S_{\mathrm{gas,h2}}}{\mathrm{d}t} = -\frac{S_{gas,h2}RTV_{\mathrm{liq}}(\frac{\rho_{T,8}}{16} + \frac{\rho_{T,9}}{64} + \rho_{\mathrm{T},10})}{(p_{\mathrm{atm}} - p_{\mathrm{gas,h2o}})V_{\mathrm{gas}}} + \rho_{\mathrm{T},8}\frac{V_{\mathrm{liq}}}{V_{\mathrm{gas}}} \tag{62}$$

$$\frac{\mathrm{d}S_{\mathrm{gas,ch4}}}{\mathrm{d}t} = -\frac{S_{\mathrm{gas,ch4}}RTV_{\mathrm{liq}}(\frac{\rho_{\mathrm{T},8}}{16} + \frac{\rho_{\mathrm{T},9}}{64} + \rho_{\mathrm{T},10})}{(p_{\mathrm{atm}} - p_{\mathrm{gas,h2o}})V_{\mathrm{gas}}} + \rho_{\mathrm{T},9}\frac{V_{\mathrm{liq}}}{V_{\mathrm{gas}}} \tag{63}$$

$$\frac{\mathrm{d}S_{\mathrm{gas,co2}}}{\mathrm{d}t} = -\frac{S_{\mathrm{gas,co2}}RTV_{\mathrm{liq}}(\frac{\rho_{\mathrm{T},8}}{16} + \frac{\rho_{\mathrm{T},9}}{64} + \rho_{\mathrm{T},10})}{(p_{\mathrm{atm}} - p_{\mathrm{gas,h2o}})V_{\mathrm{gas}}} + \rho_{\mathrm{T},10}\frac{V_{\mathrm{liq}}}{V_{\mathrm{gas}}} \tag{64}$$

The sum in Equation (45) is:

$$\begin{aligned}&\sum_{j=1}^{19}\left(\sum_{i=1-9,11-24} C_i v_{i,j}\rho_j\right)\\ &= \sum_{k=1}^{12} s_k\rho_k + s_{13}(\rho_{13} + \rho_{14} + \rho_{15} + \rho_{16} + \rho_{17} + \rho_{18} + \rho_{19})\end{aligned} \tag{65}$$

where:

$$s_1 = -C_{\mathrm{xc}} + f_{\mathrm{sI,xc}}C_{\mathrm{sI}} + f_{\mathrm{ch,xc}}C_{\mathrm{ch}} + f_{\mathrm{pr,xc}}C_{\mathrm{pr}} + f_{\mathrm{li,xc}}C_{\mathrm{li}}$$

Journal homepage: http://www.sciencedirect.com/science/journal/00255564
Original file available at: http://www.sciencedirect.com/science/article/pii/S0025556417300780

$$+ f_{\mathrm{xI,xc}} C_{\mathrm{xI}} \tag{66}$$

$$s_2 = -C_{\mathrm{ch}} + C_{\mathrm{su}} \tag{67}$$

$$s_3 = -C_{\mathrm{pr}} + C_{\mathrm{aa}} \tag{68}$$

$$s_4 = -C_{\mathrm{li}} + (1 - f_{\mathrm{fa,li}}) C_{\mathrm{su}} + f_{\mathrm{fa,li}} C_{\mathrm{fa}} \tag{69}$$

$$s_5 = -C_{\mathrm{su}} + (1 - Y_{\mathrm{su}})(f_{\mathrm{bu,su}} C_{\mathrm{bu}} + f_{\mathrm{pro,su}} C_{\mathrm{pro}} + f_{\mathrm{ac,su}} C_{\mathrm{ac}}) + Y_{\mathrm{su}} C_{\mathrm{bac}} \tag{70}$$

$$s_6 = -C_{\mathrm{aa}} + (1 - Y_{\mathrm{aa}})(f_{\mathrm{va,aa}} C_{\mathrm{va}} + f_{\mathrm{bu,aa}} C_{\mathrm{bu}} + f_{\mathrm{pro,aa}} C_{\mathrm{pro}} + f_{\mathrm{ac,aa}} C_{\mathrm{ac}}) + Y_{\mathrm{aa}} C_{\mathrm{bac}} \tag{71}$$

$$s_7 = -C_{\mathrm{fa}} + (1 - Y_{\mathrm{fa}}) 0.7 C_{\mathrm{ac}} + Y_{\mathrm{fa}} C_{\mathrm{bac}} \tag{72}$$

$$s_8 = -C_{\mathrm{va}} + (1 - Y_{\mathrm{c4}}) 0.54 C_{\mathrm{pro}} + (1 - Y_{\mathrm{c4}}) 0.31 C_{\mathrm{ac}} + Y_{\mathrm{c4}} C_{\mathrm{bac}} \tag{73}$$

$$s_9 = -C_{\mathrm{bu}} + (1 - Y_{\mathrm{c4}}) 0.8 C_{\mathrm{ac}} + Y_{\mathrm{c4}} C_{\mathrm{bac}} \tag{74}$$

$$s_{10} = -C_{\mathrm{pro}} + (1 - Y_{\mathrm{pro}}) 0.57 C_{\mathrm{ac}} + Y_{\mathrm{pro}} C_{\mathrm{bac}} \tag{75}$$

$$s_{11} = -C_{\mathrm{ac}} + (1 - Y_{\mathrm{ac}}) C_{\mathrm{ch4}} + Y_{\mathrm{ac}} C_{\mathrm{bac}} \tag{76}$$

$$s_{12} = (1 - Y_{\mathrm{h2}}) C_{\mathrm{ch4}} + Y_{\mathrm{h2}} C_{\mathrm{bac}} \tag{77}$$

$$s_{13} = -C_{\mathrm{bac}} + C_{\mathrm{xc}} \tag{78}$$

The N-differences between the states are the following:

$$r_1 = N_{\mathrm{xc}} - f_{\mathrm{xI,xc}} N_{\mathrm{I}} - f_{\mathrm{sI,xc}} N_{\mathrm{I}} - f_{\mathrm{pr,xc}} N_{\mathrm{aa}} \tag{79}$$

$$r_2 = - Y_{\mathrm{su}} N_{\mathrm{bac}} \tag{80}$$

$$r_3 = (N_{\mathrm{aa}} - Y_{\mathrm{aa}} N_{\mathrm{bac}}) \tag{81}$$

$$r_4 = - Y_{\mathrm{fa}} N_{\mathrm{bac}} \tag{82}$$

$$r_5 = - Y_{\mathrm{c4}} N_{\mathrm{bac}} \tag{83}$$

$$r_6 = - Y_{\mathrm{pro}} N_{\mathrm{bac}} \tag{84}$$

$$r_7 = - Y_{\mathrm{ac}} N_{\mathrm{bac}} \tag{85}$$

$$r_8 = - Y_{\mathrm{h2}} N_{\mathrm{bac}} \tag{86}$$

$$r_9 = N_{\mathrm{bac}} - N_{\mathrm{xc}} \tag{87}$$

The 10 AEs for the DAE-implementation of ADM1.

$$0 = S_{\mathrm{cat^+}} + S_{\mathrm{nh4^+}} + S_{\mathrm{h^+}} - S_{\mathrm{hco3^-}} - \frac{S_{\mathrm{ac^-}}}{64} - \frac{S_{\mathrm{pro^-}}}{112} - \frac{S_{\mathrm{bu^-}}}{160} - \frac{S_{\mathrm{va^-}}}{208} - S_{\mathrm{oh^-}} - S_{\mathrm{an^-}} \tag{88}$$

$$0 = S_{\mathrm{oh^-}} - \frac{K_{\mathrm{w}}}{S_{\mathrm{h^+}}} \tag{89}$$

$$0 = S_{\mathrm{va^-}} - \frac{K_{\mathrm{a,va}} S_{\mathrm{va}}}{K_{\mathrm{a,va}} + S_{\mathrm{h^+}}} \tag{90}$$

$$0 = S_{\mathrm{bu^-}} - \frac{K_{\mathrm{a,bu}} S_{\mathrm{bu}}}{K_{\mathrm{a,bu}} + S_{\mathrm{h^+}}} \tag{91}$$

$$0 = S_{\mathrm{pro^-}} - \frac{K_{\mathrm{a,pro}} S_{\mathrm{pro}}}{K_{\mathrm{a,pro}} + S_{\mathrm{h^+}}} \tag{92}$$

Journal homepage: http://www.sciencedirect.com/science/journal/00255564
Original file available at: http://www.sciencedirect.com/science/article/pii/S0025556417300780

$$0 = S_{\mathrm{ac^-}} - \frac{K_{\mathrm{a,ac}} S_{\mathrm{ac}}}{K_{\mathrm{a,ac}} + S_{\mathrm{h^+}}} \tag{93}$$

$$0 = S_{\mathrm{hco3^-}} - \frac{K_{\mathrm{a,co2}} S_{\mathrm{IC}}}{K_{\mathrm{a,co2}} + S_{\mathrm{h^+}}} \tag{94}$$

$$0 = S_{\mathrm{nh4^+}} - \frac{S_{\mathrm{h^+}} S_{\mathrm{IN}}}{K_{\mathrm{a,IN}} + S_{\mathrm{h^+}}} \tag{95}$$

$$0 = S_{\mathrm{IC}} - S_{\mathrm{co2}} - S_{\mathrm{hco3^-}} \tag{96}$$

$$0 = S_{\mathrm{IN}} - S_{\mathrm{nh3}} - S_{\mathrm{nh4^+}} \tag{97}$$

The gaseous outflow:

$$q_{\mathrm{gas}} = k_{\mathrm{p}}(p_{\mathrm{gas}} - P_{\mathrm{atm}}) \tag{98}$$

with

$$p_{\mathrm{gas}} = S_{\mathrm{gas,h2}} \frac{RT}{16} + S_{\mathrm{gas,ch4}} \frac{RT}{64} + S_{\mathrm{gas,co2}} RT + p_{\mathrm{gas,h2o}} \tag{99}$$

Postprint version of paper published in Mathematical Biosciences 2017, vol. 288, p. 21-34.
The content is identical to the published paper, but without the final typesetting by the publisher.

Appendix B. Numerical values of states and parameters

Over the course of this work numerical values are substituted for states, e.g., as initial conditions and parameters. Unless otherwise stated, the numerical values presented in this appendix are used.

Table 1: Steady-state state variables with $q_{\mathrm{liq}} = 170.0\ \mathrm{m^3 d^{-1}}$, calculated by applying the input variables of Table 3 for 1000 days.

State	Value	State	Value
S_{su}	0.01195	X_{c4}	0.43192
S_{aa}	0.00531	X_{pro}	0.13731
S_{fa}	0.09862	X_{ac}	0.76056
S_{va}	0.01162	X_{h2}	0.31702
S_{bu}	0.01325	X_{I}	25.61740
S_{pro}	0.01578	$S_{\mathrm{cat^+}}$	0.04
S_{ac}	0.19762	$S_{\mathrm{an^-}}$	0.02
S_{h2}	2.3595E−7	$S_{\mathrm{h^+}}$	3.4234E−8
S_{ch4}	0.05509	S_{va}	0.011560
S_{IC}	0.15268	S_{bu}	0.01322
S_{IN}	0.13023	S_{pro}	0.01574
S_{I}	0.32870	S_{ac}	0.19724
X_{xc}	0.30869	$S_{\mathrm{hco3^-}}$	0.14278
X_{ch}	0.02795	S_{co2}	0.00990
X_{pr}	0.10258	S_{nh3}	0.00409
X_{li}	0.02948	$S_{\mathrm{nh4^+}}$	0.12613
X_{su}	0.42017	$S_{\mathrm{gas,h2}}$	1.0241E−5
X_{aa}	1.17918	$S_{\mathrm{gas,ch4}}$	1.6256
X_{fa}	0.24303	$S_{\mathrm{gas,co2}}$	0.014151

Table 2: Steady-state state variables with $q_{\mathrm{liq}} = 85.0\ \mathrm{m^3 d^{-1}}$, calculated by applying the input variables of Table 3 for 1000 days.

State	Value	State	Value
S_{su}	0.00762	X_{pro}	0.10899
S_{aa}	0.0033953	X_{ac}	0.60874
S_{fa}	0.05728	X_{h2}	0.25345
S_{va}	0.0072466	X_{I}	25.804
S_{bu}	0.0082609	$S_{\mathrm{cat^+}}$	0.04
S_{pro}	0.0093745	$S_{\mathrm{an^-}}$	0.02
S_{ac}	0.095295	$S_{\mathrm{h^+}}$	3.2168E−8
S_{h2}	1.4997E−7	$S_{\mathrm{oh^-}}$	6.4622E−7

Journal homepage: http://www.sciencedirect.com/science/journal/00255564
Original file available at: http://www.sciencedirect.com/science/article/pii/S0025556417300780

S_{ch4}	0.050567	S_{va}	0.0072298
S_{IC}	0.15725	S_{bu}	0.0082434
S_{IN}	0.13375	S_{pro}	0.0093517
S_{I}	0.42216	S_{ac}	0.095119
X_{xc}	0.20108	S_{hco3^-}	0.14763
X_{ch}	0.014475	S_{co2}	0.009619
X_{pr}	0.051881	S_{nh3}	0.0044624
X_{li}	0.015478	S_{nh4^+}	0.12929
X_{su}	0.33899	$S_{gas,h2}$	$7.1083\text{E}{-6}$
X_{aa}	0.92778	$S_{gas,ch4}$	1.5829
X_{fa}	0.19973	$S_{gas,co2}$	0.013788
X_{c4}	0.34071		

Table 3: Input variables.

Input	**Value**	**Input**	**Value**		
$S_{su,in}$	0.01	$S_{IC,in}$	0.04	$X_{aa,in}$	0.01
$S_{aa,in}$	0.001	$S_{IN,in}$	0.01	$X_{fa,in}$	0.01
$S_{fa,in}$	0.001	$S_{I,in}$	0.02	$X_{c4,in}$	0.01
$S_{va,in}$	0.001	$S_{cat,in}$	0.04	$X_{pro,in}$	0.01
$S_{bu,in}$	0.001	$S_{an,in}$	0.02	$X_{ac,in}$	0.01
$S_{pro,in}$	0.001	$X_{ch,in}$	5.0	$X_{h2,in}$	0.01
$S_{ac,in}$	0.001	$X_{pr,in}$	20.0	$X_{I,in}$	25.0
$S_{h2,in}$	$1.0\text{E}{-8}$	$X_{li,in}$	5.0	$X_{xc,in}$	2.0
$S_{ch4,in}$	$1.0\text{E}{-5}$	$X_{su,in}$	0.0		

Table 4: Numerical values stoichiometric parameters.

Parameter	**Value**	**Parameter**	**Value**		
$f_{sI,xc}$	0.1	$f_{bu,su}$	0.13	Y_{pro}	0.04
$f_{xI,xc}$	0.2	$f_{va,aa}$	0.23	Y_{aa}	0.08
$f_{ch,xc}$	0.2	$f_{va,aa}$	0.23	Y_{c4}	0.06
$f_{pr,xc}$	0.2	$f_{h2,aa}$	0.06	Y_{fa}	0.06
$f_{li,xc}$	0.3	$f_{ac,aa}$	0.40	Y_{h2}	0.06
$f_{ac,su}$	0.41	$f_{bu,aa}$	0.26	Y_{ac}	0.05
$f_{pro,su}$	0.27	$f_{fa,li}$	0.95		
$f_{h2,su}$	0.19	Y_{su}	0.1		

Table 5: Numerical value composition parameters.

Journal homepage: http://www.sciencedirect.com/science/journal/00255564
Original file available at: http://www.sciencedirect.com/science/article/pii/S0025556417300780

Postprint version of paper published in Mathematical Biosciences 2017, vol. 288, p. 21-34.
The content is identical to the published paper, but without the final typesetting by the publisher.

Parameter	Value	Parameter	Value
N_{xc}	0.0027	C_{su}	0.0313
N_I	0.0043	C_{aa}	0.03
N_{aa}	0.007	C_{fa}	0.0217
N_{bac}	0.0057	C_{bac}	0.0313
C_{xc}	0.027863	C_{bu}	0.025
C_{sI}	0.03	C_{pro}	0.0268
C_{ch}	0.0313	C_{ac}	0.0313
C_{pr}	0.03	C_{va}	0.024
C_{li}	0.022	C_{ch4}	0.0156
C_{xI}	0.03		

Table 6: Numerical values kinetic parameters.

Parameter	Value	Parameter	Value
k_{dis}	0.5	$K_{I,nh3}$	0.0018
$k_{hyd,ch}$	10	$K_{I,h2,pro}$	3.5E−6
$k_{hyd,pr}$	10	$K_{I,h2,c4}$	1E−5
$k_{hyd,li}$	10	$K_{I,h2,fa}$	5E−6
$k_{m,su}$	30	$K_{S,IN}$	1E−4
$K_{S,su}$	0.5	$k_{dec,Xaa}$	0.02
$k_{m,aa}$	50	$k_{dec,Xc4}$	0.02
$K_{S,aa}$	0.3	$k_{dec,Xfa}$	0.02
$k_{m,fa}$	6	$k_{dec,Xpro}$	0.02
$K_{S,fa}$	0.4	$k_{dec,Xac}$	0.02
$k_{m,c4}$	20	$k_{dec,Xh2}$	0.02
$K_{S,c4}$	0.2	$k_{dec,Xsu}$	0.02
$k_{m,pro}$	13	$pH_{LL,aa}$	5.5
$K_{S,pro}$	0.1	$pH_{UL,aa}$	4
$k_{m,ac}$	8	$pH_{LL,h2}$	6
$K_{S,ac}$	0.15	$pH_{UL,h2}$	5
$k_{m,h2}$	35	$pH_{LL,ac}$	7
$K_{S,h2}$	7E−6	$pH_{UL,ac}$	6
k_La	200		

Table 7: Numerical values physico-chemical constants.

Parameter	Value	Unit	Parameter	Value	Unit
R	8.3145e-2	bar M^{-1} K^{-1}	$K_{a,co2}$	4.9371E−7	M
K_w	2.0788E−14	M	$K_{a,IN}$	1.1110E−9	M
$K_{a,va}$	1.3804E−5	M	$K_{H,co2}$	2.7147E−2	M_{liq} bar^{-1}
$K_{a,bu}$	1.5136E−5	M	$K_{H,h2}$	7.3847E−4	M_{liq} bar^{-1}
$K_{a,pro}$	1.3183E−5	M	$K_{H,ch4}$	1.1619E−3	M $_{liq}$ bar^{-1}

Journal homepage: http://www.sciencedirect.com/science/journal/00255564
Original file available at: http://www.sciencedirect.com/science/article/pii/S0025556417300780

Postprint version of paper published in Mathematical Biosciences 2017, vol. 288, p. 21-34.
The content is identical to the published paper, but without the final typesetting by the publisher.

$K_{\mathrm{a,ac}}$	1.7378E−5	M	

Table 8: Numerical values operating parameters.

Parameter	**Value**	**Unit**	**Parameter**	**Value**	**Unit**
V_{liq}	3400	m^3	$p_{\mathrm{gas,h2o}}$	0.0313	bar
V_{gas}	300	m^3	T	308.15	K
P_{atm}	1.013	bar	k_{p}	5E4	$\mathrm{m}^3\ \mathrm{d}^{-1}\ \mathrm{bar}^{-1}$

Journal homepage: http://www.sciencedirect.com/science/journal/00255564
Original file available at: http://www.sciencedirect.com/science/article/pii/S0025556417300780

Postprint version of paper published in Mathematical Biosciences 2017, vol. 288, p. 21-34.
The content is identical to the published paper, but without the final typesetting by the publisher.

Appendix C. Relations between ADM1 model structure and structural identifiability results

Interactions

Following interactions are found in the model structure of ADM1:

- Through the different degradation processes $\rho_i, \quad i = 1, \ldots, 19$ each state directly influences the concentration of its degradation products, and for $\rho_5 - \rho_{12}$ the biomass performing this degradation.
- Each biomass (X_{su}, X_{aa}, X_{fa}, X_{pro}, X_{c4}, X_{h2}, X_{ac}) influences the concentration of the component it degrades and its degradation products.
- All biomass decays to X_{xc} which is the component at the beginning of the reaction network. In that way, each biomass has an indirect influence on *every* component in the reaction scheme.
- For each reaction, there is an interaction with the source/sink components S_{IC} and S_{IN} to compensate for an excess/deficiency of carbon and nitrogen between the component and its degradation products. The flows from/to S_{IC} and S_{IN} are indicated with $s_i, \quad i = 1, \ldots, 1$, $r_i, i = 1, \ldots, 9$, respectively on Figure 1. Thus, S_{IC} and S_{IN} are influenced by almost all reactions.
- Inorganic nitrogen S_{IN} directly influences the acetate degradation since its ammonia fraction S_{nh3} is inhibiting. If nitrogen is a limiting component in biomass growth, it also influences the reactions performed by microbial groups, i.e., $\rho_5 - \rho_{12}$.
- There are three gaseous components $S_{\mathrm{gas,co2}}$, $S_{\mathrm{gas,h2}}$ and $S_{\mathrm{gas,ch4}}$. The outflow of each of these gases q_{gas} out of the system is determined by the quantity of *all* of each of these gases, thus, they influence each other.
- Each of the gases exchanges mass with its soluble form, i.e., S_{h2}, S_{ch4}, S_{co2}. Thus, the soluble forms, through the gaseous form, interact with each other. S_{co2} is a pH-determined fraction of the inorganic carbon S_{IC}, thus through S_{co2} and $S_{\mathrm{gas,co2}}$, S_{IC} has an influence on S_{h2}, S_{ch4}, S_{co2}.
- Valeric acid (S_{va}), butyric acid (S_{bu}), acetic acid (S_{ac}), propionic acid (S_{pro}), inorganic nitrogen (S_{IN}) and inorganic carbon (S_{IC}) directly influence the pH.
- The pH has a direct inhibition effect on reactions $\rho_5 - \rho_{12}$, and determines the fraction of S_{IC} and S_{IN} existing as S_{co2} and S_{nh3}, respectively.
- Hydrogen S_{h2} inhibits the degradation of S_{bu}, S_{va}, S_{fa} and S_{pro}.

Journal homepage: http://www.sciencedirect.com/science/journal/00255564
Original file available at: http://www.sciencedirect.com/science/article/pii/S0025556417300780

Postprint version of paper published in Mathematical Biosciences 2017, vol. 288, p. 21-34.
The content is identical to the published paper, but without the final typesetting by the publisher.

Identifiability and interconnectivity

To decrease the connectivity, three hypothetical 'storage' states were introduced γ_1, γ_2 and γ_3. γ_1 collects all COD from decayed biomass and γ_2 and γ_3 collects the excess of C and N originating from the decay of biomass. In this manner, the COD, C and N is not recirculated to the particulate composites X_{xc} via the 'decay' recirculation (see Figure 1).

The observability results of this 'modified' reaction network are then the following. When X_{xc} is measured, only $X_{\mathrm{xc}}(0)$ is observable. When only S_{su} is measured, only $X_{\mathrm{xc}}(0)$, $X_{\mathrm{ch}}(0)$ and $S_{\mathrm{su}}(0)$ are observable. Thus, only information from the states themselves or of states 'upstream' in the reaction pathway can be observed. Because of the removal of the feedback via the decay, there is no information pathway linking $X_{\mathrm{xc}}(0)$ or S_{su} to the rest of the system. When one goes further downstream in the altered reaction network, the observability results become applicable again. For instance when only S_{pro} is measured almost all states and parameters are observable with the exception of the parameters and initial conditions already listed in Table 1: $f_{\mathrm{sI,xc}}$, $f_{\mathrm{xI,xc}}$, C_{sI}, C_{xI}, $S_{\mathrm{I}}(0)$, $X_{\mathrm{I}}(0)$, $S_{\mathrm{cat^+}}$, $S_{\mathrm{an^-}}$, and $\gamma_1(0)$, $\gamma_2(0)$,$\gamma_3(0)$ and the composition parameters N_I, C_{xc} and N_{xc}. The composition parameters become non-observable because of the carbon and nitrogen captured in the non-observable $\gamma_2(0)$ and $\gamma_3(0)$. Since S_{pro} is connected to the rest of the system via multiple mechanisms, measuring it is thus sufficiently informative from an observability or identifiability point of view. Finally, note that it was necessary to introduce *all* 'storage' states γ_1, γ_2 and γ_3 to break open the connectivity. One or two of them was insufficient.

Table 1: The results of the parameters of ADM1 for the scenarios with inputs q_{liq} and/or $S_{x,in}$. Observability is equivalent to structurally locally identifiable.

Measurement	**Result**
All states	All parameters observable excl. C_{sI}, C_{xI}
Any state excl. S_{I}, X_{I}, $S_{\mathrm{cat^+}}$, $S_{\mathrm{an^-}}$	All parameters observable excl. $f_{\mathrm{sI,xc}}$, $f_{\mathrm{xI,xc}}$, C_{sI}, C_{xI}, $S_{\mathrm{I}}(0)$, $X_{\mathrm{I}}(0)$, $S_{\mathrm{cat^+}}(0)$, $S_{\mathrm{an^-}}(0)$
S_{I}	All parameters observable excl. C_{sI}, C_{xI}, $X_{\mathrm{I}}(0)$, $S_{\mathrm{cat^+}}(0)$, $S_{\mathrm{an^-}}(0)$
X_{I}	All parameters observable excl. C_{sI}, C_{xI}, $S_{\mathrm{I}}(0)$, $S_{\mathrm{cat^+}}(0)$, $S_{\mathrm{an^-}}(0)$
$S_{\mathrm{cat^+}}$	None observable excl. $S_{\mathrm{cat^+}}(0)$
$S_{\mathrm{an^-}}$	None observable excl. $S_{\mathrm{an^-}}(0)$

Journal homepage: http://www.sciencedirect.com/science/journal/00255564
Original file available at: http://www.sciencedirect.com/science/article/pii/S0025556417300780

Postprint version of paper published in Mathematical Biosciences 2017, vol. 288, p. 21-34.
The content is identical to the published paper, but without the final typesetting by the publisher.

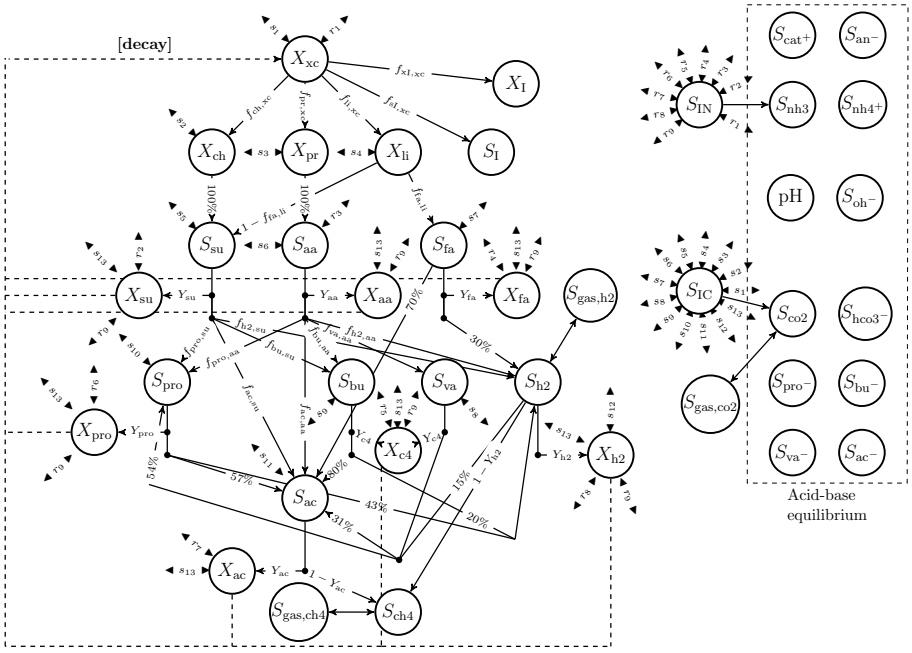

Figure 1: **The structure of ADM1, on which the stoichiometric parameters $f_{i,j}$ and Y_i are indicated.** Inorganic nitrogen S_{IC} and carbon S_{IN} are source/sink components that collect or make up excess or deficiencies of carbon and nitrogen, due to different N- or C-compositions of the different components in the system, indicated with r_i and s_i respectively. A separate system defines the acid-base equilibrium. The microbial metabolism on the substrates is inhibited by the pH-level, limiting inorganic nitrogen, ammonia and hydrogen.

Journal homepage: http://www.sciencedirect.com/science/journal/00255564
Original file available at: http://www.sciencedirect.com/science/article/pii/S0025556417300780

Postprint version of paper published in Mathematical Biosciences 2017, vol. 288, p. 21-34.
The content is identical to the published paper, but without the final typesetting by the publisher.

Appendix D. In-depth discussion of the state profiles in Experiment 2

The state profiles for Experiment 2 are shown in Figure 1. Notable are the rises in the particulates X_{xc}, X_{ch}, X_{pr} and X_{li} due to the change of liquid inflow at $t = 25$ d and the peaks in S_{su} and S_{aa} due to the elevated inflow and lowered pH. Note that the lowering of the pH also inhibits the degradation of S_{fa}, S_{va}, S_{bu}, S_{pro} and S_{h2} allowing the concentrations of these state to rise dramatically. For S_{va}, S_{bu}, S_{pro}, the fermentation of the added S_{su} and S_{aa} gives an additional rise. After reactivation of the biomass by raising the pH to a normal level, the concentrations of the mentioned states drop significantly. The concentration of S_{ac} also increases due to the biomass inhibition, but increases even more after reactivation of the biomass. This is because S_{ac} is the product of the degradation of S_{va}, S_{bu}, S_{pro}.

The concentrations of biomass (X_{su}, X_{aa}, X_{fa}, X_{c4}, X_{pro}, X_{ac} and X_{h2}) decrease during the period of low pH. Important to note is the drop in inorganic carbon S_{IC} when the pH drops. In the acidification, a large portion of the inorganic carbon effervesces to gas, i.e., $S_{\mathrm{gas,co2}}$ and leaves the CSTR in the gas outflow. When the digestion 're-activates' when the pH is raised again, the C-consuming reaction also re-activates, further decreasing the C-content. However, since the inorganic carbon content is low, the limiting C-inhibition becomes active. The effect of this artificially added inhibition is negligible for almost all the states, i.e., the profiles with or without this inhibition are visually almost indiscernible. Only, for the lipids X_{li} a noticeable peak around $t = 60$ days can be observed, because of the inhibition of lipid uptake.

Journal homepage: http://www.sciencedirect.com/science/journal/00255564
Original file available at: http://www.sciencedirect.com/science/article/pii/S0025556417300780

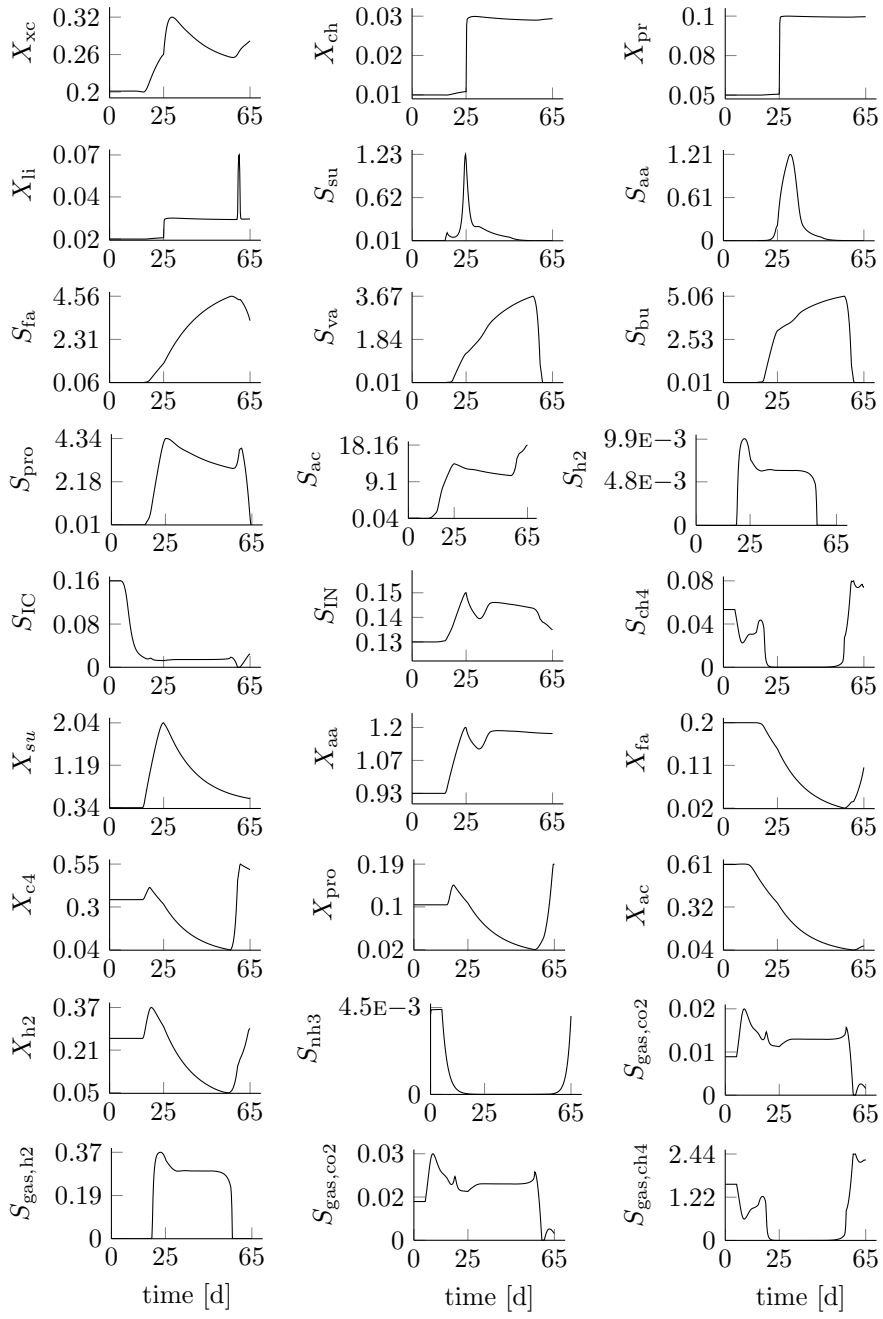

Figure 1: **Concentration profiles of most states in Experiment 2.**

Journal homepage: http://www.sciencedirect.com/science/journal/00255564
Original file available at: http://www.sciencedirect.com/science/article/pii/S0025556417300780

Postprint version of paper published in Mathematical Biosciences 2017, vol. 288, p. 21-34.
The content is identical to the published paper, but without the final typesetting by the publisher.

Appendix E. Parameter estimation results

This appendix reports the parameter estimation results for the two experiments at different noise levels.

Experiment 1

The degradation of the states S_{su}, S_{aa}, S_{pro} S_{fa}, S_{bu}, S_{va} S_{h2}, S_{ac} by biomass is described by Monod kinetics and inhibited by H_2, pH and NH_3. The fact that the Monod parameter estimates are strongly interrelated and are not estimated well is not entirely surprising. No accurate results could have been expected if the values of the associated states are not below and above the K_S reference value. Because of the larger spread of acetic acid S_{ac} on the kinetic profiles, as shown in Figure 1, it is expected that both maximum uptake rate $k_{m,ac}$ (54.) and saturation constant $K_{S,ac}$ (55.) show accurate estimations.

Surprisingly, this is *only* so for the saturation constant and *not* for the maximum uptake rate. The reason for this poor estimation is most likely the strong negative interdependence with the NH_3 inhibition parameter $K_{I,nh3}$ (56.). This parameter appears indeed together with $k_{m,ac}$ in the equations for ρ_{11}. Since the NH_3-values are generally very low and do not change much, $K_{I,nh3}$ is expected to be inaccurately estimated, and due to the exhibited interdependence with $k_{m,ac}$, the latter will also be estimated poorly. A similar reasoning can be made to explain the interdependence between (i) the Monod parameters of the degradation of S_{fa} (45.-46.) and the parameter related to its inhibition (47.), (ii) the Monod parameters of the degradation of S_{bu}, S_{va} (48.-49.) and the parameters related to its inhibition (50.), and (iii) the Monod parameters of the degradation of S_{pro} (51.-52.) and the parameter related to its inhibition (53.). Besides these interdependence between the Monod parameters and its inhibition constants, there is also a strong interdependence between the different sets of Monod parameters (42.-43.), (43.-44.), (45.-46.), (48.-49.), (51.-52.) and (54.) and the associated stoichiometric parameters (14.-22.). This interdependence is quite understandable, since there are multiple reactions pathways interconnecting the states S_{su}, S_{aa}, S_{va}, S_{pro} S_{fa}, S_{bu}, S_{h2}, S_{ac}. Any change in the value of state induced by a bias in the estimate of a parameter, can then approximately be corrected by a change in value of another parameter in the network. Consider for instance the degradation of S_{su} to S_{pro}. Imagine that for some reason the value of $k_{m,su}$ is estimated too high. There are several ways to 'correct' this: the saturation constant $K_{S,su}$ could be increased, the stoichiometric parameter $f_{pro,su}$ can be decreased or the kinetic parameter $k_{m,pro}$ can be increased to alleviate the increase in the degradation product S_{pro}.

Finally, the connection between the composition parameters (23.-35.) and many of the stoichiometric parameters (10.-22.) and kinetic parameters (41.-58.) is explained. The fact that the C and N composition parameters are strongly connected to each other and the stoichiometric parameters most likely stem from the fact that they are primarily observed by the measurement of a single variable, i.e., the inorganic carbon S_{IC} or the inorganic nitrogen S_{IN}. A bias

Journal homepage: http://www.sciencedirect.com/science/journal/00255564
Original file available at: http://www.sciencedirect.com/science/article/pii/S0025556417300780

Postprint version of paper published in Mathematical Biosciences 2017, vol. 288, p. 21-34.
The content is identical to the published paper, but without the final typesetting by the publisher.

in the estimate of one of the composition parameters can then approximately be offset by a change in any other composition parameters, or, by an off-set in the stoichiometric parameters. Since the stoichiometric parameters (10.-22.) are strongly related to the kinetic parameters (41.58.), a strong interdependence between the composition parameters and the stoichiometric parameters implies also a strong interdependence between the composition parameters and the kinetic parameters.

Table 1: Parameter estimation results of Experiment 1 for Gaussian measurement noise with a magnitude of 5% and 10% of the initial conditions. The true parameter values (θ_i^*), the relative deviation of the Monte Carlo estimate $\hat{\theta}_{\mathrm{MC},i_\theta}$ and the relative standard deviation of the Monte Carlo estimate $\sigma_{\mathrm{MC},i_\theta}$ are shown. $^{(\dagger)}C_I = f_{\mathrm{sI,xc}}C_{\mathrm{sI}} + f_{\mathrm{xI,xc}}C_{\mathrm{xI}}$. A bias or standard deviation of less than 5%, between 5% and 25% and more than 25% is indicated in white, light gray and dark gray respectively.

		5%		10%	
θ_{i_θ}	$\theta^*_{i_\theta}$	$\mathrm{Bias}_{\mathrm{rel},i_\theta}$	$\sigma_{\mathrm{rel},i_\theta}$	$\mathrm{Bias}_{\mathrm{rel},i_\theta}$	$\sigma_{\mathrm{rel},i_\theta}$
Stoichiometric parameters					
1. $f_{\mathrm{fa,li}}$	0.95	2.6%	10.3%	−0.6%	19.2%
2. Y_{ac}	0.05	−1.2%	8.2%	−2.8%	12.2%
3. Y_{h2}	0.06	4.4%	15.9%	3.6%	25.6%
4. Y_{pro}	0.04	−0.6%	16.3%	−2.0%	26.5%
5. Y_{c4}	0.06	−3.2%	15.9%	−4.3%	26.7%
6. Y_{fa}	0.06	−3.9%	16.1%	−5.0%	27.5%
7. Y_{su}	0.1	1.7%	13.6%	−6.9%	37.2%
8. Y_{aa}	0.08	0.8%	6.6%	−2.8%	13.9%
9. $f_{\mathrm{sI,xc}}$	0.1	−1.5%	5.5%	1.1%	8.6%
10. $f_{\mathrm{ch,xc}}$	0.2	−3.3%	34.4%	−12.4%	64.9%
11. $f_{\mathrm{pr,xc}}$	0.2	9.3%	50.2%	8.1%	76.5%
12. $f_{\mathrm{li,xc}}$	0.3	−0.2%	23.7%	5.1%	42.0%
13. $f_{\mathrm{xI,xc}}$	0.2	−4.8%	24.4%	−4.0%	50.5%
14. $f_{\mathrm{bu,su}}$	0.13	−54.8%	152.1%	−48.6%	154.2%
15. $f_{\mathrm{pro,su}}$	0.27	−5.3%	78.5%	1.3%	83.7%
16. $f_{\mathrm{ac,su}}$	0.41	32.9%	55.4%	23.1%	64.9%
17. $f_{\mathrm{h2,su}}$	0.19	−26.0%	104.6%	−18.6%	114.6%
18. $f_{\mathrm{va,aa}}$	0.23	1.6%	15.0%	−1.0%	23.2%
19. $f_{\mathrm{bu,aa}}$	0.26	10.3%	20.9%	6.4%	29.3%
20. $f_{\mathrm{pro,aa}}$	0.05	1.4%	78.8%	−19.6%	100.7%
21. $f_{\mathrm{ac,aa}}$	0.4	−7.1%	19.0%	1.7%	29.2%
22. $f_{\mathrm{h2,aa}}$	0.06	−5.0%	83.2%	−18.7%	115.1%
23. C_{xc}	0.02786	−193.9%	151.4%	−192.4%	132.4%
24. N_{xc}	0.00269	−98.8%	182.2%	−79.2%	174.4%
25. C_{bac}	0.0313	−162.7%	141.8%	−175.2%	121.5%
26. N_{bac}	0.0057	−43.3%	128.7%	−79.4%	155.5%
27. N_{I}	0.0043	−162.6%	178.4%	−161.1%	170.8%
28. $C_{\mathrm{I}}^{(\dagger)}$	0.009	−120.6%	21.2%	−108.7%	19.7%
29. N_{aa}	0.007	−7.5%	22.3%	−13.4%	23.7%
30. C_{ch}	0.0313	−48.5%	154.5%	−65.5%	160.1%
31. C_{su}	0.0313	−76.5%	162.6%	−78.9%	173.3%
32. C_{pr}	0.03	−13.6%	63.8%	−16.3%	64.7%
33. C_{aa}	0.03	−78.9%	182.4%	−68.6%	171.4%
34. C_{li}	0.022	−63.2%	153.2%	−42.8%	149.7%
35. C_{fa}	0.0217	−61.0%	98.2%	−61.7%	106.6%

Journal homepage: http://www.sciencedirect.com/science/journal/00255564
Original file available at: http://www.sciencedirect.com/science/article/pii/S0025556417300780

Kinetic parameters					
36. $k_{\mathrm{L}}a$	200	0.1%	1.8%	0.7%	4.9%
37. k_{dis}	0.5	1.3%	5.2%	−1.6%	9.0%
38. $k_{\mathrm{hyd,ch}}$	10	−0.2%	3.6%	−1.5%	7.0%
39. $k_{\mathrm{hyd,pr}}$	10	0.3%	1.5%	0.2%	2.4%
40. $k_{\mathrm{hyd,li}}$	10	0.2%	3.5%	0.5%	6.7%
41. $k_{\mathrm{m,su}}$	30	−111.0%	180.3%	−140.7%	165.5%
42. $K_{\mathrm{S,su}}$	0.5	−100.9%	171.1%	−139.4%	162.7%
43. $k_{\mathrm{m,aa}}$	50	−113.0%	180.8%	−114.5%	177.0%
44. $K_{\mathrm{S,aa}}$	0.3	−110.8%	181.1%	−113.2%	178.1%
45. $k_{\mathrm{m,fa}}$	6	−39.7%	76.5%	−61.4%	96.2%
46. $K_{\mathrm{S,fa}}$	0.4	−47.8%	96.3%	−73.2%	126.2%
47. $K_{\mathrm{I,h2,fa}}$	5E−6	−138.7%	190.4%	−93.7%	180.3%
48. $k_{\mathrm{m,c4}}$	20	−119.3%	139.2%	−110.2%	134.4%
49. $K_{\mathrm{S,c4}}$	0.2	−130.8%	153.9%	−123.7%	153.5%
50. $K_{\mathrm{I,h2,c4}}$	1E−5	−130.5%	185.8%	−154.9%	173.5%
51. $k_{\mathrm{m,pro}}$	13	−99.8%	141.4%	−100.7%	120.1%
52. $K_{\mathrm{S,pro}}$	0.1	−92.0%	136.6%	−101.0%	130.9%
53. $K_{\mathrm{I,h2,pro}}$	3.5E−6	−115.8%	188.4%	−111.0%	179.1%
54. $k_{\mathrm{m,ac}}$	8	−113.0%	128.9%	−124.5%	125.9%
55. $K_{\mathrm{S,ac}}$	0.15	−0.7%	7.8%	−3.7%	14.4%
56. $K_{\mathrm{I,nh3}}$	0.0018	9.7%	88.7%	−11.0%	133.3%
57. $k_{\mathrm{m,h2}}$	35	−124.0%	163.8%	−91.8%	160.7%
58. $K_{\mathrm{S,h2}}$	7E−5	−93.2%	150.8%	−57.3%	146.8%
59. $k_{\mathrm{dec,Xsu}}$	0.02	−0.3%	35.2%	−8.7%	61.3%
60. $k_{\mathrm{dec,Xaa}}$	0.02	3.7%	25.8%	−9.8%	53.2%
61. $k_{\mathrm{dec,Xfa}}$	0.02	1.1%	32.7%	−3.1%	57.6%
62. $k_{\mathrm{dec,Xc4}}$	0.02	2.8%	20.1%	2.4%	34.0%
63. $k_{\mathrm{dec,Xpro}}$	0.02	1.9%	23.4%	−0.5%	41.4%
64. $k_{\mathrm{dec,Xac}}$	0.02	2.1%	25.5%	1.5%	37.4%
65. $k_{\mathrm{dec,Xh2}}$	0.02	7.4%	29.5%	3.7%	50.5%
66. $\mathrm{pH}_{\mathrm{UL,aa}}$	5.5	−18.0%	14.3%	−13.7%	15.3%
67. $\mathrm{pH}_{\mathrm{LL,aa}}$	4	−35.0%	12.8%	−34.3%	16.3%
68. $\mathrm{pH}_{\mathrm{UL,h2}}$	7	4.5%	11.1%	6.5%	12.8%
69. $\mathrm{pH}_{\mathrm{LL,h2}}$	6	6.4%	6.8%	7.2%	7.9%
70. $\mathrm{pH}_{\mathrm{UL,ac}}$	6	−15.5%	16.2%	−10.9%	18.8%
71. $\mathrm{pH}_{\mathrm{LL,ac}}$	5	−13.5%	11.2%	−12.4%	12.2%
Initial conditions					
72. $S_{\mathrm{su}}(0)$	0.00762	0.4%	4.8%	0.1%	10.5%
73. $S_{\mathrm{aa}}(0)$	0.00340	−0.9%	5.3%	0.0%	9.7%
74. $S_{\mathrm{fa}}(0)$	0.0573	−0.1%	4.0%	−0.2%	9.6%
75. $S_{\mathrm{va}}(0)$	0.00725	0.2%	3.2%	−1.0%	7.8%
76. $S_{\mathrm{bu}}(0)$	0.00826	−0.3%	3.7%	−0.7%	6.9%
77. $S_{\mathrm{pro}}(0)$	0.00937	−0.8%	3.7%	0.4%	7.1%
78. $S_{\mathrm{ac}}(0)$	0.09540	0.3%	3.6%	0.1%	6.3%
79. $S_{\mathrm{h2}}(0)$	1.500E−7	0.4%	4.8%	−0.5%	10.2%
80. $S_{\mathrm{ch4}}(0)$	0.0505	0.5%	4.3%	0.5%	9.0%
81. $S_{\mathrm{IC}}(0)$	0.157	0.0%	0.5%	−0.1%	0.9%
82. $S_{\mathrm{IN}}(0)$	0.1337	0.0%	0.5%	−0.1%	1.0%
83. $S_{\mathrm{I}}(0)$	0.422	−0.1%	0.9%	−0.2%	1.8%
84. $X_{\mathrm{xc}}(0)$	0.201	0.2%	2.4%	0.5%	4.7%
85. $X_{\mathrm{ch}}(0)$	0.0145	0.5%	4.9%	0.1%	10.3%
86. $X_{\mathrm{pr}}(0)$	0.0520	−0.7%	4.8%	0.0%	9.6%
87. $X_{\mathrm{li}}(0)$	0.0155	−0.7%	4.8%	0.1%	10.0%

Journal homepage: http://www.sciencedirect.com/science/journal/00255564
Original file available at: http://www.sciencedirect.com/science/article/pii/S0025556417300780

Postprint version of paper published in Mathematical Biosciences 2017, vol. 288, p. 21-34.
The content is identical to the published paper, but without the final typesetting by the publisher.

88. $X_{su}(0)$	0.339	−0.1%	0.9%	0.2%	1.6%
89. $X_{aa}(0)$	0.928	−0.3%	0.9%	−0.2%	1.7%
90. $X_{fa}(0)$	0.200	0.0%	1.0%	−0.4%	1.9%
91. $X_{c4}(0)$	0.341	0.0%	0.9%	−0.2%	1.7%
92. $X_{pro}(0)$	0.109	−0.1%	1.0%	0.0%	1.9%
93. $X_{ac}(0)$	0.608	−0.1%	0.8%	0.1%	1.6%
94. $X_{h2}(0)$	0.253	−0.2%	0.9%	−0.5%	1.6%
95. $X_{I}(0)$	25.8	0.1%	1.0%	0.2%	2.0%
96. $S_{cat^+}(0)$	0.04	−0.1%	0.8%	0.1%	1.5%
97. $S_{an^-}(0)$	0.02	0.0%	0.8%	0.0%	1.5%
98. $S_{gas,h2}(0)$	7.108E−6	−0.3%	5.0%	1.6%	9.9%
99. $S_{gas,ch4}(0)$	1.582	0.2%	4.9%	−1.1%	9.8%
100. $S_{gas,co2}(0)$	0.0138	−0.1%	5.2%	−0.1%	11.2%

Table 2: Parameter estimation results of Experiment 1 for Gaussian measurement noise with a magnitude of 15% and 25% of the initial conditions. The true parameter values (θ_i^*), the relative deviation of the Monte Carlo estimate $\hat{\theta}_{MC,i_\theta}$ and the relative standard deviation of the Monte Carlo estimate σ_{MC,i_θ} are indicated. $^{(\dagger)}C_I = f_{sI,xc}C_{sI} + f_{xI,xc}C_{xI}$. A bias or standard deviation of less than 5%, between 5% and 25% and more than 25% is indicated in white, light gray and dark gray respectively.

		15%		25%	
θ_{i_θ}	$\theta^*_{i_\theta}$	$\text{Bias}_{\text{rel},i_\theta}$	$\sigma_{\text{rel},i_\theta}$	$\text{Bias}_{\text{rel},i_\theta}$	$\sigma_{\text{rel},i_\theta}$
Stoichiometric parameters					
1. $f_{fa,li}$	0.95	−4.43%	29.4%	−6.16%	45.1%
2. Y_{ac}	0.05	−4.54%	18.3%	−16.22%	34.8%
3. Y_{h2}	0.06	4.89%	34.2%	−5.64%	52.6%
4. Y_{pro}	0.04	−10.50%	39.1%	−13.12%	60.3%
5. Y_{c4}	0.06	−10.38%	36.2%	−26.12%	59.8%
6. Y_{fa}	0.06	−7.73%	41.0%	−33.53%	79.8%
7. Y_{su}	0.1	−25.61%	73.7%	−60.57%	109.2%
8. Y_{aa}	0.08	−7.77%	21.1%	−18.16%	34.5%
9. $f_{sI,xc}$	0.1	3.71%	13.1%	13.22%	18.3%
10. $f_{ch,xc}$	0.2	−9.57%	74.7%	−21.90%	105.9%
11. $f_{pr,xc}$	0.2	6.03%	84.7%	7.04%	100.2%
12. $f_{li,xc}$	0.3	5.52%	54.1%	11.63%	67.0%
13. $f_{xI,xc}$	0.2	−6.59%	75.3%	−9.20%	91.3%
14. $f_{bu,su}$	0.13	−51.97%	159.2%	−17.48%	146.2%
15. $f_{pro,su}$	0.27	1.09%	88.1%	−3.33%	99.5%
16. $f_{ac,su}$	0.41	18.99%	65.8%	17.64%	71.3%
17. $f_{h2,su}$	0.19	−6.97%	122.1%	−21.36%	142.0%
18. $f_{va,aa}$	0.23	−0.13%	28.4%	1.89%	30.4%
19. $f_{bu,aa}$	0.26	7.03%	36.1%	5.91%	41.3%
20. $f_{pro,aa}$	0.05	−18.71%	112.8%	−56.26%	148.5%
21. $f_{ac,aa}$	0.4	7.32%	37.3%	12.15%	45.7%
22. $f_{h2,aa}$	0.06	−63.16%	145.9%	−67.00%	159.9%
23. C_{xc}	0.02786	−204.14%	120.1%	−165.36%	144.0%
24. N_{xc}	0.00269	−71.49%	173.4%	−94.76%	183.5%
25. C_{bac}	0.0313	−160.57%	129.6%	−170.15%	136.1%
26. N_{bac}	0.0057	−64.65%	160.5%	−64.30%	165.9%
27. N_I	0.0043	−141.66%	177.1%	−155.72%	177.1%
28. $C_I^{(\dagger)}$	0.009	−107.43%	23.0%	−109.47%	17.9%

Journal homepage: http://www.sciencedirect.com/science/journal/00255564
Original file available at: http://www.sciencedirect.com/science/article/pii/S0025556417300780

29. N_{aa}	0.007	−11.19%	21.9%	−12.38%	21.2%
30. C_{ch}	0.0313	−76.26%	161.9%	−45.07%	150.4%
31. C_{su}	0.0313	−75.81%	176.1%	−68.58%	174.1%
32. C_{pr}	0.03	−4.65%	65.7%	−22.21%	69.2%
33. C_{aa}	0.03	−83.80%	178.5%	−95.75%	182.4%
34. C_{li}	0.022	−76.93%	162.2%	−47.79%	163.2%
35. C_{fa}	0.0217	−39.34%	116.6%	−46.52%	123.9%
Kinetic parameters					
36. k_La	200	2.12%	8.5%	0.82%	10.3%
37. k_{dis}	0.5	−5.75%	14.4%	−21.53%	26.9%
38. $k_{hyd,ch}$	10	−1.70%	8.5%	−4.78%	14.0%
39. $k_{hyd,pr}$	10	−0.03%	2.8%	−0.56%	4.2%
40. $k_{hyd,li}$	10	0.12%	8.8%	−1.05%	12.8%
41. $k_{m,su}$	30	−103.60%	163.2%	−71.84%	160.1%
42. $K_{S,su}$	0.5	−114.44%	165.8%	−77.91%	153.5%
43. $k_{m,aa}$	50	−90.77%	174.7%	−104.84%	176.9%
44. $K_{S,aa}$	0.3	−86.70%	173.7%	−96.34%	174.4%
45. $k_{m,fa}$	6	−63.78%	93.0%	−77.68%	111.8%
46. $K_{S,fa}$	0.4	−75.58%	129.8%	−104.79%	154.3%
47. $K_{I,h2,fa}$	5.00E−6	−84.41%	175.8%	−141.24%	178.2%
48. $k_{m,c4}$	20	−77.34%	132.9%	−85.21%	153.3%
49. $K_{S,c4}$	0.2	−92.57%	154.2%	−96.66%	163.7%
50. $K_{I,h2,c4}$	1.00E−5	−204.52%	152.8%	−144.35%	178.0%
51. $k_{m,pro}$	13	−93.31%	121.4%	−89.83%	127.8%
52. $K_{S,pro}$	0.1	−112.80%	152.2%	−103.68%	155.7%
53. $K_{I,h2,pro}$	3.50E−6	−116.53%	172.2%	−172.49%	167.5%
54. $k_{m,ac}$	8	−151.33%	115.3%	−150.37%	129.7%
55. $K_{S,ac}$	0.15	−9.02%	36.7%	−17.56%	69.5%
56. $K_{I,nh3}$	0.0018	2.63%	131.4%	−26.54%	151.7%
57. $k_{m,h2}$	35	−109.12%	162.7%	−117.56%	164.6%
58. $K_{S,h2}$	7.00E−6	−77.93%	154.6%	−68.35%	148.5%
59. $k_{dec,Xsu}$	0.02	−24.26%	94.1%	−77.27%	142.6%
60. $k_{dec,Xaa}$	0.02	−29.80%	80.0%	−70.16%	132.0%
61. $k_{dec,Xfa}$	0.02	−11.77%	80.9%	−49.62%	127.2%
62. $k_{dec,Xc4}$	0.02	−2.87%	44.9%	−29.30%	84.2%
63. $k_{dec,Xpro}$	0.02	−7.94%	61.4%	−15.34%	86.6%
64. $k_{dec,Xac}$	0.02	3.66%	50.9%	−24.18%	87.0%
65. $k_{dec,Xh2}$	0.02	9.20%	62.5%	−29.99%	108.7%
66. $pH_{UL,aa}$	5.5	−12.17%	15.2%	−15.85%	15.5%
67. $pH_{LL,aa}$	4	−31.97%	15.3%	−34.53%	16.0%
68. $pH_{UL,h2}$	7	4.59%	14.9%	1.25%	14.5%
69. $pH_{LL,h2}$	6	5.82%	10.7%	2.26%	12.8%
70. $pH_{UL,ac}$	6	−6.92%	16.0%	−14.15%	18.1%
71. $pH_{LL,ac}$	5	−11.53%	12.9%	−13.30%	12.5%
Initial conditions					
72. $S_{su}(0)$	0.00762	0.53%	14.3%	0.64%	27.4%
73. $S_{aa}(0)$	0.0034	−0.97%	15.9%	2.01%	25.3%
74. $S_{fa}(0)$	0.0573	−1.18%	14.1%	−0.08%	20.2%
75. $S_{va}(0)$	0.00725	1.47%	10.8%	0.32%	16.8%
76. $S_{bu}(0)$	0.00826	−0.44%	10.6%	1.32%	15.2%
77. $S_{pro}(0)$	0.00937	−0.31%	10.4%	0.42%	16.7%
78. $S_{ac}(0)$	0.0954	−0.95%	10.8%	−1.71%	20.5%
79. $S_{h2}(0)$	1.500E−7	−0.52%	13.3%	−2.52%	22.3%
80. $S_{ch4}(0)$	0.0505	2.73%	14.6%	5.25%	24.8%

81. $S_{\mathrm{IC}}(0)$	0.157	−0.02%	1.4%	1.15%	6.8%
82. $S_{\mathrm{IN}}(0)$	0.1337	−0.03%	1.3%	0.84%	6.2%
83. $S_{\mathrm{I}}(0)$	0.422	−0.28%	2.7%	0.36%	7.2%
84. $X_{\mathrm{xc}}(0)$	0.201	1.10%	7.3%	2.38%	14.1%
85. $X_{\mathrm{ch}}(0)$	0.0145	−1.18%	14.9%	−3.71%	25.9%
86. $X_{\mathrm{pr}}(0)$	0.052	−3.29%	13.6%	−3.15%	24.6%
87. $X_{\mathrm{li}}(0)$	0.0155	−0.32%	14.8%	−0.90%	26.3%
88. $X_{\mathrm{su}}(0)$	0.339	0.30%	2.3%	1.28%	4.0%
89. $X_{\mathrm{aa}}(0)$	0.928	0.38%	2.1%	1.29%	4.2%
90. $X_{\mathrm{fa}}(0)$	0.2	−0.33%	2.4%	0.70%	5.3%
91. $X_{\mathrm{c4}}(0)$	0.341	−0.18%	1.9%	0.36%	5.3%
92. $X_{\mathrm{pro}}(0)$	0.109	0.14%	2.8%	0.37%	3.7%
93. $X_{\mathrm{ac}}(0)$	0.608	0.21%	2.2%	0.73%	6.6%
94. $X_{\mathrm{h2}}(0)$	0.253	−0.55%	2.1%	−0.08%	3.2%
95. $X_{\mathrm{I}}(0)$	25.8	0.00%	2.5%	1.34%	7.4%
96. $S_{\mathrm{cat}+}(0)$	0.04	0.02%	2.0%	0.84%	7.1%
97. $S_{\mathrm{an}-}(0)$	0.02	0.11%	2.3%	−0.13%	5.1%
98. $S_{\mathrm{gas,h2}}(0)$	7.108E−6	−2.14%	15.1%	−0.29%	24.0%
99. $S_{\mathrm{gas,ch4}}(0)$	1.582	−1.12%	15.2%	−0.78%	23.5%
100. $S_{\mathrm{gas,co2}}(0)$	0.0138	1.44%	13.6%	0.68%	21.3%

Experiment 2

Generally speaking, the results are acceptable. Some interesting results can be obtained for certain subsets. The degradation kinetics of the particulates and the liquid-gas mass transfer coefficient (36.-40.) are estimated well for the noise levels 5%-15%. At 25% these results become very poor for the disintegration constant k_{dis} and $k_{\mathrm{hyd,li}}$. Concerning the pH-inhibition levels (65.-71.), estimates for amino acid degradation (66.-67.) and acetoclastic methanogenesis (70.-71.) are accurate and precise for all noise levels. Some variation is observed in the levels for the hydrogenotrophic methanogenesis step (69.-70.). At 25% this variation can be considered to be bad. However, for lower noise levels, the estimates can still be considered to be moderately good. For the sugar and amino acid degradation, the kinetic parameters (41.-44.) as well as the associated stoichiometric parameters (14.-22.) are estimated well for noise levels 5%-15%. At 25%, the estimates are still moderately accurate. The estimates of the other kinetic parameters (45.-65.) are generally poor, regardless of the noise level. The stoichiometric parameters concerning the disintegration of X_{xc} (9.-13.) are generally also poor, regardless of the noise level. The stoichiometric biomass yield parameters have inaccurate estimates, except for the biomass yields of monosaccharides and amino acid degraders (7.-8.) for 5% and 10% noise. The C- and N-composition (23.-35.) estimation results are mixed. The composition of monosaccharide and amino acids (29., 33., 35) is generally well estimated, except for the noise level of 25%. The other compositions show appalling results. Finally, the initial conditions (72.-98.) are moderately well estimated for 5% and 10% noise, except for the acetic acid concentrations (78.) and the LCFA concentrations (74.). For higher noise levels, the estimates generally become unacceptable.

The results can be compared to the covariances of Experiment 1 shown in

Journal homepage: http://www.sciencedirect.com/science/journal/00255564
Original file available at: http://www.sciencedirect.com/science/article/pii/S0025556417300780

Postprint version of paper published in Mathematical Biosciences 2017, vol. 288, p. 21-34.
The content is identical to the published paper, but without the final typesetting by the publisher.

Figure 2. There are some similarities: for instance a large part of the kinetic parameters (45.-65.) still shows a great interdependence with each other, i.e., the stoichiometric parameters (9.-13.), the biomass yields (2.-8.) and the composition parameters (23.-35.). There are some differences though. First, the estimates of the initial conditions (72.-98.) now have considerable interdependency with themselves *and* with the other parameters. This is in line with the results in Appendix D that show that the initial conditions estimates are only moderately good. It is also clear that there are more groups of parameters that exhibit little or no interdependency with other parameters. These are the stoichiometric (14.-21.) and kinetic parameters (41.-44.) associated with the degradation of S_{su} and S_{aa}, the first-order kinetic parameters (36.-40.), 4 of the pH-inhibition levels, (66.-67., 70.-71.), and several initial conditions (79.-83., 94.-98.). On the other hand, there are several parameters that show interdependencies with a large set of other parameters. These are the biomass yields (2., 6.) associated with the degradation of S_{ac} and S_{fa}, the composition of X_{xc} (23.-24.), X_{ch} (23.), X_{li} (34.) and S_{fa} (35.). Finally, the pH-inhibition levels of the hydrogenotrophic methanogenesis (68.-69.) show considerable interdependency with the other parameters.

Table 3: Parameter estimation results of Experiment 2 for Gaussian measurement noise with a magnitude of 5% and 10% of the initial conditions. The true parameter values (θ_i^*), the relative deviation of the Monte Carlo estimate $\hat{\theta}_{\mathrm{MC},i_\theta}$ and the relative standard deviation of the Monte Carlo estimate $\sigma_{\mathrm{MC},i_\theta}$ are shown. $^{(\dagger)}C_I = f_{\mathrm{sI,xc}}C_{\mathrm{sI}} + f_{\mathrm{xI,xc}}C_{\mathrm{xI}}$. A bias or standard deviation of less than 5%, between 5% and 25% and more than 25% is indicated in white, light gray and dark gray respectively.

		5%		10%	
θ_{i_θ}	$\theta^*_{i_\theta}$	$\mathrm{Bias}_{\mathrm{rel},i_\theta}$	$\sigma_{\mathrm{rel},i_\theta}$	$\mathrm{Bias}_{\mathrm{rel},i_\theta}$	$\sigma_{\mathrm{rel},i_\theta}$
Stoichiometric parameters					
1. $f_{\mathrm{fa,li}}$	0.95	−1.80%	3.6%	−0.41%	4.9%
2. Y_{ac}	0.05	−12.91%	29.5%	−0.45%	34.1%
3. Y_{h2}	0.06	10.64%	2.9%	10.09%	4.7%
4. Y_{pro}	0.04	−0.89%	9.9%	−0.34%	6.5%
5. Y_{c4}	0.06	5.23%	9.4%	6.09%	7.2%
6. Y_{fa}	0.06	−16.62%	67.7%	−14.91%	56.8%
7. Y_{su}	0.1	−2.41%	8.5%	0.13%	8.2%
8. Y_{aa}	0.08	−0.99%	3.1%	−1.29%	6.0%
9. $f_{\mathrm{sI,xc}}$	0.1	1.24%	1.9%	1.13%	2.7%
10. $f_{\mathrm{ch,xc}}$	0.2	−18.49%	40.2%	−13.66%	44.4%
11. $f_{\mathrm{pr,xc}}$	0.2	22.19%	20.1%	18.81%	17.0%
12. $f_{\mathrm{li,xc}}$	0.3	16.00%	27.5%	4.53%	36.3%
13. $f_{\mathrm{xI,xc}}$	0.2	−28.31%	63.5%	−12.50%	49.4%
14. $f_{\mathrm{bu,su}}$	0.13	1.35%	1.8%	1.76%	1.5%
15. $f_{\mathrm{pro,su}}$	0.27	−0.72%	1.5%	−0.36%	1.3%
16. $f_{\mathrm{ac,su}}$	0.41	−0.57%	3.9%	−1.40%	3.2%
17. $f_{\mathrm{h2,su}}$	0.19	1.34%	5.3%	2.33%	4.2%
18. $f_{\mathrm{va,aa}}$	0.23	−0.48%	0.7%	−0.42%	0.9%
19. $f_{\mathrm{bu,aa}}$	0.26	−1.14%	0.8%	−1.03%	0.8%
20. $f_{\mathrm{pro,aa}}$	0.05	1.43%	3.9%	2.80%	4.4%
21. $f_{\mathrm{ac,aa}}$	0.4	0.96%	2.4%	0.42%	2.0%
22. $f_{\mathrm{h2,aa}}$	0.06	−0.77%	7.6%	0.94%	6.2%
23. C_{xc}	0.02786	−2.28%	59.6%	−17.78%	89.3%
24. N_{xc}	0.00269	2.52%	140.9%	−47.86%	177.1%

Journal homepage: http://www.sciencedirect.com/science/journal/00255564
Original file available at: http://www.sciencedirect.com/science/article/pii/S0025556417300780

25. C_{bac}	0.0313	11.29%	6.7%	11.79%	8.3%
26. N_{bac}	0.0057	2.01%	25.1%	11.06%	37.0%
27. N_{I}	0.0043	−63.27%	152.4%	−37.90%	166.2%
28. $C_{\mathrm{I}}^{(\dagger)}$	0.009	−96.40%	12.3%	−97.80%	9.2%
29. N_{aa}	0.007	−2.39%	7.4%	0.56%	8.9%
30. C_{ch}	0.0313	35.18%	103.8%	36.99%	106.6%
31. C_{su}	0.0313	1.11%	0.8%	1.23%	0.9%
32. C_{pr}	0.03	12.24%	26.6%	11.24%	26.4%
33. C_{aa}	0.03	1.14%	0.9%	1.44%	1.3%
34. C_{li}	0.022	−98.35%	38.0%	−105.12%	34.9%
35. C_{fa}	0.0217	10.96%	38.2%	0.86%	45.3%
Kinetic parameters					
36. $k_{\mathrm{L}}a$	200	0.68%	4.2%	1.40%	3.4%
37. k_{dis}	0.5	−1.13%	2.4%	−1.24%	3.2%
38. $k_{\mathrm{hyd,ch}}$	10	−1.99%	4.1%	−1.72%	4.3%
39. $k_{\mathrm{hyd,pr}}$	10	0.96%	1.0%	0.86%	0.8%
40. $k_{\mathrm{hyd,li}}$	10	4.63%	7.1%	2.10%	10.2%
41. $k_{\mathrm{m,su}}$	30	3.32%	1.9%	3.58%	2.4%
42. $K_{\mathrm{S,su}}$	0.5	2.50%	2.7%	3.06%	2.9%
43. $k_{\mathrm{m,aa}}$	50	1.77%	4.7%	3.14%	5.3%
44. $K_{\mathrm{S,aa}}$	0.3	0.18%	0.6%	0.25%	0.8%
45. $k_{\mathrm{m,fa}}$	6	−8.11%	41.9%	−4.04%	41.1%
46. $K_{\mathrm{S,fa}}$	0.4	−28.90%	60.7%	−15.50%	41.0%
47. $K_{\mathrm{I,h2,fa}}$	5.00E−6	−21.51%	88.2%	−35.08%	99.1%
48. $k_{\mathrm{m,c4}}$	20	−5.37%	7.6%	−7.21%	10.8%
49. $K_{\mathrm{S,c4}}$	0.2	−138.06%	84.5%	−165.01%	91.4%
50. $K_{\mathrm{I,h2,c4}}$	1.00E−5	−111.37%	92.9%	−134.54%	98.1%
51. $k_{\mathrm{m,pro}}$	13	−9.91%	8.7%	−9.95%	7.3%
52. $K_{\mathrm{S,pro}}$	0.1	−29.60%	16.1%	−29.90%	17.5%
53. $K_{\mathrm{I,h2,pro}}$	3.50E−6	1.67%	16.7%	6.70%	12.3%
54. $k_{\mathrm{m,ac}}$	8	−229.89%	115.2%	−204.38%	138.9%
55. $K_{\mathrm{S,ac}}$	0.15	45.06%	40.5%	47.01%	39.5%
56. $K_{\mathrm{I,nh3}}$	0.0018	52.14%	88.1%	27.47%	123.8%
57. $k_{\mathrm{m,h2}}$	35	37.61%	4.8%	38.00%	7.5%
58. $K_{\mathrm{S,h2}}$	7.00E−6	16.66%	13.2%	20.38%	14.3%
59. $k_{\mathrm{dec,Xsu}}$	0.02	−6.57%	16.3%	−1.38%	16.4%
60. $k_{\mathrm{dec,Xaa}}$	0.02	0.83%	7.8%	−1.27%	17.6%
61. $k_{\mathrm{dec,Xfa}}$	0.02	−4.73%	42.6%	−15.04%	67.2%
62. $k_{\mathrm{dec,Xc4}}$	0.02	−9.27%	24.7%	−17.06%	27.2%
63. $k_{\mathrm{dec,Xpro}}$	0.02	13.31%	17.2%	13.88%	13.6%
64. $k_{\mathrm{dec,Xac}}$	0.02	−13.11%	50.4%	−21.28%	66.0%
65. $k_{\mathrm{dec,Xh2}}$	0.02	5.22%	3.3%	5.76%	2.6%
66. $\mathrm{pH}_{\mathrm{UL,aa}}$	5.5	−0.02%	0.2%	0.03%	0.2%
67. $\mathrm{pH}_{\mathrm{LL,aa}}$	4	0.06%	0.3%	0.15%	0.3%
68. $\mathrm{pH}_{\mathrm{UL,h2}}$	7	−4.69%	20.7%	−0.76%	18.1%
69. $\mathrm{pH}_{\mathrm{LL,h2}}$	6	−5.61%	23.1%	−0.29%	18.0%
70. $\mathrm{pH}_{\mathrm{UL,ac}}$	6	1.67%	0.3%	1.70%	0.4%
71. $\mathrm{pH}_{\mathrm{LL,ac}}$	5	1.42%	0.2%	1.42%	0.3%
Initial conditions					
72. $S_{\mathrm{su}}(0)$	0.00762	2.36%	11.4%	−0.14%	13.2%
73. $S_{\mathrm{aa}}(0)$	0.0034	2.76%	12.0%	1.54%	14.4%
74. $S_{\mathrm{fa}}(0)$	0.0573	−0.03%	18.0%	2.58%	25.4%
75. $S_{\mathrm{va}}(0)$	0.00725	10.93%	12.5%	12.42%	14.6%
76. $S_{bu}(0)$	0.00826	7.83%	13.5%	8.75%	22.0%

Journal homepage: http://www.sciencedirect.com/science/journal/00255564
Original file available at: http://www.sciencedirect.com/science/article/pii/S0025556417300780

77. $S_{\mathrm{pro}}(0)$	0.00937	3.75%	12.6%	2.89%	19.3%
78. $S_{\mathrm{ac}}(0)$	0.0954	−14.22%	26.5%	−14.46%	34.9%
79. $S_{\mathrm{h2}}(0)$	1.500E−7	−0.72%	5.2%	−0.02%	10.3%
80. $S_{\mathrm{ch4}}(0)$	0.0505	−0.06%	4.8%	0.68%	11.7%
81. $S_{\mathrm{IC}}(0)$	0.157	−0.81%	1.9%	−0.90%	2.6%
82. $S_{\mathrm{IN}}(0)$	0.1337	0.62%	4.2%	2.00%	6.2%
83. $S_{\mathrm{I}}(0)$	0.422	0.15%	1.6%	0.76%	2.3%
84. $X_{\mathrm{xc}}(0)$	0.201	6.43%	13.6%	8.11%	16.2%
85. $X_{\mathrm{ch}}(0)$	0.0145	2.17%	11.7%	1.06%	11.9%
86. $X_{\mathrm{pr}}(0)$	0.052	4.03%	11.3%	2.16%	12.0%
87. $X_{\mathrm{li}}(0)$	0.0155	3.20%	11.6%	4.10%	13.4%
88. $X_{\mathrm{su}}(0)$	0.339	2.61%	9.7%	−0.31%	10.4%
89. $X_{\mathrm{aa}}(0)$	0.928	2.62%	3.6%	2.34%	3.5%
90. $X_{\mathrm{fa}}(0)$	0.2	2.32%	10.7%	1.25%	7.9%
91. $X_{\mathrm{c4}}(0)$	0.341	−17.28%	14.4%	−22.38%	15.6%
92. $X_{\mathrm{pro}}(0)$	0.109	8.20%	1.2%	8.14%	2.5%
93. $X_{\mathrm{ac}}(0)$	0.608	−1.44%	16.3%	−5.80%	23.4%
94. $X_{\mathrm{h2}}(0)$	0.253	−13.80%	3.2%	−13.00%	4.3%
95. $X_{\mathrm{I}}(0)$	25.8	0.56%	1.3%	0.13%	1.5%
96. $S_{\mathrm{gas,h2}}(0)$	7.108E−6	0.57%	5.1%	0.55%	9.4%
97. $S_{\mathrm{gas,ch4}}(0)$	1.582	0.13%	5.3%	1.12%	9.3%
98. $S_{\mathrm{gas,co2}}(0)$	0.0138	−0.22%	4.4%	0.89%	9.9%

Table 4: Parameter estimation results of Experiment 2 for Gaussian measurement noise with a magnitude of 15% and 25% of the initial conditions. The true parameter values (θ_i^*), the relative deviation of the Monte Carlo estimate $\hat{\theta}_{\mathrm{MC},i_\theta}$ and the relative standard deviation of the Monte Carlo estimate $\sigma_{\mathrm{MC},i_\theta}$ are shown. $^{(*)}C_I = f_{\mathrm{sI,xc}}C_{\mathrm{sI}} + f_{\mathrm{xI,xc}}C_{\mathrm{xI}}$. A bias or standard deviation of less than 5%, between 5% and 25% and more than 25% is indicated in white, light gray and dark gray respectively.

		15%		25%	
θ_{i_θ}	$\theta^*_{i_\theta}$	$\mathrm{Bias}_{\mathrm{rel},i_\theta}$	$\sigma_{\mathrm{rel},i_\theta}$	$\mathrm{Bias}_{\mathrm{rel},i_\theta}$	$\sigma_{\mathrm{rel},i_\theta}$
Stoichiometric parameters					
1. $f_{\mathrm{fa,li}}$	0.95	−0.39%	5.7%	2.46%	11.0%
2. Y_{ac}	0.05	−1.74%	41.4%	3.14%	83.0%
3. Y_{h2}	0.06	8.42%	11.0%	1.91%	34.3%
4. Y_{pro}	0.04	−2.05%	12.7%	−7.43%	19.9%
5. Y_{c4}	0.06	5.64%	14.4%	0.34%	31.3%
6. Y_{fa}	0.06	−24.88%	73.0%	−69.05%	120.0%
7. Y_{su}	0.1	1.35%	12.4%	4.77%	19.6%
8. Y_{aa}	0.08	−3.71%	20.3%	−11.64%	32.3%
9. $f_{\mathrm{sI,xc}}$	0.1	2.47%	10.1%	9.69%	21.5%
10. $f_{\mathrm{ch,xc}}$	0.2	−23.11%	46.3%	−26.55%	78.3%
11. $f_{\mathrm{pr,xc}}$	0.2	22.59%	24.2%	27.24%	43.1%
12. $f_{\mathrm{li,xc}}$	0.3	7.47%	34.0%	−5.55%	62.5%
13. $f_{\mathrm{xI,xc}}$	0.2	−11.93%	67.0%	2.79%	103.2%
14. $f_{\mathrm{bu,su}}$	0.13	2.09%	3.1%	2.55%	3.9%
15. $f_{\mathrm{pro,su}}$	0.27	−0.12%	2.1%	0.31%	3.7%
16. $f_{\mathrm{ac,su}}$	0.41	−1.94%	5.6%	−4.30%	9.8%
17. $f_{\mathrm{h2,su}}$	0.19	2.92%	7.6%	7.11%	16.2%
18. $f_{\mathrm{va,aa}}$	0.23	−0.74%	1.9%	−1.65%	4.1%
19. $f_{\mathrm{bu,aa}}$	0.26	−1.27%	1.9%	−1.59%	3.1%

Journal homepage: http://www.sciencedirect.com/science/journal/00255564
Original file available at: http://www.sciencedirect.com/science/article/pii/S0025556417300780

20. $f_{\mathrm{pro,aa}}$	0.05	3.99%	9.6%	10.02%	18.1%
21. $f_{\mathrm{ac,aa}}$	0.4	0.46%	2.8%	−0.49%	5.3%
22. $f_{\mathrm{h2,aa}}$	0.06	1.95%	11.1%	8.12%	21.4%
23. C_{xc}	0.02786	−35.13%	109.4%	−84.74%	147.6%
24. N_{xc}	0.00269	−67.12%	190.4%	−86.86%	192.9%
25. C_{bac}	0.0313	9.53%	34.1%	14.09%	62.0%
26. N_{bac}	0.0057	23.04%	43.9%	35.73%	66.9%
27. N_{I}	0.0043	−58.13%	179.3%	−66.18%	189.7%
28. $C_{\mathrm{I}}^{(*)}$	0.009	−97.43%	13.4%	−98.51%	7.2%
29. N_{aa}	0.007	1.34%	9.8%	2.38%	11.8%
30. C_{ch}	0.0313	28.15%	109.3%	−1.53%	126.8%
31. C_{su}	0.0313	1.27%	2.0%	2.60%	7.1%
32. C_{pr}	0.03	13.74%	26.6%	29.41%	36.8%
33. C_{aa}	0.03	0.97%	7.0%	2.41%	9.7%
34. C_{li}	0.022	−111.14%	59.1%	−135.19%	100.3%
35. C_{fa}	0.0217	−1.58%	61.2%	6.45%	82.0%
Kinetic parameters					
36. $k_{\mathrm{L}}a$	200	1.94%	6.6%	5.78%	15.4%
37. k_{dis}	0.5	−2.62%	12.2%	−25.45%	74.5%
38. $k_{\mathrm{hyd,ch}}$	10	−2.70%	4.8%	−3.39%	10.5%
39. $k_{\mathrm{hyd,pr}}$	10	0.90%	1.2%	2.00%	6.0%
40. $k_{\mathrm{hyd,li}}$	10	−1.02%	25.7%	−11.86%	38.4%
41. $k_{\mathrm{m,su}}$	30	3.67%	9.4%	7.05%	12.0%
42. $K_{\mathrm{S,su}}$	0.5	3.67%	5.3%	7.10%	12.9%
43. $k_{\mathrm{m,aa}}$	50	4.48%	8.7%	8.41%	14.3%
44. $K_{\mathrm{S,aa}}$	0.3	0.32%	1.4%	−0.94%	5.1%
45. $k_{\mathrm{m,fa}}$	6	−0.88%	32.8%	−30.41%	116.5%
46. $K_{\mathrm{S,fa}}$	0.4	−25.82%	59.2%	−42.53%	112.5%
47. $K_{\mathrm{I,h2,fa}}$	5.00E−6	−48.36%	116.4%	−101.71%	153.6%
48. $k_{\mathrm{m,c4}}$	20	−9.05%	34.1%	−17.57%	66.1%
49. $K_{\mathrm{S,c4}}$	0.2	−159.23%	88.3%	−180.39%	98.0%
50. $K_{\mathrm{I,h2,c4}}$	1.00E−5	−129.15%	99.8%	−151.35%	124.5%
51. $k_{\mathrm{m,pro}}$	13	−10.21%	21.4%	−5.61%	17.8%
52. $K_{\mathrm{S,pro}}$	0.1	−33.24%	26.8%	−47.09%	63.6%
53. $K_{\mathrm{I,h2,pro}}$	3.50E−6	3.82%	32.3%	−5.28%	70.3%
54. $k_{\mathrm{m,ac}}$	8	−179.34%	152.5%	−102.65%	169.6%
55. $K_{\mathrm{S,ac}}$	0.15	52.67%	37.2%	37.69%	92.9%
56. $K_{\mathrm{I,nh3}}$	0.0018	11.42%	140.5%	−75.02%	174.2%
57. $k_{\mathrm{m,h2}}$	35	32.05%	45.2%	26.13%	60.1%
58. $K_{\mathrm{S,h2}}$	7.00E−6	21.08%	15.9%	34.41%	24.7%
59. $k_{\mathrm{dec,Xsu}}$	0.02	1.22%	24.2%	4.52%	51.6%
60. $k_{\mathrm{dec,Xaa}}$	0.02	−5.39%	40.2%	−34.04%	85.5%
61. $k_{\mathrm{dec,Xfa}}$	0.02	−20.96%	72.6%	−65.01%	130.7%
62. $k_{\mathrm{dec,Xc4}}$	0.02	−14.78%	30.3%	−28.31%	58.6%
63. $k_{\mathrm{dec,Xpro}}$	0.02	11.95%	19.1%	0.51%	44.0%
64. $k_{\mathrm{dec,Xac}}$	0.02	−35.84%	85.9%	−62.58%	124.2%
65. $k_{\mathrm{dec,Xh2}}$	0.02	6.07%	4.8%	6.39%	13.6%
66. $\mathrm{pH}_{\mathrm{UL,aa}}$	5.5	0.04%	0.6%	0.22%	0.8%
67. $\mathrm{pH}_{\mathrm{LL,aa}}$	4	0.22%	0.6%	0.60%	1.1%
68. $\mathrm{pH}_{\mathrm{UL,h2}}$	7	1.49%	20.8%	7.24%	32.2%
69. $\mathrm{pH}_{\mathrm{LL,h2}}$	6	1.25%	21.2%	7.69%	33.5%
70. $\mathrm{pH}_{\mathrm{UL,ac}}$	6	1.59%	1.1%	1.67%	1.8%
71. $\mathrm{pH}_{\mathrm{LL,ac}}$	5	1.30%	1.1%	1.12%	1.5%
Initial conditions					

Journal homepage: http://www.sciencedirect.com/science/journal/00255564
Original file available at: http://www.sciencedirect.com/science/article/pii/S0025556417300780

72. $S_{su}(0)$	0.00762	2.07%	21.6%	−4.91%	42.9%
73. $S_{aa}(0)$	0.0034	1.21%	22.6%	−3.08%	46.4%
74. $S_{fa}(0)$	0.0573	7.61%	30.0%	6.16%	55.0%
75. $S_{va}(0)$	0.00725	7.98%	24.8%	1.67%	57.1%
76. $S_{bu}(0)$	0.00826	2.40%	34.0%	−1.07%	48.7%
77. $S_{pro}(0)$	0.00937	1.77%	26.0%	−12.10%	52.8%
78. $S_{ac}(0)$	0.0954	−14.79%	42.1%	−20.51%	55.7%
79. $S_{h2}(0)$	1.500E−7	−3.12%	19.0%	−3.31%	30.6%
80. $S_{ch4}(0)$	0.0505	−0.08%	14.8%	4.50%	24.7%
81. $S_{IC}(0)$	0.157	−1.86%	4.9%	−2.92%	9.4%
82. $S_{IN}(0)$	0.1337	3.58%	8.6%	6.90%	10.4%
83. $S_{I}(0)$	0.422	0.43%	5.6%	−1.07%	12.0%
84. $X_{xc}(0)$	0.201	11.66%	19.6%	17.50%	27.3%
85. $X_{ch}(0)$	0.0145	0.85%	17.9%	1.00%	33.2%
86. $X_{pr}(0)$	0.052	1.66%	22.1%	3.14%	40.0%
87. $X_{li}(0)$	0.0155	3.27%	17.3%	8.83%	31.7%
88. $X_{su}(0)$	0.339	−1.60%	14.9%	−4.32%	22.2%
89. $X_{aa}(0)$	0.928	3.67%	7.0%	−1.18%	26.6%
90. $X_{fa}(0)$	0.2	2.61%	11.8%	6.43%	24.7%
91. $X_{c4}(0)$	0.341	−21.31%	15.8%	−23.23%	21.6%
92. $X_{pro}(0)$	0.109	7.44%	6.3%	10.62%	10.5%
93. $X_{ac}(0)$	0.608	−8.65%	28.8%	−18.29%	34.5%
94. $X_{h2}(0)$	0.253	−11.73%	9.8%	−3.13%	27.4%
95. $X_{I}(0)$	25.8	0.40%	2.1%	−0.40%	3.8%
96. $S_{gas,h2}(0)$	7.108E−6	1.38%	15.6%	−3.67%	31.1%
97. $S_{gas,ch4}(0)$	1.582	0.36%	15.6%	−1.90%	26.9%
98. $S_{gas,co2}(0)$	0.0138	−0.05%	15.1%	−2.19%	26.7%

Journal homepage: http://www.sciencedirect.com/science/journal/00255564
Original file available at: http://www.sciencedirect.com/science/article/pii/S0025556417300780

Postprint version of paper published in Mathematical Biosciences 2017, vol. 288, p. 21-34.
The content is identical to the published paper, but without the final typesetting by the publisher.

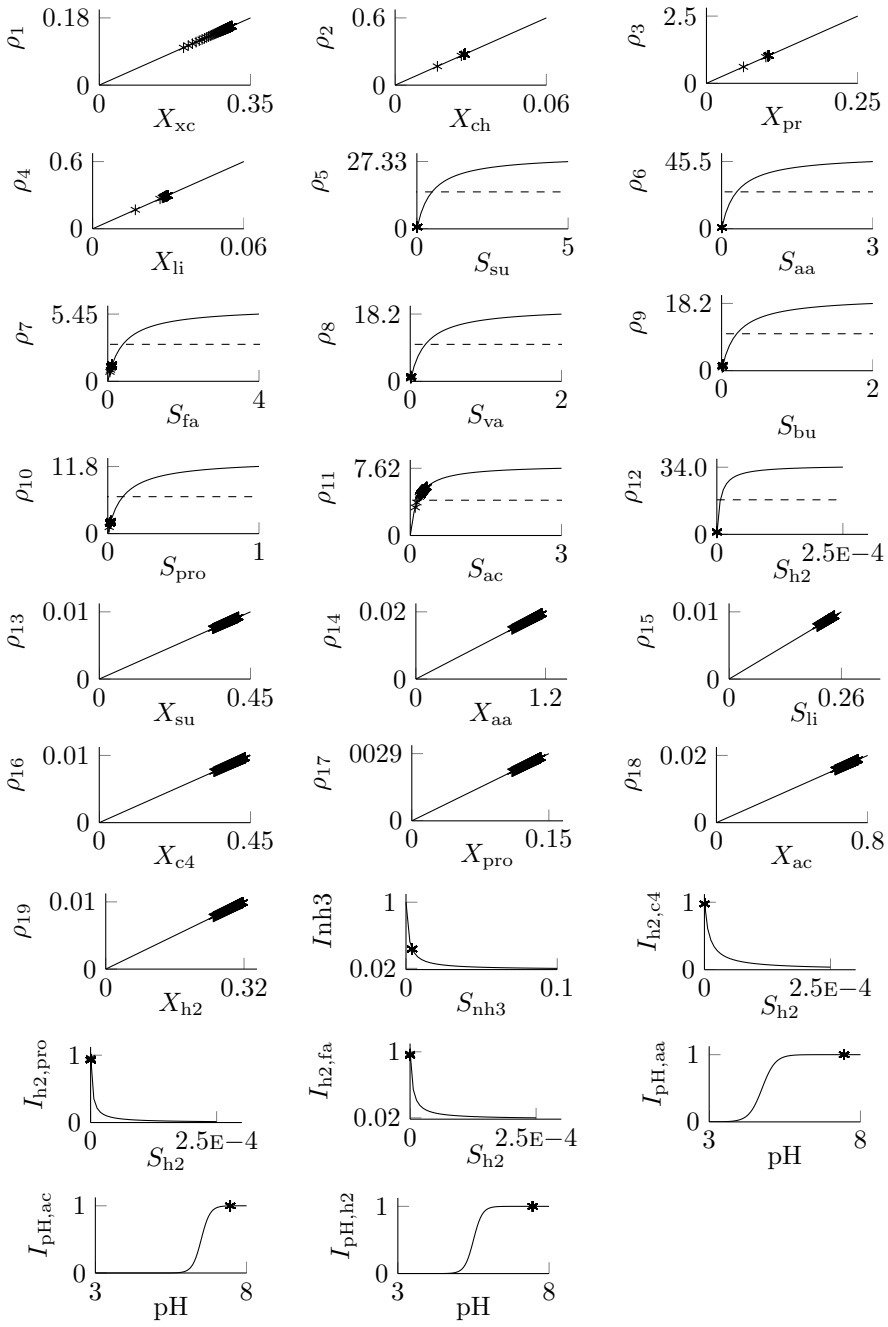

Figure 1: **Plot of the simulation results of Experiment 1 on the reaction rates of ADM1.** The value $\mu_{\max}/2$ is indicated by a dashed line (- -).

Journal homepage: http://www.sciencedirect.com/science/journal/00255564
Original file available at: http://www.sciencedirect.com/science/article/pii/S0025556417300780

Postprint version of paper published in Mathematical Biosciences 2017, vol. 288, p. 21-34.
The content is identical to the published paper, but without the final typesetting by the publisher.

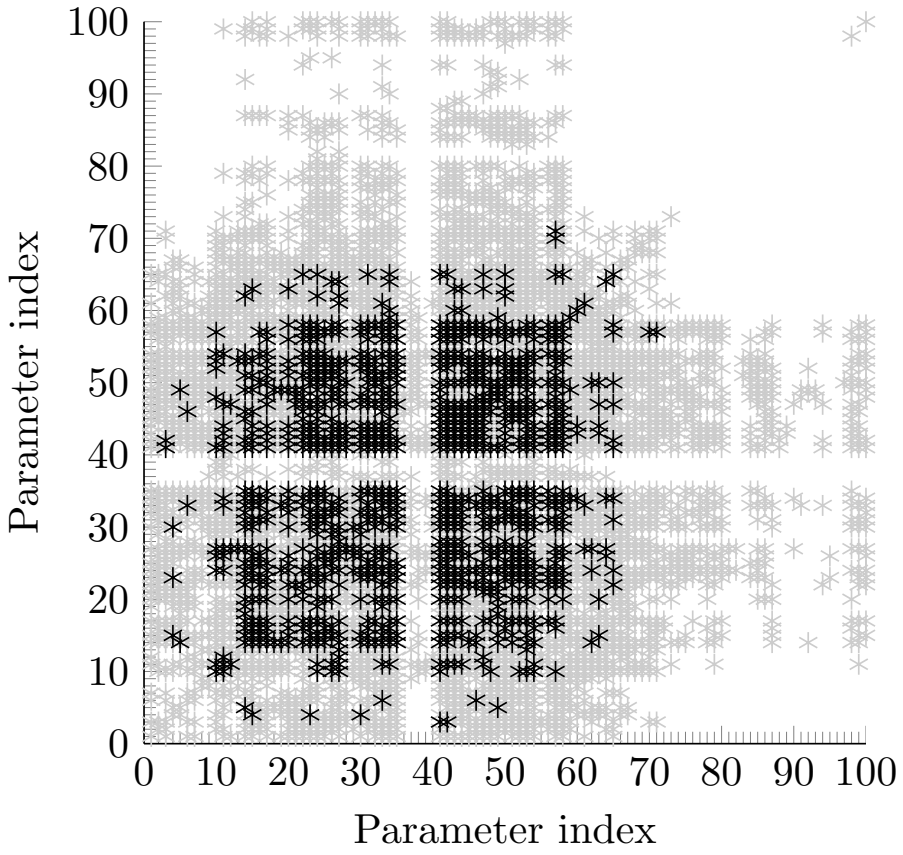

Figure 2: **Square root of the absolute relative covariances for the parameters estimates at a 5% noise level for Experiment 1.** A root of an absolute covariance higher than 25% is indicated in black. A root of an absolute covariance in between 5% and 25% is indicated in grey. Roots of absolute covariances lower than 5 % are not indicated.

Journal homepage: http://www.sciencedirect.com/science/journal/00255564
Original file available at: http://www.sciencedirect.com/science/article/pii/S0025556417300780